Sustainability Assessment of Community Scale Integrated Energy Systems: Conceptual Framework and Applications

by

Salim Moslehi

A Dissertation Presented in Partial Fulfillment
of the Requirements for the Degree
Doctor of Philosophy

Approved June 2018 by the
Graduate Supervisory Committee:

T. Agami Reddy, Chair
Klaus Lackner
Kristen Parrish
Ram Pendyala
Patrick Phelan

ARIZONA STATE UNIVERSITY

August 2018

ABSTRACT

One of the key infrastructures of any community or facility is the energy system which consists of utility power plants, distributed generation technologies, and building heating and cooling systems. In general, there are two dimensions to “sustainability” as it applies to an engineered system. It needs to be designed, operated, and managed such that its environmental impacts and costs are minimal (energy efficient design and operation), and also be designed and configured in a way that it is resilient in confronting disruptions posed by natural, manmade, or random events. In this regard, development of quantitative sustainability metrics in support of decision-making relevant to design, future growth planning, and day-to-day operation of such systems would be of great value. In this study, a pragmatic performance-based sustainability assessment framework and quantitative indices are developed towards this end whereby sustainability goals and concepts can be translated and integrated into engineering practices.

New quantitative sustainability indices are proposed to capture the energy system environmental impacts, economic performance, and resilience attributes, characterized by normalized environmental/health externalities, energy costs, and penalty costs respectively. A comprehensive Life Cycle Assessment is proposed which includes externalities due to emissions from different supply and demand-side energy systems specific to the regional power generation energy portfolio mix. An approach based on external costs, i.e. the monetized health and environmental impacts, was used to quantify adverse consequences associated with different energy system components.

Further, this thesis also proposes a new performance-based method for characterizing and assessing resilience of multi-functional demand-side engineered systems. Through

modeling of system response to potential internal and external failures during different operational temporal periods reflective of diurnal variation in loads and services, the proposed methodology quantifies resilience of the system based on imposed penalty costs to the system stakeholders due to undelivered or interrupted services and/or non-optimal system performance.

A conceptual diagram called “Sustainability Compass” is also proposed which facilitates communicating the assessment results and allow better decision-analysis through illustration of different system attributes and trade-offs between different alternatives. The proposed methodologies have been illustrated using end-use monitored data for whole year operation of a university campus energy system.

This dissertation is dedicated to my kind parents, my caring sisters, Saba and Nasim, and to my kind-hearted and loving wife, Maryam, who have been extremely supportive and encouraging. I am truly thankful for having you all in my life. I LOVE you.

ACKNOWLEDGMENTS

I have had the pleasure to work with amazing and knowledgeable individuals during my studies and have learned a lot from them. I am intended to thank my research committee members, Professor Klaus Lackner, Professor Ram Pendyala, and Professor Patrick Phelan, and especially Professor Kristen Parrish who have provided me with brilliant suggestions and feedbacks which considerably improved this work. I would like to express my deepest appreciation to my advisor, Professor T. Agami Reddy, for giving me the opportunity to work with him and for his tremendous and invaluable support which made my PhD studies an amazing experience. Words can not describe how grateful I am.

Finally, I would like to thank my family and my friends for always being there and for everything they have done for me.

TABLE OF CONTENTS

CHAPTER Page

CHAPTER Page

CHAPTER Page

LIST OF TABLES

Table Page

Table Page

LIST OF FIGURES

Figure Page

Figure Page

Figure Page

Figure Page

Chapter 1 – Introduction

1.1 Sustainability and Sustainable Development- Definitions and Approaches

Sustainability is a complex multifaceted concept with direct implications towards all activities associated with human development, and consequently, has been the focus of researchers from various disciplines as well as practitioners from a wide range of disciplines. It has gained enormous attention in a variety of fields during the past few decades. The numerous definitions and approaches one comes across in the published literature have to be viewed in the context in which they appear. The definition of sustainable development proposed in 1987 by the World Commission on Environment and Development is probably the most cited: “Development that meets the needs of the present without compromising the ability of future generations to meet their own needs” [1]. Such aspirational definitions, despite providing insight into the ultimate goal of sustainable development, lack one basic feature, i.e. the necessary specificity to be operationalized.

In ecology, healthy endurance of biological systems over a long period of time requires that the system remain diverse and productive which are two critical attributes of such systems. This approach can suggest a more generalized definition of sustainability applicable to a variety of systems from different domains. The sustainability criteria need to be customized pertinent to the domain and its specifications tailored to a particular system to include those attributes which guarantee “healthy endurance of the system”. For example, a sustainable educational system should be more impacted, or characterized by, equity, diversity, etc. In this study we have defined sustainability as:

“Ability of a system to endure while consistently meeting requirements pertinent to critical aspects of the system and its surrounding environment”

This definition is applicable to different systems as the critical aspects of different systems are different. Such critical aspects, hereafter referred to as *“sustainability criteria”* or *“sustainability attributes”*, are crucial to system endurance and should not be compromised. Sustainability criteria are broad categories comprised of various metrics (also known as indicators) capturing certain features of the system. In selecting and defining sustainability criteria and metrics relevant to a particular system, critical aspects of the system and its interactions with the surrounding environment, including both physical environmental and society, should be considered. Such criteria and related limitations would change in time, location, and system scale. For instance, “water consumption” would be extremely critical in a location with arid climate but not so important in another location with heavy rainfall. Of course, these sustainability criteria ought to be selected by consensus of different stakeholders and authorities, after which the goal would be to find solutions able to satisfy all sustainability criteria, i.e. fall within the desired solution space. The system stakeholders (users, owners, etc.) may prioritize different sustainability criteria in order to magnify or lessen their relative importance, and so one single “best” solution even for a relatively well defined spatial region may be a simplistic goal.

In the context of energy and energy systems, there is consensus on the important sustainability criteria, i.e. environmental impacts, economic impacts, and social impacts, known as the triple bottom line. Figure 1-1 graphically represents the concept of sustainability for energy systems. The overlapped area or intersection of three sustainability criteria denote the solution space in which system performance is able to satisfy all sustainability criteria.

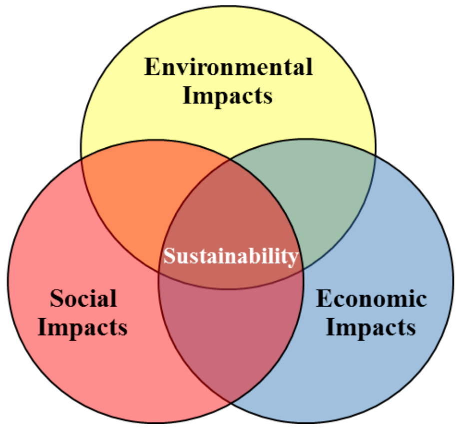

Figure 1-1- Triple bottom line: sustainability solution space

1.2 Current Issues with Complex Energy Systems

Finding a sustainable solution for the energy crisis is becoming more and more controversial both in terms of technical solutions as well as satisfying the perspectives of different stakeholders in terms of assigning acceptable environmental burden and economic costs. Integration of energy systems with other infrastructures, the whole society, and the environment introduces even higher levels of complexities which makes energy policy definitions and decision making extremely challenging. To overcome such challenges and find solutions for these “wicked” problems, a clear roadmap that can support sustainable development is essential.

Much of the dialogue about sustainability and sustainable development tends to be largely at odds with current engineering analysis methods. Further, it is often heuristic and normative due to the introduction of “soft” issues such as social interactions and human values. Moving toward more sustainable energy systems and infrastructure requires that the sustainability concept to be cast in the context of engineering practices and serves as a pointer to design and planning goals. In this regard, sustainability or sustainable performance of energy systems should be characterized using well-defined metrics which : (a) can capture critical features/attributes and primary sustainability criteria; (b) can be aggregated into a single (or a small few) sustainability index (indices); (c) can be calculated for different types of systems and facilities; (d) is based on data which can be gathered from monitoring, or public records or even by system simulation; and (e) can serve as a means to compare different systems and design alternatives. Such multi-dimensional traits should be able to capture the tradeoffs associated with different development paths, design alternatives, and planning options, and thereby facilitate and support multi-criteria decision making.

On the other hand, with the current technological and market barriers, fossil fuels will be in use for several decades into the future and cannot be immediately replaced by renewables. Therefore, ranking different power generation facilities may not provide useful insight for a sustainable energy infrastructure unless a longer time timeframe is considered during the analysis. Environmental impacts of electricity depend heavily on the energy portfolio mix. The fuel mix varies across utility companies and also changes over time (seasonally and hourly) since it is dictated by the magnitude and variability of the loads to be met, the costs and availability of primary resources and the specific mix of power plant generation units [2]. In addition, similar types of power generation facilities would have different emission rates due to utilization of emission control strategies; consequently, environmental impacts assessment of energy systems, and essentially the sustainability assessment frameworks, would be case-specific and multidimensional.

1.3 Research Gaps and Objectives of This Study

There are two dimensions to “sustainability” as it applies to an energy system. It needs to be: (a) designed, operated, managed, and supported in such a manner that its environmental impacts and costs are minimal- this is the concept of energy efficient design and operation; and (b) designed such that it is robust to disruptions and shocks posed by natural, manmade, or random events and, if possible, can dynamically transform and adapt, and be able to recover and deal with the aftermaths; these capabilities are generally referred to as “*resilience*”. Increased complexity of urban infrastructure systems on one hand, and more severe and more frequent natural disasters due to global climate change on the other hand, have forced researchers to consider resilience as an important and integral element of sustainability assessment of energy infrastructure and systems Therefore, sustainability criteria should explicitly include environmental, economic, and resilience considerations of any energy system, be it at an individual building level, at community scale, and at regional scale.

This study will attempt to provide a more practical and general working definition of sustainable energy systems that includes criteria and metrics which capture all critical aspects of energy systems farmed in such a manner that it can be adopted in engineering design and planning practices. In other words, instead of common metrics and objective functions (usually maximizing system financial performance), this thesis is aimed at adapting sustainability criteria into the engineering practices. This would help designers, developers, and planners make informed and sustainability-conscious decisions accounting for different system attributes and acknowledging different perspectives regarding design of new systems, operation of existing ones, and planning for future growth. To achieve this goal, a new quantitative sustainability assessment framework and indices have been developed which is described and illustrated in this thesis.

In this research, in addition to the sustainability assessment framework itself, new methodologies have been developed for assessment and quantification of location and circumstance-specific environmental impacts and resilience performance of energy systems. The scope of this study is limited to community scale energy systems which have a well-defined central authority wherein policy decisions regarding social practices and engineering systems are easier to implement. At point of use, community-scale energy systems, including energy inputs from utilities (in the form of electricity and fuel), distributed power generation technologies, and building heating and cooling systems, are crucial in achieving sustainable development due to involvement of end-use consumers on one hand [3], and their large contribution in the world's energy use and GHG emissions on the other hand (according to [4] in 2017, 40% of total U.S. primary energy consumption was for residential and commercial buildings).

1.4 Thesis Structure

The thesis is primarily concerned with integrated energy systems which comprise of utility power plants, distributed generation technologies, and building heating and cooling systems. Hence, typical end-uses will be electricity loads, and heating and cooling thermal loads. Chapter 2 will provide a detailed description of how to assess environmental impacts of energy systems through a comprehensive life cycle assessment. Chapter 3 addresses resilience of energy systems which is as an important and integral sustainability criterion pertinent to energy systems, and describes and illustrates a way by which it can be quantified and incorporated into the whole framework. Chapter 4 considers the applicability of the proposed framework in designing, planning, and operating the energy systems and how the framework can support decision making with regard to sustainable development. Finally, a summary of this research study along with possible extensions are presented in chapter 5. Chapter 2, 3, and 4 have been written as three journal papers (all of which have been submitted to a engineering journal).

Chapter 2 – A Methodology to Assess Location-Specific Environmental Externalities

Abstract

A community scale integrated energy system (IES), which consists of utility power plants, distributed generation systems, and building heating and cooling systems, is a key element of any community or facility. Development of quantitative sustainability metrics in support of decision-analysis relevant to design, future growth planning and day-to-day operation of such systems would be of great value. This paper addresses one of the basic issues in this regard, i.e. quantification of location-specific environmental and health effects attributable to IES. This paper proposes a pragmatic methodology towards this end that incorporates Life Cycle Assessment which considers emission rates from different supply and demand-side energy systems, accounting for regional power generation energy portfolio mix. External cost approach, i.e. the monetized adverse health and environmental impacts, was used to quantify impacts associated with utility scale power generation, solar photovoltaics (PV) manufacturing, transportation, and installation, as well as those associated with the operation of combined heat and power (CHP) systems, boilers, and chillers. Uncertainties associated with various numerical inputs to this analysis are large, and the Monte Carlo approach is adopted to quantify their propagation into the final results. The proposed methodology has been illustrated using end-use monitored data for a whole year of operation of a university campus IES with a CHP system and large solar PV penetration. We found average external costs of purchased electricity, specific to the local power utility fuel mix, to be about 1.93 ¢/kWh, with minimal diurnal and seasonal variations, while the power generated by the PV systems are four times less detrimental. Accounting for recovered heat, the externalities

associated with the CHP system (which has a total efficiency of 71%) are of the same order of magnitude as those associated with the purchased electricity. External cost of heating generated by on-site boilers are estimated to be 6.7 $/GJ. These values can be effectively used by planner and operators to make sustainable-conscious decisions regarding design, expansion, and operation of integrated energy systems.

Nomenclature

EF_E	Emission factor (kg/MWh, kg/MW) from electricity generation
EF_O	Emission factor (kg/MWh, kg/MW) from systems operation
EF_M	Emission factor (kg/MWh, kg/MW) from systems manufacturing
ExC	External costs ($, $/kg, ¢/kWh, $/GJ)
FuCo	Cumulative fuel energy consumption (kJ)
HC	Heat content of the fuel (kJ/m^3)
i	Pollutant index
j	System index
PuEl	Purchased electricity (MWh)
SysCap	System Capacity (MW)
t	time (hr)
TH	Time horizon (years)
$T\&D_{loss}$	Electricity transmission and distribution loss fraction
σ	Standard deviation

Subscripts

PE	Purchased electricity
SO	System operation

SM System manufacturing

T Total

2.1 Introduction

Meeting the energy needs of mankind imposes huge burdens on both society and the environment in the form of externalities, which are typically not accounted for either by energy providers or by consumers. Price tags of monetized externalities, referred to as external costs, are representative of the amount of money that should be spent to either offset the pollutant emissions or to deal with the associated adverse consequences. Just the health-related external damages of burning fossil fuels in the U.S. are estimated to be about $120 billion per year and said to result in 20,000 premature deaths each year [5].

Hohmeyer, in 1988, conducted one of the very first studies [6] on external costs of fossil fuels power generation using pollutant damages estimated by Wicke [7]. Since then, the external costs of various power generation sources have been examined extensively and in more depth. Rabl and Rabl estimated externalities of nuclear power generation inclusive of the frequency of nuclear accidents and compared them with external costs associated with wind plus NGCC (natural gas combined cycle) power generation which is an alternative with lowest external costs; they found that the external damages of the latter to be 1.22 €cent /kWh which was found to be higher than that of nuclear power (0.79 €cent /kWh) [8]. Rabl and Spadaro performed a life cycle assessment to evaluate the power generation externalities throughout the lifecycle of various power generation technologies in Europe for the purpose of environmental policies development; they found that coal power generation results in average external costs around 6.7 €cent /kWh, while wind energy external cost is only 0.18 €cent /kWh

[9]. The U.S. National Research Council (NRC) committee studied external costs of power generation and transportation from particulate matter (PM), sulfur dioxide (SO_2), and nitrogen oxide (NO_x), over the entire lifecycle of conventional power generation facilities and of transportation across the U.S.; they found that the mean damages associated with electricity generation from coal were 3.2 ¢/kWh (5th percentile < 0.5 ¢/kWh and 95th percentile > 12 ¢/kWh). On the other hand, mean damages from natural-gas-fired power plants were estimated to be 0.16 ¢/kWh (5th percentile < 0.05 ¢/kWh and 95th percentile = 1 ¢/kWh) [10].

Numerous in-depth studies focusing on individual energy/power technologies provide valuable insights in evaluation of associated environmental impacts. For example, Corona et al. investigated life cycle externalities of concentrating solar power (CSP) plants (parabolic troughs) in both basic and hybrid modes, and concluded that hybridizing CSP with natural gas will result in rapid increase in environmental damages from 2 €/MWh, from the solar-only mode, to around 13 €/MWh from the 30% Natural Gas mode [11]. Mattmann et al. focused on valuation of both positive and negative externalities associated with hydropower electricity generation from previously published studies and identified avoidance of greenhouse gas emissions as the main positive externality of the hydropower generation given the share of the hydropower in national energy production [12]. Zhang et al. evaluated and compared the externalities of small and large scale hydropower projects in China and found that the hydropower potentials to offset the GHG emissions have been overestimated as the externalities due to reservoir impoundment and occupation are overlooked [13]. Hacatoglu et al. assessed and compared GHG emissions, ozone-depleting substance emissions of wind-battery systems and gas-fired technologies finding that wind-battery would emit 78% less ozone-depleting substances and 87% less GHG [14].

The traditional remedy, in order to overcome market failures to appropriately consider and price such externalities, is government interventions in the form of taxes or tradable permits [10]. Using ExternE project results, Krewitt pointed out that the uncertainties of external costs estimates is a barrier to proper internalization of externalities [15]. Georgakellos evaluated effects of internalizing greenhouse-related external costs with electricity price generated in thermal power plants in Greece and found that this would increase the power generation costs by more than 52% [16]. Kosugi et al. studied the externalities of major global environmental issues and the effects of internalizing such impacts on economic growth [17]; they found that global warming is likely to account for 10% to 40% of total environmental externalities in the 21st century.

Analysis and comparison of the external costs associated with various energy resources would provide valuable insights into some of the controversies surrounding energy and sustainability. Owen investigated the effects of environmental externalities of renewable and conventional energy technologies on penetration of renewables, and concluded that such externalities, if internalized into the price of the electricity, could lead to wind and some application of biomass power generation technologies becoming economically competitive with coal-based power generation [18]. In addition, external costs estimation can be incorporated into quantitative sustainability assessment of energy infrastructure and system such as those proposed by Moslehi and Arababadi [19], Afgan et al. [20], and Evans et al. [21]. Furthermore, external costs can be considered to be a decision criterion in energy systems design and development both in supply and demand sides. For example, Diakoulaki et al. evaluated the energy-related externalities of two industrial units so as to compare different pollution abatement policies [22]; they found that substitution of fuel oil with Natural Gas could lead to 90% reduction in environmental damages and is by far the most effective strategy compared to “increasing the stack height” and “relocating the facilities hundreds of kilometers far form the urban area”. Anastaselos et al. evaluated environmental performance of numerous energy systems commonly used in Greek residential buildings, focusing on production, disposal and transportation of the materials used in those energy systems; they found that a Natural Gas-fired boiler with floor heating and evacuated tube solar collector or poly-Si PV system would have the least environmental impacts [23]. Gaterell and McEvoy investigated the impacts of external costs and associated uncertainties on relative performance of insulation measures applied to number of residential houses and found that large variations in the external costs have significant impact on the cost-effectiveness of such energy conservation measures [24].

In order to address environmental challenges pertinent to energy systems, aggregated sustainability goals have to be translated to community level targets to be met by energy systems designers, developers, and operators [25]; however, we contend that studies carried out with focus on energy-related externalities are limited to aggregated levels, i.e. to utility scale power generation (such as done in [8,12,26,27]). Therefore, the current study aims to bridge the gap between generic pathways and specific products by evaluating and quantifying the environmental and health externalities associated with community scale energy systems taking an Life Cycle Assessment (LCA) approach. We shall identify environmental and health impacts over the lifecycle of the system components, which includes utility power generation facilities, distributed on-site power generation systems, and building heating and cooling equipment. Externalities of different sources and systems shall be estimated using external cost values associated with pollutant emissions. Hourly and seasonal variations in pollutant emissions due to changes in the power generation fuel mix shall be considered; to the best of our knowledge, there is only one published study that accounts for temporal variations in the power generation carbon footprint [28]. The proposed methodology will facilitate real-time sustainable operation of energy systems in terms of dynamic/active building load management and optimal control and operation of integrated energy systems (IES)which would be of great importance as buildings operation corresponds to significant portion of total environmental impacts throughout life cycle of the building [29,30]. It will also allow evaluations into future system expansion and re-design options in terms of sustainability considerations

2.2 Methodology

Evaluating environmental and health impacts associated with a community IES requires a comprehensive LCA of each and every energy system and energy carrier. Such analysis would ideally include all life stages of energy technologies starting from material extraction and fuel mining, to construction of required infrastructure, fuels processing, power generation, distribution and transmission, for both utility and on-site energy system components.

2.2.1 Life Cycle Assessment

An extensive LCA is required to estimate the emissions associated with a community scale IES over its lifecycle. According to ISO 14040 standard [31], an LCA study is comprised of four steps: goal and scope definition, life cycle inventory (LCI), life cycle impacts assessment (LCIA), and results interpretation. Each of theses steps are discussed in more detail and adopted to the scope of our analysis.

(a) *Goal and Scope Definition*: This step includes defining goals and scopes of the LCA study, identifying systems boundaries, and defining the functional unit. Regarding the scope of this study, this should involve assessing the environmental and health impacts associated with meeting the service needs of a community (ranging from one building to hundreds of buildings) in terms of electricity or fuel. An attributional or comparative LCA approach (i.e., one which is meant to evaluate two or more existing systems) is more appropriate to identify and compare the impacts from various existing energy sources and systems. Figure 2-1 depicts the life cycle of the whole system along with the boundaries of this LCA study. It includes explicit consideration of various stages in the extraction and manufacturing of raw materials needed for various types of components, the subsequent conversion (or core) processes needed to meet the energy service load of the building. Location-specific power generation technologies/fuel mix, as well as heating, cooling, and on-site power generation equipment need to be considered. The environmental and health impacts should be identified during systems operation (for example, burning Natural Gas (NG) in boilers for heating) including upstream effects (for example, processing NG), as well as for system/infrastructure manufacturing and construction (for example, construction of a NG-fired power plant).

Previous studies reveal that emission rates of on-site boilers and CHP systems manufacturing and end-of-life stages are negligible compared to other lifecycle phases [32–35]. Beccali et al. performed a comprehensive life cycle assessment on chillers finding that operation of electric and absorption chillers (as appose to solar-driven absorption chillers) is the most impactful life stage accounting for more than 96% of global warming potentials (GWP) and more than 98% of global energy requirement (GER) [36]. Therefore, manufacturing and end-of life impacts of on-site boilers, CHP systems and chillers are excluded from the current analysis.

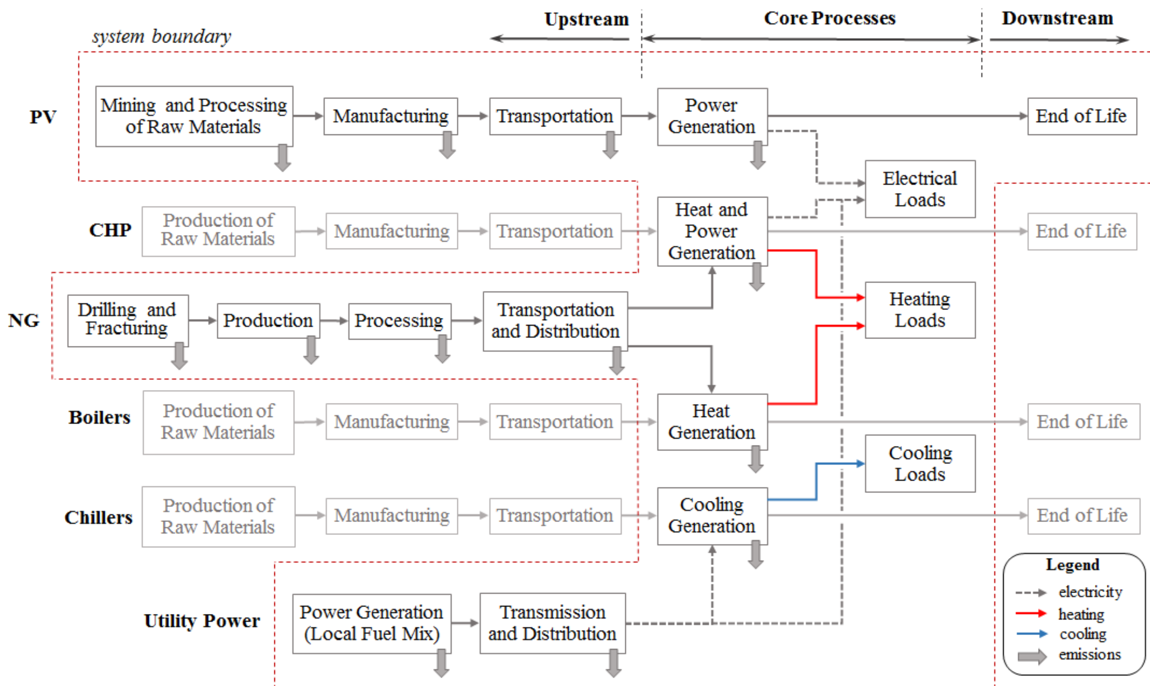

Figure 2-1- Scope of the LCA analysis for a typical community Integrated Energy System (IES). Emissions associated with each step are represent as thick arrows.

(b) *Life cycle inventory*: Here, emission data should be collected for all systems and during their lifecycle stages that are included in the scope of analysis. The impact categories, i.e. damage criteria, and the reference substances should be identified such that most of the adverse impacts imposed on the environment and on society are captured. Failing to include important damage criteria would likely bias the final decision.

Instead of being exhaustive, it would be more appropriate to identify important damage criteria/insults pertinent to energy systems. In order to do so, the share of each pollutant in the total external cost of power generation had to be estimated (Figure 2-2) using previous studies and based on the U.S. average power generation fuel mix (taken from [9]). It was found that more than 95% of the total externalities of power generation in the U.S. can be attributed to four damage criteria, i.e. CO_2, SO_2, NO_x, and $PM_{2.5}$. Therefore, we have chosen to limit our assessment to include only these four damage criteria

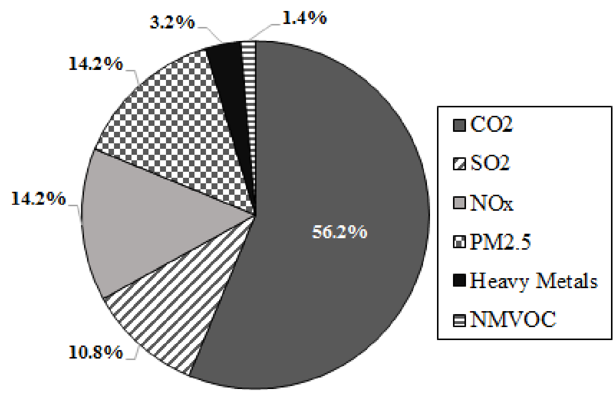

Figure 2-2- Contribution of different pollutants to external costs attributable to electricity generation in the U.S., estimated based on external costs of utility scale power generation technologies estimated by Dones et al. [37]

(c) ***Life cycle impact assessment***: This step should involve translating the pollutant emissions from various systems and sources, gathered in the previous step (life cycle inventory), into negative impacts on the environment, natural resources, human health, flora and fauna, building materials, and other social assets. External cost approach was adopted in this study in order to capture environmental and health impacts associated with the selected pollutant types. Such effects may include local impacts and/or global consequences, such as climate change. Assigning monetary costs to the impacts from CO_2, SO_2, NO_x, and $PM_{2.5}$ will enable us to aggregate them into one number which reflects overall impact of a particular system or energy source. This will facilitate comparison among various energy sources and alternative systems.

(d) ***Results Interpretation***: The final step of the LCA should be to analyze the data and results of the assessment in order to identify life stages, systems, or resources which have relatively high environmental and health impacts. This can help policy/decision makers and designers make informed decisions regarding short-term and long-term emission curtailment strategies.

2.2.2 External (Hidden) Costs

Monetizing externalities can be done through different means depending on type of the impacts which can be divided into two broad groups: (a) those with market value, such as loss in crops or loss in work days, and (b) those with no clear market values, such as premature death, quality of life degradation. Assessment of health externalities is usually done by allocating monetary values to premature death and other health endpoints, loss in work days, and costs imposed to the healthcare system. The estimated values of health impacts vary widely in the literature depending on the population density, the models used to evaluate pollutant concentration and concentration-response function to estimate the adverse health effects of change in a particular pollutant concentration [38]. The external costs and damages from different criteria air pollutants also vary significantly depending on the location of the emitting sources [39].

A relatively simple approach to monetize adverse health effects is the use of the “willingness to pay” concept, abbreviated as WTP, to infer the valuation that people place on a particular effect. These WTP values are often determined through surveys [40].

2.2.3 Calculating the External Costs

The objective of this study is to evaluate the overall environmental and health impacts associated with supplying a community with its energy needs which include electricity, and heating-cooling energy. The external cost approach allows us to quantify and aggregate environmental and health effects of various resources and systems used to generate, process, and transmit the required energy. Total impacts attributed to the IES, ExC_T, can be expressed as:

$$ExC_T = ExC_{PE} + ExC_{SO} + ExC_{SM} \tag{2-1}$$

where ExC_{PE} is the external costs associated with purchased electricity generation; ExC_{SO} is the external costs of on-site systems during their operation to generate electrical power, heating, and cooling, such as burning natural gas in a boiler or by a CHP system; this term also includes upstream impacts of required fuel during extraction, processing, and distribution. The term ExC_{SM} captures external costs attributable to on-site systems manufacturing and on-site plant constructions. Each of these terms will be explained in more details in this paper. Regarding the manufacturing externalities, since the lifespan and age of energy systems and components are different, external costs associated with systems and manufacturing were simply spread over the life span of the corresponding system neglecting time value of money. On the other hand, the uncertainties associated with the external cost values are much higher than the discount rates (see Table 2-1 and [41]), and so there is little benefit in adopting a discounted cash flow approach.

2.2.3.1 External Costs of Purchased Electricity

Total external cost of purchased electricity (in \$) over a specified time period (say, one year) can be formulated as:

$$ExC_{PE} = (1 + T\&D_{loss}).\left[\sum_t \left(PuEl_t \sum_i (EF\_E_{it}.ExC_i)\right)\right] \quad (2\text{-}2)$$

where $T\&D_{loss}$ is the fraction of transmission and distribution electrical power losses, $PuEl_t$ is the total purchased electricity at time step *t* (say, one hour) in kWh which can be obtained from monitored data or from system simulations, EF_E_{it} is the i^{th} pollutant emission factor correspond to purchased electricity, in kg/MWh during hour t of the year, and ExC_i is external cost of the i^{th} pollutant in $/kg.

The electrical power generation fuel mix varies greatly across the U.S. depending on the electric utility provider and available resources. Such huge differences will also be reflected in the corresponding environmental and health impacts. Therefore, it is crucial to consider the fuel mix of the specific location for estimating the external costs of purchased electricity.

(a) *Emission Factors*: The fuel/energy mix varies by location and changes over time (long-term and short-term) and is dictated by costs and availability of resources and power plants [2]. Monthly-averaged hourly emission factors are available from National Renewable Energy Laboratory (NREL) [42] for different eGRID sub-regions (map can be found in [43]). The emission factor data on CO_2, NO_x, and SO_2 take into account the utility scale facilities being used in each region (i.e. power generation fuel mix), electricity imports and exports across sub-regions, diurnal and seasonal changes in the fuel mix, and transmission and distribution losses [42]. Figure 2-3 shows the hourly CO_2, SO_2, and NO_x emission factors of power generation for the AZNM (Arizona and New Mexico) eGRID (Emissions & Generation Resource Integrated Database) sub-region for four different months representative of seasonal and diurnal variations. It is evident that the emission rates change only slightly during a day and also throughout a year.

Since hourly data on emission of $PM_{2.5}$ were not available, we have assumed a constant emission rate for this pollutant based on emission factors from each facility type, i.e. coal, natural gas, nuclear, etc. and power generation fuel mix specific to each eGRID sub-region. For example, we estimated the $PM_{2.5}$ emissions rate to be 0.094 kg per MWh of purchased electricity in the state of Arizona (energy mix were taken from [44]). This would be a reasonable assumption since according to [37], health and environmental effects of $PM_{2.5}$ emissions is a considerable portion of total damages from hydro, PV, and wind power plants only during the manufacturing stage.

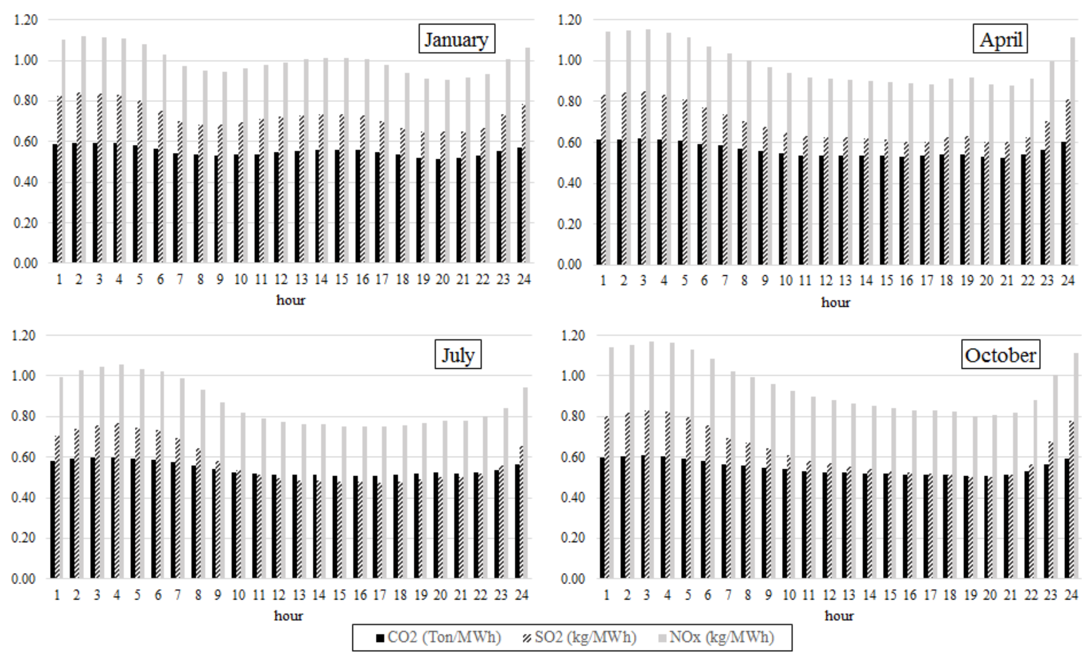

Figure 2-3- Hourly (monthly-averaged) emission factors of electricity generation for AZNM eGRID sub-region for CO_2 (in Ton/MWh) and SO_2 and NO_x (in kg/MWh), reported by NREL [42]

(b) ***Transmission and Distribution Losses***: The U.S. average electricity losses in transmission and distribution grids has been estimated by Energy Information Administration (EIA) to be about 5% [45]. This effect is already included in the emission factors estimated by NREL stated in (a) above. In case the emission factor data from another source excludes such losses, the term $T\&D_{loss}$ in Eq. 2-2 can be obtained from [46].

(c) *External Cost Values per Damage Criteria*: In this study, we have used the National Research Council (NRC) report for damage values (in $/Ton) estimated for SO_2, NO_x, and $PM_{2.5}$ for most of the coal and natural gas power plants across the U.S. [10]. The estimated damages are assembled in Table 2-1 in terms of mean, standard deviation and the 5th and 95th percentiles (which are helpful for subsequent uncertainty analysis). Note that the distribution of the pollutant damages from coal power plants are close to normal while those from NG-fired power plants seem to be closer to log-normal. The wide range of damages per pollutant criteria is mainly due to the variations in the population size affected by the pollution; effective height of the stack is also an influential factor [10].

The NRC analysis considers the entire life cycle of each power generation technology whereas most other studies exclude upstream activities in the life cycle. It investigated emissions from 406 coal-fired power plants and 498 natural-gas-fired power plants considering location of each power plant, applied emission control strategies, population density and demographics. The analysis applied the APEEP model (Air Pollution Emissions Experiments and Policy) in order to link the ambient concentration of each pollutant to emissions from pollution sources which are then translated to damages using population-weighted exposure-response function in six categories, namely health (including premature mortality and morbidity), visibility, crop yields (major field crops), timber yields, building materials and recreation (limited to pollution damages to forests)

[10]. We chose to use this dataset due to comprehensiveness of the NRC analysis in terms of damages and the breadth of the pollutants source locations.

Table 2-1- Distribution of criteria-air-pollutant damages in 2007 U.S. $/Ton from 406 coal-fired and 498 NG-fired power plants across the U.S. reported by NRC [10]

	Coal-Fired Power Plants ($/Ton)				NG-Fired Power Plants ($/Ton)			
Pollutant	Mean	Standard Deviation	5th Percentile	95th Percentile	Mean	Standard Deviation	5th Percentile	95th Percentile
SO_2	5,800	2,600	1,800	11,000	13,000	29,000	1,800	44,000
NO_x	1,600	780	680	2,800	2,200	2,000	460	4,900
$PM_{2.5}$	9,500	8,300	2,600	26,000	32,000	59,000	2,600	160,000

The external costs associated with global warming and climate change are usually reported per ton of carbon dioxide equivalent or carbon equivalent. Values found in the literature vary greatly depending on the assumptions of the analysis. The uncertainty mainly stems from unknown spatial scale and temporal horizons of the associated consequences. Although climate change is always regarded as a global dilemma, damages are, and will be, pronounced in specific locations. For example, local effects of extreme heat and cold conditions would affect people in mild climate who are more vulnerable due to human physiological adaptation. Based on different studies that have quantified global warming effects across the U.S., such as [47] and [39], we have assumed the CO_2 external costs to be 30 $/Ton with a low (i.e. 5^{th} percentile) of 10 $/Ton and a high (i.e. 95^{th} percentile) of 50 $/Ton.

2.2.3.2 External costs of System Operation (for on-site systems)

The term ExC_{SO} in Eq. 2-1 accounts for external costs associated with on-site energy systems, such as CHPs, boilers, and chillers, meant to generate electrical power, heating, and cooling thermal energy streams during their operation. Such externalities are mainly attributable to burning fuels, typically natural gas, in boilers or CHP systems to generate power and heat for domestic hot water, heating and cooling (via absorption chillers). Electrical equipment operation is already accounted for by the ExC_{PE} term. Upstream impacts of supplying required fuel during extraction, processing, and distribution, altogether referred to as pre-combustion stages, are also considered. The term ExC_{SO} ($) can be expressed as:

$$ExC_{SO} = \sum_t \sum_j \left(\frac{FuCo_{jt}}{HC_j} \sum_i EF\_O_{ij}.ExC_i\right) \tag{2-3}$$

where, $FuCo_{jt}$ is fuel energy consumption (in Joules) of the j^{th} system during time step t; EF_O_{ij} is the i^{th} pollutant emission factor in kg/m^3 for supplying and burning the fuel in the j^{th} system; HC_j is the heat content of the fuel in Joules/m^3 for the j^{th} system and ExC_i is the external damage costs of the i^{th} pollutant in $/kg. Emission factors for combustion and delivering the NG to buildings are listed in Table 2-2. Heat content of the natural gas can be obtained from [48] for each state in the U.S separately for each year for the past five years.

Table 2-2- Emission factors of supplying and burning natural gas [49]

Pollutant	Pre-combustion Emission Factors for Fuel Delivered to Buildings (kg/1000m^3)	NG combustion in a Commercial Boiler (kg/1000m^3)	NG combustion in Other Equipment (CHP) (kg/1000m^3)
CO_2	4.46e-1	1.97e0	2.00e0
SO_2	1.95e-2	1.00e-5	1.00e-5
NO_x	2.62e-4	1.78e-3	5.62e-3

2.2.3.3 External Costs in Manufacturing and Construction

The last term in Eq. 2-1, i.e. ExC_{SM}, accounts for the damages from on-site systems during manufacturing or construction stage which annualizes the external costs over the life span of the system. This parameter can be calculated from:

$$ExC_{SM} = \sum_j \sum_i \frac{SysCap_j.EF\_M_{ij}.ExC_i}{LS_j} \times TH \qquad (2\text{-}4)$$

where, $SysCap_j$ is the j^{th} system capacity or size (in MW); EF_M_{ij} is the i^{th} pollutant emission factor (in kg/MW) from the j^{th} on-site system during its manufacturing or construction; LS_j is the j^{th} system life span (in years) used to annualize the total external costs of system manufacturing/construction; ExC_i is the i^{th} pollutant external cost in $\$/kg$, and TH is the time horizon of the analysis in years.

For systems that do not emit any pollution during the operation phase, such as solar photovoltaic (PV) systems, embodied emissions have been estimated by considering panels manufacturing, transportation, and installation. The type of PV technology and the size of the installation are important factors. Solar PVs emission factors are sometimes reported in kg/kWh; however, it would be more accurate (and technically correct) if they are reported in kg/m^2 or kg/kW since PV system efficiency and capacity factor would vary based on the location and other factors such as type of PV system mount. In this study, we have used the ecoinvent database to determine emission factors of solar PVs manufacturing and transportation [50].

Solar PV systems installed in the U.S. have been manufactured in different countries such as China, Malaysia, Mexico, Canada as well as in the U.S. Therefore, some panels have to be transported over long distances which might have considerable emissions and impacts on the environment. In this study, we have assumed marine transport for long distances (for instance, from China) and truck transport for shorter distances (for example, from Canada and Mexico). The emission factors associated with the transportation phase taken from various sources are gathered in Table 2-3.

Table 2-3- Emission factors due to transportation-g/Tkm (data is taken from [50]*)*

Transportation Mode	CO_2	NO_x	SO_2	$PM_{2.5}$
Marine	10	0.14	0.02	0.04
Truck	133	1.1	0.9	0.12

In addition, installation of solar panels as well as the balance of systems (inverters and supporting structures and foundations), were found to be quite energy-intensive [51]. The embodied energy has been considered in this analysis to include the effects of solar PVs installation as well as the operation and maintenance effects.

2.2.4 Uncertainty Analysis

Evaluation of externalities involves large uncertainties in addition to the type of simplified models assumed. Two major sources of uncertainties associated with estimating the IES external costs are:

(i) Uncertainties in emission rates for different types of pollutants: these depend mainly on the technology type, age and efficiency of energy systems and power plants, and implemented emission control devices. Since statistical data on emission rates are not available for all systems, we shall instead estimate total emission rates corresponding to purchased electricity from each individual power plant. As mentioned earlier, such data is provided by NREL for different regions across the U.S. in terms of average, minimum, maximum, and standard deviation of emission rates for CO_2, NO_x, and SO_2 on an hourly basis.

(ii) Uncertainties in damages resulting from the pollutants: results of the external costs analysis depend largely on the pollution concentration model used to link emissions to ambient air quality, selected concentration-response functions, and the VSL (value of statistical life) used to monetize premature death [10].

The Monte Carlo approach was adopted in this study in order to estimate the uncertainties in external costs associated with purchased electricity. This involves the following steps:

(a) *Uncertainties corresponding to emission rates of different pollutants*: NREL data was used to generate 10,000 data points for each pollutant type using the known annual mean and standard deviation values. The emission rate distributions (mean values shown in Figure 2-3) were found to be close to normal since the reported minimum and maximum values were symmetrical around the mean, and the minimum and maximum values are very close to ($mean \pm 3\sigma$).

(b) *Uncertainties of external costs per pollutant type*: data on criteria-air-pollutant damages reported by NRC (Table 2-1) was used to generate these distributions. Based on the damage percentiles, we fitted a log-normal distribution for NG-fired power plants and a normal distribution for coal-fired power plants (except for $PM_{2.5}$ for which log-normal distribution was found to be a better fit).

(c) *Generation of distributions pertinent to damage values*: in total, 10,000 data points for each pollutant type were generated. Normal distribution (assumed for coal-fired power plants) were used to generate 46% of the data points and the rest were generated using the log-normal distribution (assumed for NG-fired power plants) in order to be consistent with number of power plants of each type investigated by NRC (see part c in section *2.3.1* of this paper).

(d) *Total external costs of 1 kWh of purchased electricity*: These were calculated for all 10,000 data points using Eq. 2-2.

The same procedure was performed for the four selected months in order to investigate the seasonal changes in the mean and uncertainty bounds of the purchased electricity external costs. Results of this analysis are assembled in Table 2-4 in terms of percentiles, mean, and standard deviation of the external costs. We note that (*i*) the mean values are all close to 3 ¢/kWh and seasonal variations are not significant; and (*ii*) the distributions are right-skewed with the 5th and 95th percentiles around 1.1 ¢/kWh and 6.8 ¢/kWh respectively. Since the distributions are not normal, standard deviation is not a proper measure to characterize the distributions and thus, percentiles are shown in Table 2-4 which are more meaningful.

Table 2-4- Distribution of damages from generation and distribution of electricity in AZNM eGRID sub-region (¢/kWh) generated through Monte Carlo analysis

	Mean	Standard Deviation	5th Percentile	25th Percentile	50th Percentile	75th Percentile	95th Percentile
Annual	3.00	3.67	1.06	1.70	2.29	3.06	7.02
January	3.08	3.74	1.12	1.78	2.38	3.16	6.82
April	3.08	3.53	1.09	1.78	2.38	3.20	7.17
July	2.88	3.16	1.07	1.70	2.25	2.99	6.55
Oct	3.03	4.02	1.04	1.71	2.30	3.11	6.76

Note that we have not considered the possible changes to the utility energy portfolio mixes across the U.S. and limited our assessment to the current situation.

2.3 Case Study

2.3.1 Energy System Description

The methodology described above has been applied to IES of a university campus, located in Arizona, U.S., with more than 280 buildings. The entire energy system is extensively instrumented by an Energy Information System which collects and stores end-use data from various systems at 15-minute time intervals. Currently, the overall energy demand of the campus is met through a variety of sources ranging from electricity purchases from a local power company to solar PV systems installed on several campus buildings and parking lots (15.5 MW total) and also from a 9 MW CHP plant. The cooling plant comprises of 10 centrifugal chillers each of capacity 2,000 Tons (one refrigeration Ton is 3.517 kW or 12,000 Btu/h), and 6 chilled water TES (Thermal Energy Storage) tanks each having a capacity of one million gallons of water. Solar panels are mostly polycrystalline and are either stationary or one-axis trackers. They are assumed to have an average of 1.7 m^2 each across all PV systems installed. The lifetime of solar panels is assumed to be 25 years in order to estimate the annualized environmental and health impacts. Whole year of hourly monitored data on electricity and natural gas consumption was used in this analysis.

2.3.2 Location-specific Damages

It was assumed that the population density is the most important factor in assessing the external costs of different pollutants. In order to customize the damages from various pollutants, population density around each power plant owned by the local electrical utility provider had to be identified. Therefore, we have associated different percentiles of the external costs, obtained from the Monte Carlo analysis, to different tiers of population densities (see Table 2-5). More specifically, the 5^{th} percentile corresponds to remote, sparsely populated areas while the 95^{th} percentile to dense urban locations. Subsequently, we have identified the location of (and thereby the population density around) each power plant using the Census Bureau 2010 summary map [52], and then associated each power plant to the corresponding damage percentiles. Next, location-specific average of the damages corresponding to each pollutant criteria (rightmost column in Table 2-5) were estimated by calculating the capacity-weighted average (weighted based on each power plant capacity) of damages for each pollutant type.

Since locations of the utility power plants range from remote areas (with population density < 50 people/sq.mile) to densely populated cities (with population density > 5000 people/sq.mile), upper and lower limits for the purchased electricity external costs were assumed to be equal to those estimated through the uncertainty analysis. The external cost value was assumed to be \$30/Ton for CO_2 emissions representing a global value, rather than a location-specific one, recognizing that such damages are considered to occur globally.

Table 2-5- Pollutant damage costs (\$/Ton) obtained from our Monte Carlo analysis. The percentiles are somewhat arbitrarily assigned to specific population densities as shown

		Population Density (population per sq. mile)					Location-Specific Mean Values
		< 50	50 .. 500	500 .. 2500	2500 .. 5000	>5000	
Pollutant	Mean	5th Percentile	25th Percentile	50th Percentile	75th Percentile	95th Percentile	
SO_2	9,427	732	3,127	5,698	8,617	30,140	3,048
NO_x	1,902	392	1,017	1,616	2,330	4,458	818
$PM_{2.5}$	9,522	2,005	4,319	7,194	11,815	24,976	3,984

The utility company power plants are mostly located in remote areas while only one gas-fired power plant, which contributes to 5% of the total capacity, is located in an urban area. Therefore, as can be seen in Table 2-5, the location-specific mean values are lower than those obtained from the distribution of damages across the U.S.

2.4 Results and Discussions

(a) *Purchased electricity*: External costs associated with generation and distribution of electricity were calculated for the whole year in hourly time steps consistent with how the campus energy information system stores the monitored data. Results are depicted in Figure 2-4 for the four selected months showing mean, 5^{th}, and 95^{th} percentile values. The mean of estimated damage cost is found to be about 2 ¢/kWh for purchased electricity with the diurnal and seasonal variations being relatively minor. Uncertainty bands are relatively large compared to diurnal and seasonal changes. The values obtained in this study are consistent with values found in the literature (NRC values ranges from 0.16 to 3.2 ¢/kWh). Maximum values can reach a high of 7.2 ¢/kWh which is obtained from the Monte Carlo analysis. The campus has purchased 116,841 MWh electricity from the grid during the investigated year which result in external costs of purchased electricity, ExC_{PE}, ranging from $1,235,000 to $8,198,750 (calculated based on the annual 5th and 95th percentile of the purchased electricity external costs) with a mean of $2,250,000 over the course of one year.

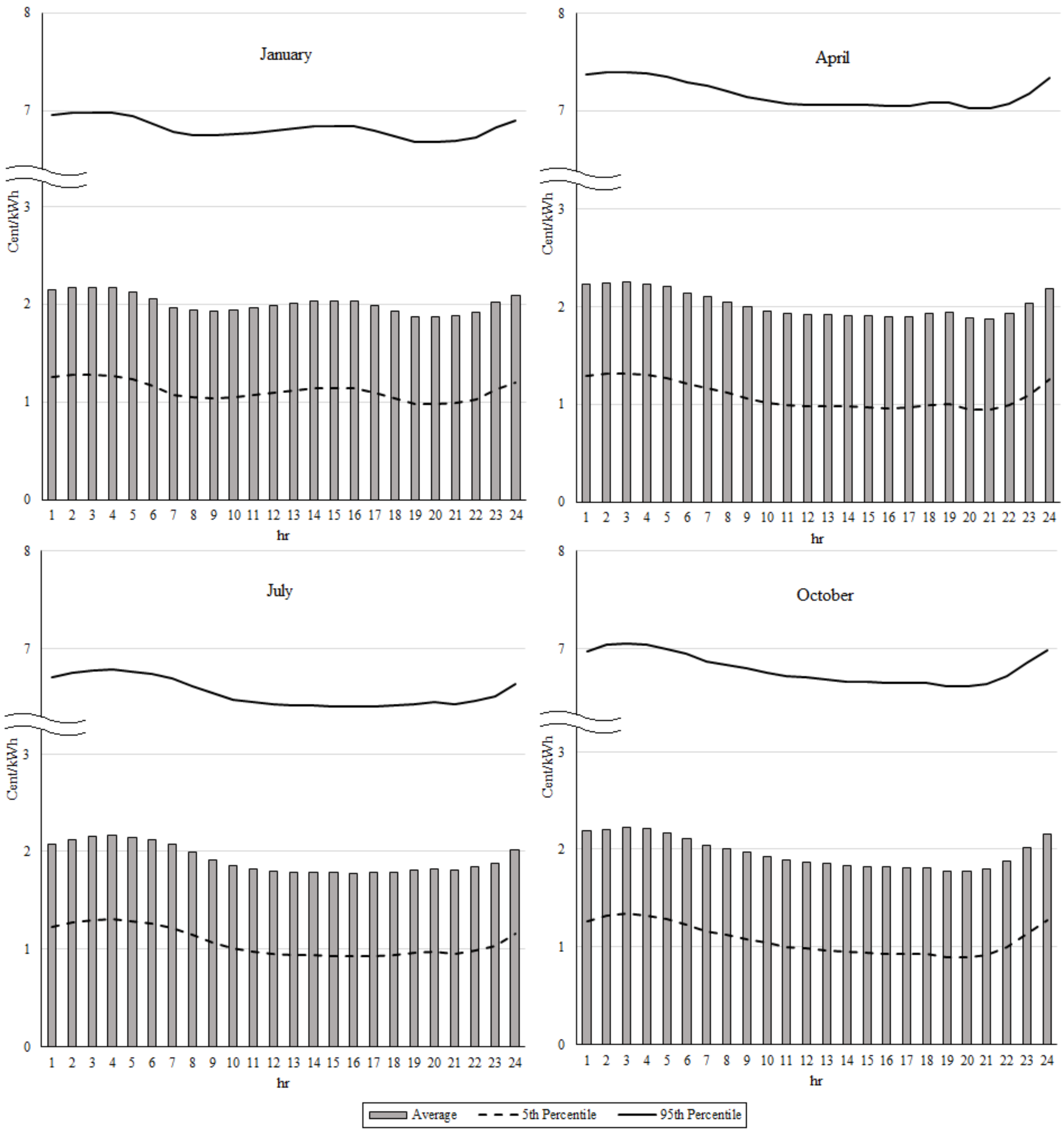

Figure 2-4- Hourly variation of purchased electricity external costs for the case study campus

Figure 2-5 illustrates the month-by-month contribution of each pollutant to the average external costs of purchased electricity. We note that damages corresponding to CO_2 emissions have the largest share in externalities of power generation and distribution (about 83.3%) followed by SO_2 emissions (average of 10.3% of total externalities). NO_x and $PM_{2.5}$ related damages account for 6.4% of the total damages whereby NO_x-related damages are twice than those from the $PM_{2.5}$ emissions. Note also that the month-by-month variation of the external costs of the individual pollutants is relatively minor (about ±5%).

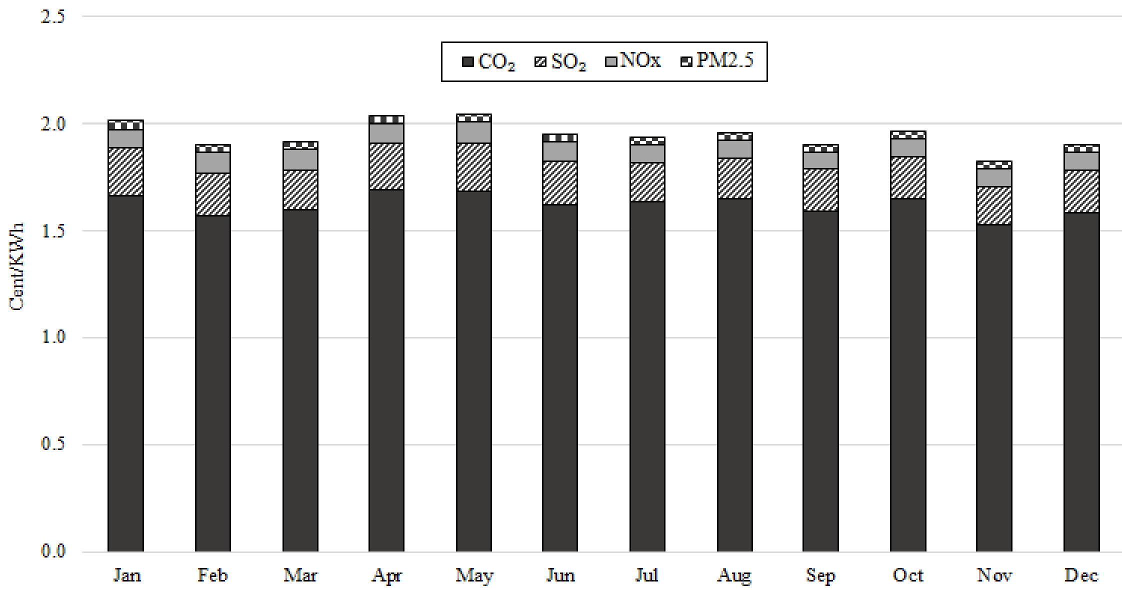

Figure 2-5- Breakdown of monthly averaged external costs of purchased electricity by pollutant type

(b) *NG-fired equipment*: External costs associated with boilers and the CHP plant were estimated separately for the upstream (pre-combustion) and after combustion using the emission factors given in Table 2-2 and the heat content of NG for Arizona (38.2 MJ/m^3). From the mean external costs of the CHP plant over one year of operation, it is noted that the upstream (pre-combustion) impacts are more severe, around \$3.4 million, compared to burning NG in the engine which causes \$1.25 million in terms of externalities (see Figure 2-6). It was also found that SO_2 emissions during processing NG (specifically the sweetening step) is the most impactful stage, and can be considered to be a critical process.

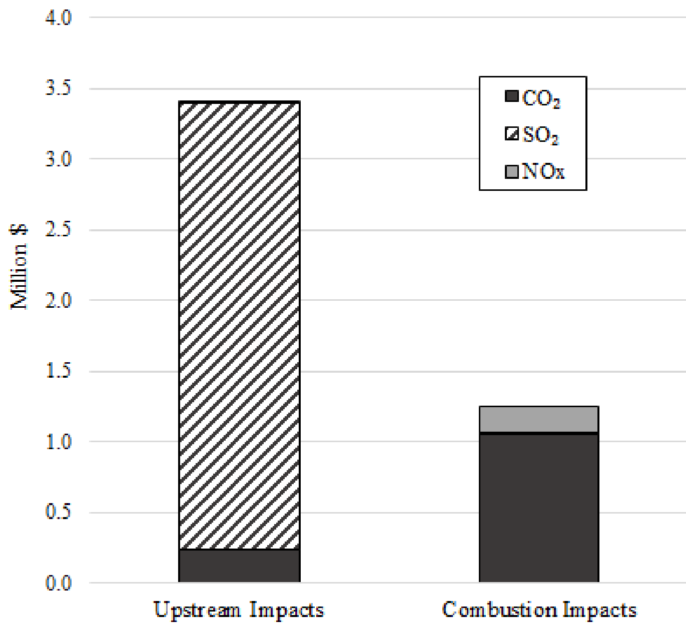

Figure 2-6- Mean annual external costs of the CHP system operation

The CHP system generated 45,908 MWh electricity and 288,725 GJ recovered heat over the year. Total external costs of the CHP plant were estimated to be $4.66 million with a minimum (5th percentile) of $0.73 million and a maximum (95th percentile) of $12.26 million. Figure 2-7 depicts the total external costs caused by each pollutant type pertinent to the CHP system along with the uncertainty bands showing the variability of the damage values associated with each pollutant. External costs of the $SO_{2\text{-eq}}$ emissions has the largest share among different pollutant types (due to the NG sweetening step) followed by damaged from $CO_{2\text{-eq}}$ emissions due to Methane leakage during the upstream processes as well as from the fuel combustion.

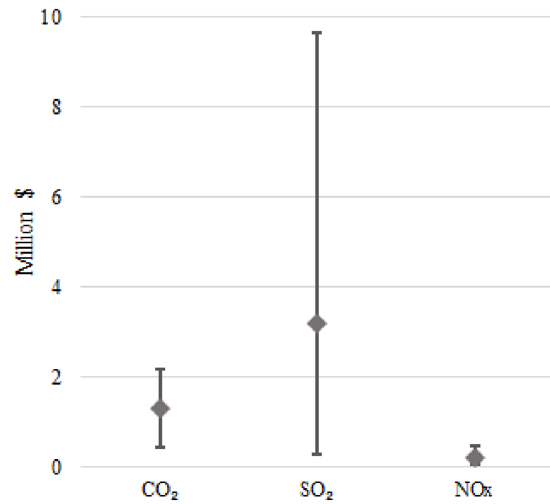

Figure 2-7- Annual external costs of the CHP system during the operation by pollutant type with 5^{th} and 95^{th} percentile bands

From Figure 2-8, the external costs of the on-site boilers serving the community, which generate 118,615 GJ of heating over the year, is found to be around $0.8 million. Therefore, the normalized external cost of the heating loads is 6.74 $/GJ. Again, pre-combustions effects are considerable and dominated by SO_2 impacts while external costs of fuel combustion are mainly due to CO_2 emissions.

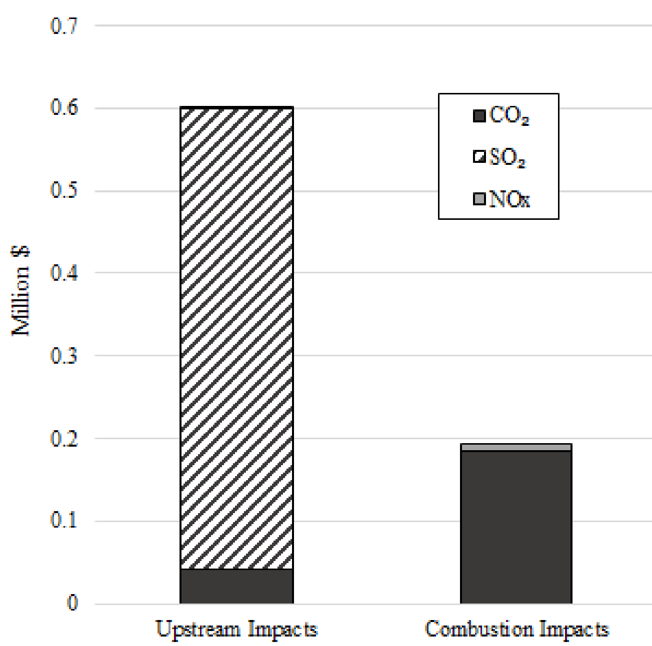

Figure 2-8- Mean annual external costs of operating boilers

Figure 2-9 depicts the total external costs caused by each pollutant criteria pertinent to boilers along with the uncertainty bands. It can be seen that the NO_x-related external costs are almost negligible compared to CO_2 and SO_2 related damages.

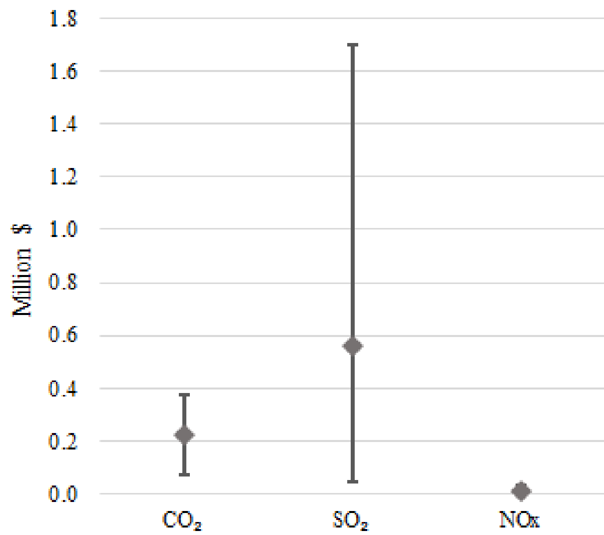

Figure 2-9- Annual external costs of boilers during their operation by pollutant type with 5th and 95th percentile bands

The CHP system also provides heating energy besides the electrical power, and thereby less fuel will be consumed by the boilers. In order to account for this avoided external costs, we estimated the extra external costs associated with the boilers if recovered heat from the CHP system was not available. We found that by utilizing the recovered heat from the CHP systems we can avoid about $1.15 million in external costs which would otherwise occur from burning NG in boilers.

(c) *Solar PV Systems*: As discussed earlier, pollutant emissions attributable to solar PV systems mostly occur during panels manufacturing, transportation and installation. The campus has installed 15.5 MW solar panels in 54 sites in the form of roof-mount panels and parking shades. Total external cost from solar PVs manufacturing was estimated using ecoinvent inventory database [50] which was found to be $45,200 per year assuming the system lifetime to be 25 years. Figure 2-10 shows the breakdown of total annual external costs of solar PV panels manufacturing by pollutant type. It is observed that CO_2 and SO_2 emissions have the largest contributions to the external costs of solar PVs manufacturing.

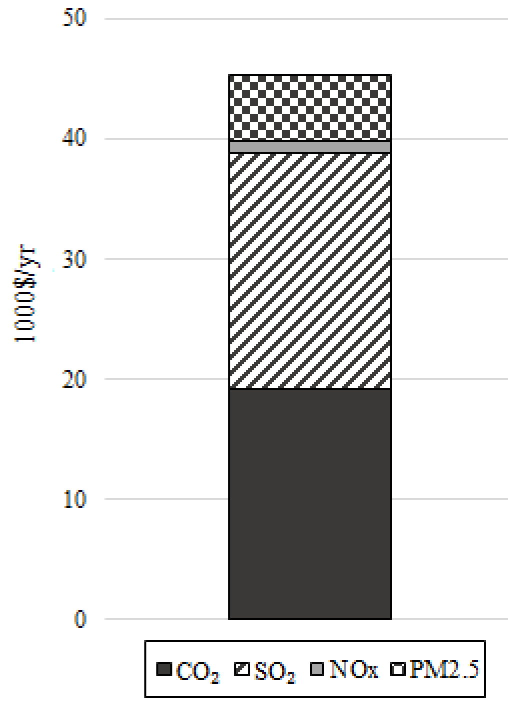

Figure 2-10- Total damages from PV systems manufacturing per year

In order to evaluate the transportation effects of solar panels, we have identified location of manufacturing facilities for each of the 54 sites. We estimated that 13 kW solar panels have been shipped from Philippines, 7.03 MW from China (both assumed to be marine transport), 1.15 MW from Canada via truck, and the rest is assumed to be manufactured in the U.S. and shipped from close distances and therefore excluded from the analysis. Since transportation-related emissions happen once during the system lifetime, we have averaged the results over 25 years of the systems life span. Emission results can be found in Table 2-6.

Table 2-6- Solar panels transportation emissions and input data

Input Data					Transportation Emissions (Ton/yr)			
Shipped from	kW	Weight (Ton)	Transportation mode	Distance (km)	CO_2	NO_x	SO_2	$PM_{2.5}$
Philippine	13	11.83	marine	12,000	5.69E-02	7.96E-04	1.14E-04	2.28E-04
China	7034	6401	marine	10,500	2.71E+01	3.79E-01	5.41E-02	1.08E-01
Canada	1152	1048	truck	3,500	1.86E+01	1.63E-01	1.34E-01	1.78E-02

Then, external costs associated with these emissions have been estimated using the 5th percentile damage per ton of pollutant criteria (except for CO_2 for which the impacts are somewhat global) reported by NRC [10] assuming that pollutants are emitted in remote areas. It was found that CO_2 has the largest contribution in the external costs of both truck and marine transportation. Figure 2-11 depicts the normalized and annualized external costs of solar panels transportation. The total external costs of solar PVs transportation were found to be $2,300 per year which is around 5% of the manufacturing externalities.

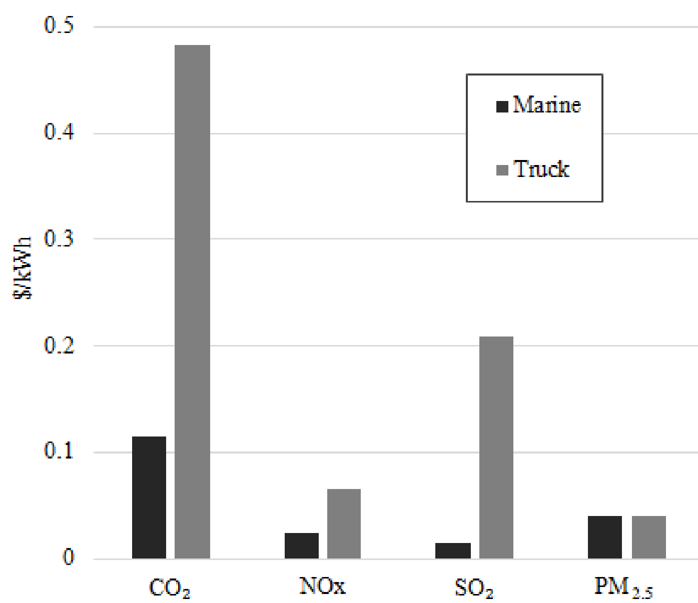

Figure 2-11- Normalized external costs of solar panels shipment through marine and truck transportation

In addition to solar panels manufacturing and transportation, externalities associated with structural supports and required foundation, as well as the inverter and system operation and maintenance, altogether referred as balance of system, should be included in the analysis. In order to evaluate such impacts, the embodied energy for the balance of system was estimated for each of the 54 solar systems across the campus. The embodied energy of the required foundation was included only for solar panels installed on parking structures. Total external cost of the balance of system was found to be $39,200 per year. Figure 2-12 shows the breakdown of the balance of system external cost.

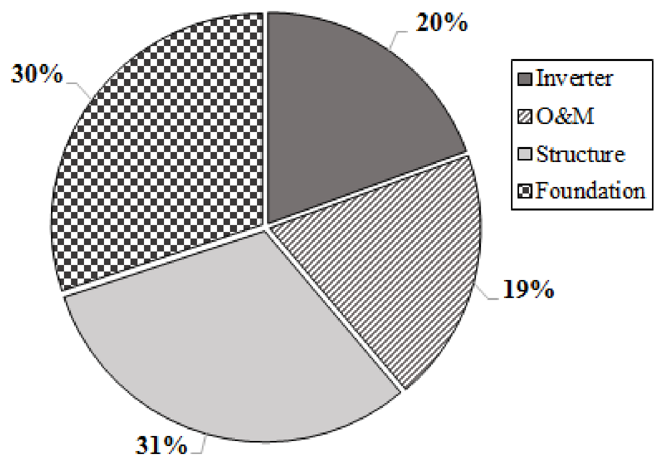

Figure 2-12- Breakdown of Solar PVs' external costs associated with balance of system (total external cost is $39,200 per year)

Therefore, results suggest that impacts associated with balance of system are in the same order as solar PVs manufacturing effects while external costs due to PV transportation are around 5% of the manufacturing related externalities.

2.5 Summary

Table 2-7 provides a summary of different life stages included in this analysis pertinent to each energy system component along with the type of the pollutants considered in the analysis. Manufacturing of the heating and cooling equipment was not included since the associated emissions were deemed negligible compared to those generated during the operational stages. Cooling systems are either electric-driven or heat-driven (absorption chillers) which are explicitly considered in other system components.

Table 2-7- Summary of the LCA analysis specifying stages and pollutants considered

System Component		Life Stages Analyzed: Construction/ Manufacturing	Transp./ Transm./ Installation	Operation/ Maintenance	Pollutants Considered: CO_2	SO_2	NO_x	$PM_{2.5}$
Purchased Electricity	Local Energy Mix	Power Plants Construction	Transmission and Distribution Losses	Operation	✓	✓	✓	✓
On-site Generated Electricity	PV	Panel Manufacturing	Transportation and Installation	Maintenance	✓	✓	✓	✓
	CHP	-	Transportation and processing of NG	Operation	✓	✓	✓	-
Heating Systems	Boilers	-	Transportation and processing of NG	Operation	✓	✓	✓	-
Cooling Systems	Chillers	-	-	Operation	✓	✓	✓	✓

In order to compare the external costs associated with various electricity generation resources, aggregated monetary damages from available sources have been calculated and normalized against total electrical energy production throughout the year (Table 2-8). Location of the pollutant sources were considered resulting in more realistic evaluation of the damages. In this regard, the location-specific mean damage values, listed in Table 2-5, were used for the purchased electricity. Regarding the CHP system, since the plant is located on campus with a high population density, maximum damage values (the 95th percentile value) were assumed for SO_2 and NO_x emissions through the CHP operation while minimum (5th percentile) damage values were considered for upstream effects (NG extraction and processing is carried out in remote areas), and average values were used for both upstream and on-site CO_2 emissions as the associated damages happen mostly at global scale. Under such assumptions, total damage values associated with the CHP system during one year of operation would be around $2 million. Results of the analysis suggest that although power generation using CHP systems might be economically beneficial (where natural gas price is low), the environmental and health effects would be more pronounced due to the location of the emitting source. If the exhaust heat from the CHP system can be recovered and used effectively, boilers loading and thereby the external costs associated with them can be reduced. The CHP external costs without and with taking the effect of thermal heat recovery into consideration are 4.36 ¢/kWh and 1.86 ¢/kWh respectively (Recall that the purchased electricity external costs are almost 2 ¢/kWh). Therefore, CHP system would be economically and environmentally beneficial if the generated heat can be used to offset boilers fuel consumption.

Solar panels external costs during manufacturing, transportation and installation of the system have been evaluated as well. Solar PVs can provide much cleaner electricity, compared to utility and on-site CHP systems, for which the external costs are around only 0.5 ¢/kWh. This information is especially useful to developers, decision and policy makers, and energy systems operators who are interested in minimizing the environmental and health effects of energy systems.

Table 2-8- Electricity generation and associated external costs from various sources

	Total Generation kWh/yr	Total External Cost- $/yr	Normalized External Cost- ¢/kWh
Purchased electricity	116,841,250	2,250,200	1.93
On-site solar-generated electricity	17,561,540	88,430	0.50
On-Site CHP-generated electricity (considering only generated electrical power)	45,907,610	2,000,860	4.36
On-Site CHP-generated electricity (considering generated electricity and heating)	45,907,610	853,554	1.86

* with the 5^{th} and 95^{th} percentiles about ¢1/kWh and ¢7/kWh respectively.

Figure 2-13 provides a summary of the external costs associated with generation and distribution of electricity from various sources and systems. For the studied campus, 65% of the total electricity needs were purchased from the grid which accounts for 70% of the total external costs associated with electricity needs of the campus. Of the latter, CO_2 emissions contribute 83% followed by SO_2 emissions which has a 10% share. The onsite CHP system supplies 25% of the total electricity consumptions of the campus while accounting for 27% of total damages; SO_2 emissions has the biggest share (68%) in the externalities from the CHP system; CO_2 emissions accounts for 28% and NO_x contributes to only 4%. The on-site solar PV systems were able to supply 10% of the campus electricity needs while being responsible for only 3% of total damage costs.

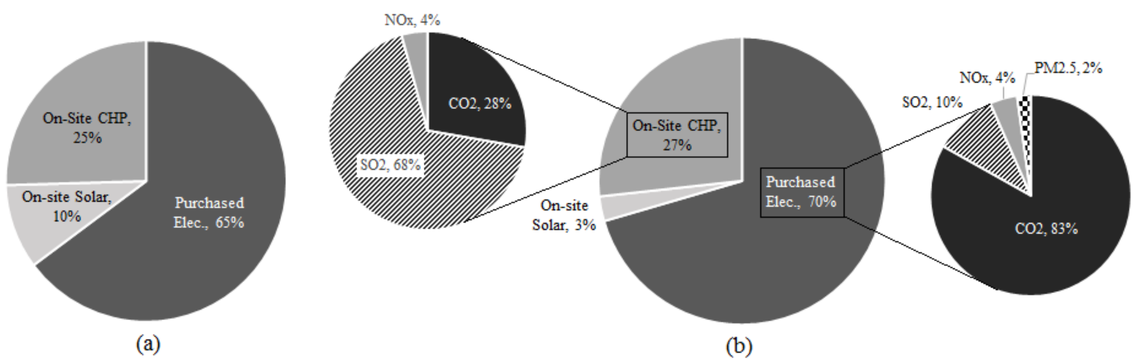

Figure 2-13- (a) Percentage of electricity supplied from and (b) Contribution of different sources/systems in total external costs along with share of each pollutant type

Assumptions and limitations of this LCA framework includes:

- The uncertainties associated with the damages from the pollutants are assumed to be derived mainly from the population density around each pollution source.
- External costs of $CO_{2\text{-eq}}$ emissions are assumed to be \$30/Ton with the high of \$50/Ton and low of \$10/Ton.
- Regarding the case study CHP system impacts, 95th percentile damage values were assumed for emissions occurring on-site, 5th percentile damages were assumed for upstream fuel processing and transport, and average values are assumed for all $CO_{2\text{-eq}}$ emissions.

2.6 Conclusions and Future Work

This paper proposes a pragmatic LCA methodology to quantitatively evaluate monetary costs of human health and environmental impacts of a specific community scale Integrated Energy Systems (IES) which capture the effect of real-time emissions from various energy systems including, utility power plants, distributed generation facilities, and building heating and cooling systems. The uncertainties associated with the results have been analyzed using the Monte Carlo techniques. The approach described in this paper can be integrated into design, operation, and development planning practices toward more sustainable engineered systems and infrastructure.

Some of the capabilities of the proposed methodology were illustrated through a case study on a large university campus with more than 280 buildings. The external costs of electricity generation using on-site CHP system were found to be about 4.4 ¢/kWh (neglecting the recovered heat) which is considerably higher than both on-site solar systems (0.5 ¢/kWh) and utility-generated electricity (2 ¢/kWh). It was found that the amount of recovered heat plays a crucial role in external costs of a CHP system. In other words, the waste heat from the exhaust flue gas and from the motor jacket can be used to offset boilers fuel consumption by reducing their loading. The campus CHP system has an overall efficiency of 71% which results in the external costs to be 1.86 ¢/kWh. Therefore, we can conclude that expanding the size of the CHP plant along with thermal heat recovery to offset the use of boilers would be a more sustainable option.

We also evaluated the variation in external costs of utility-generated electricity at the hourly level under seasonal changes in the fuel mix. One of the key findings of this analysis is that such variations are in the range of ±5% in seasonal and about ±8% in hourly changes. These diurnal and seasonal variations are much lower than the uncertainties associated with the externalities of purchased electricity. The average of the purchased electricity external costs was estimated to be around 2 ¢/kWh and the distribution was found to be highly skewed, with 5% and 95% being about 1 ¢/kWh to more than 7 ¢/kWh respectively.

Valuation of environmental and health impacts is an inherent and intrinsic part of any sustainability assessment study. Logical extensions of the proposed methodology should involve inclusion of water systems, transportation, and building materials. The proposed methodology could also be extended to the broader issue of sustainability assessment of community scale integrated energy systems as well as of other types of engineered systems and infrastructures in support of decision-analysis toward sustainable developments.

Chapter 3 – Sustainability of Integrated Energy Systems: A Performance-Based Resilience Assessment Methodology

Abstract

One of the key elements of any community or facility is the integrated energy system (IES) which consists of utility power plants, distributed generation systems, and building heating and cooling systems. Assessing the sustainability of an IES would be of great value to decision-making relevant to design, future growth planning, and operation of such systems. This paper addresses one of the basic issues in this regard, i.e. resilience assessment and quantification of IES. A new performance-based method for characterizing and assessing resilience of multi-functional demand-side engineered systems is proposed in this study. Through modeling of system response to potential internal and external failures (called failure modes) during different operational temporal periods (such as different diurnal and seasonal periods of the year), the proposed methodology quantifies resilience of the system based upon loss in the services which the system is designed to deliver. A three-dimensional matrix, called *Loss Matrix*, is introduced whose elements represent the undelivered system services under different scenarios, i.e. combinations of failure modes and different operational temporal periods. Assigning monetary penalty costs to such losses and including them in the objective function of an optimization model of the entire system allows the three-dimension loss matrix to be reframed into a two-dimensional *Consequence Matrix* where individual elements represent the imposed penalty costs to the system stakeholders due to undelivered services and/or non-optimal system performance. Normalizing the individual elements results in the *Resilience Matrix* of the system for different scenarios. The

developed methodology is illustrated for IES of a large office building meant to satisfy critical and noncritical electrical, heating, and cooling loads. The resilience assessment framework proposed in this paper would serve as a mean to identify critical components of a particular IES, thereby facilitating resilient design and operation, and also to evaluate different cost-effective resilience enhancement strategies.

Nomenclature

DP	Disruption Period
f	functionality
FL	Functionality Loss
IC	Imposed Costs
IP	Interruption Period
OC	Operational Costs
PC	Penalty Costs
Re	Resilience
t	time
T	time period
x	flow (electricity, fuel, heat, etc.)

3.1 Introduction

Increased complexity of urban infrastructure systems on one hand, and more severe and increasingly frequent natural disasters due to global climate change on the other hand, require analysis methods which can improve their preparedness, resistance, and rapid recovery against disruptions. The energy infrastructure, consisting of power generation and distribution, transporting pipelines, and transportation systems (marine, railroad, truck lines, etc.), is critical for sustainable development under normal conditions, and in confronting natural and other types of extreme events and disasters. The world energy crisis has been more pronounced in developing countries, particularly in rural areas, where people experience massive power outages in forms of planned, unplanned, unanticipated faults and burnouts. Absence of power has drastic detrimental impacts on the economy, on education, on healthcare and, more generally, on sustainable development itself. Making infrastructure systems more resilient is thus an area of research which has gained considerable momentum in recent years.

The concept of resilience was first introduced in the 19th century in physics and material science as the ability of an object to resist loads without permanent distortion [53]. This concept has then been adopted in a variety of contexts such as, medicine, psychology, as well as in engineering. Such terms as ecological resilience, psychological resilience, disaster resilience, seismic resilience, family resilience, etc. have been introduced. The scope of this paper is, however, limited to resilience of engineered systems only.

Numerous studies have been conducted trying to characterize and assess resilience of different types of systems and proposed new definition for resilience. In general, resilience assessment methods can be categorized in three groups: (i) structural assessment methods (ii) performance-based methods, and (iii) hybrid methods being a combination of the first two ones. Structural assessment methods focus on the structure and general characteristics of the system and generally tend to be qualitative or semi-quantitative, in that, systems are scored using results of numerous questions categorized based on pre-identified resilience indices or metrics (e.g. vulnerability, capability, resourcefulness, etc.) [54]. On the other hand, performance-based assessment methods evaluate system resilience based upon the functionality of the system. Through a particular interruption scenario, this method measures, or simulates, the system performance during and after the disruption. The performance-based methods specifically consider the speed with which the system can return to the post-interruption condition, known as *rapidity* [55], as one of the basic aspects of resilience. The two general resilience evaluation methods, i.e. the structural and the performance-based methods, are complementary; while the structural assessment can explain *whether* a system is likely to be resilient, the performance-based approaches specify *how much* the system is resilient.

Numerous qualitative and quantitative studies have been conducted to define and evaluate resilience of engineered systems. These studies are different in objective and scope based on type of the assessment (quantitative, qualitative, or semi-qualitative), type of the system, and type of the disruptive event. For example, Hatvani-Kovacsa et al. integrated planning and design of infrastructures and buildings in addition to public health and social research to qualitatively assess the heat stress resilience [56]; Bozza et al. proposed a framework to quantitatively assess the disaster resilience of urban systems by introducing *efficiency* and *quality of life* as indicators to be identified before and after an extreme event and also during the recovery time [53]; Zobel and Khansa proposed a new resilience measure for multiple related disastrous events adopting the concept of resilience triangle which characterizes system resilience based on the functionality loss and duration of the recovery time [57]; Chang et al. have developed a practical approach to evaluate infrastructure resilience at a community scale based on historical experiences and judgments of technical specialists to identify which critical services could be lost, to what extent, and for how long; they have also investigated the ripple effect, i.e. how disruption in one infrastructure sector can have impacts on downstream sectors [58]; Maliszewski and Perrings have investigated resilience of the power distribution systems suggesting that resilience of such systems depend on power distribution infrastructure and its biophysical environment, and also on the priority given to restoration by the power company [59]; Cimellaro et al. proposed a framework for quantitatively evaluating resilience of health care facilities subjected to earthquakes by using an analytical function that fits both technical and organizational issues [60]; Attoh-Okine et al. formulated a resilience index for urban infrastructure using Belief function accounting for interdependencies among systems [61]; Cutter et al. developed a framework to assess disaster resilience at local or community scale focusing on social resilience [62]. Ouyang et al. (2012) developed a multi-stage framework to assess and analyze infrastructure resilience. They defined resilience as the joint ability of a system/infrastructure to resist (prevent and withstand) any possible disruption or shock, absorb the initial damages, and recover to normal operation [63].

Resilience assessment frameworks are useful both during the design phase and during system retrofitting. Ouyang and Fang (2017), improved on their earlier work, and developed a tri-level decision-making model which supports critical infrastructure resilience optimization in order to find the best defensive strategies by identifying vulnerable system components and protecting them against intentional [64] and spatially localized [65] attacks. They introduced the resilience metric based on the performance of the interdependent infrastructures under natural hazards (such as hurricanes [66]) and random failures relative to target performance of the system [67]. Lin and Bie proposed a new Defender-Attacker-Defender (DAD) model to identify hardening and operational restoration measures as two main resilience aspects of power systems [68]; they found that hardening strategies are strongly influenced by topology reconfiguration and the distributed generation installation. Alderson et al. developed a resilience assessment model which quantifies operational resilience of an infrastructure system and can help developers and policy makers identify critical vulnerabilities in the system [69]. Matelli and Goebel developed a conceptual framework for resilient design of a cogeneration system through stochastic failure propagation simulation [70].

Researchers from Sandia National Laboratory (for example, Vugrin et al. [71]; Vugrin et al. [72]) have developed complex resilience assessment models to quantify operational resilience of an infrastructure system and help developers and policy makers identify critical vulnerabilities in the system. They have developed detailed methodologies and operating software ranging from an individual infrastructure to a whole region with multiple infrastructures based on both network models as well as multiagent modeling approaches. The methodology requires extensive involvement of local experts in all relevant areas such as engineering, social and governance which is needed in both gathering necessary data as well as developing the interactions between infrastructures. A book by Biringer et al. [73] describes this general approach called IRAM (Infrastructure Resilience Assessment Methodology). It is an extension of RAMCAP originally developed for hostile threats on infrastructure systems. IRAM takes into account the following considerations (which traditional methods tend to overlook): (i) Provides precise and actionable definition of resilience, (ii) Explicitly considers costs and resource requirements of adaptation and recovery, (iii) Proposes definitions and resulting measurement methods which are generally valid to all 18 infrastructure systems, (iv) Proposes a performance-based assessment that is flexible and uses different methods and models to generate performance metrics, (v) Minimizes subjective elements, (vi) Meant not only to assess resilience but also to design resilient systems.

While most of the previous studies are focused on quantifying and characterizing resilience of infrastructure systems at aggregated levels, the current study addresses how resilience of demand-side systems with multiple functions can be defined, characterized, and improved. A new quantitative performance-based resilience assessment framework is developed, and a resilience matrix is introduced which captures essential dimensions of resilience pertinent to engineered systems. The proposed methodology is illustrated for a typical integrated energy system (IES) and energy-related measures are assessed in terms of resilience improvements.

3.2 Methodology

This section describes the methodologies and mathematical approaches adopted in this study to quantitatively evaluate the resilience of demand-side engineered systems.

3.2.1 Definition of Resilience

Earlier published literature viewed resiliency of a system as its ability recover once it has been compromised due to a short-acting shock. However, the concept has evolved and has been expanded greatly, it now includes additional set of characteristics and capabilities. Such capabilities can be classified into three groups relative to the occurrence of the disruption: (1) “Pre-disruption” phase: involve capabilities to anticipate shocks and adapt in order to respond properly while minimizing initial damages; *adaptability* and *robustness* are some examples of pre-disruption capabilities. (2) “During-the-disruption” phase: involve ability to minimize functionality losses through capabilities such as *fail safe* meant to prevent failure propagation, or *resourcefulness* enabling implementation of alternative sources to maintain system functionality. (3) “Post-disruption” phase: involve the capacity to deal with the consequences of failure and with the *rapidity* i.e., how fast the interrupted system can be recovered. Numerous definitions have been proposed in the literature for resilience of systems to include these capabilities relative to the type of the interruption and to the type of the system itself.

When supply-side systems, such as power generation infrastructure are targeted, fast recovery, would be an important resilience characteristic; but, when demand-side systems are investigated, robustness, reliability, and adoptability should be given more importance. For an IES, which can be considered a demand-side system, system performance depends on the performance of up-stream systems, i.e. the supply side electric grid and fuel distribution system and if they fail, the system performance will be adversely affected. In this case, the recovery process is outside the control of the owner or user of the system. Internal failures (for example failure of a chiller), will also affect the system performance and can be addressed through *reliability* improvements aimed at lowering the probability of random failures (for example by performing regular maintenance), or through *redundancy* to prevent functionality losses (for example by having a stand-by chiller), and any other possible measure to help the system deliver its services/products when disrupted. In transmission and distribution networks, the ability of the system to prevent propagation of failures is the main focus of resilience studies rather than recovery features [74]. Therefore, a new definition for resilience of engineered systems is proposed which is focused on functionality of the system of interest, rather than on the system characteristics as:

"Resilience is the ability of the system to minimize the costs imposed to the stakeholders due to functionality losses, damages to assets and people, and recovery processes when interrupted by either external or internal disruptions"

This definition is holistic, in that it is not limited to the type of engineered system nor to a specific characteristic of the system, nor to a specific type of disruption. In other words, there are numerous resilience characteristics pertinent to engineered systems and no definition can contain them all. Instead, the suggested definition relates the system resilience to the level of system functionality losses since the primary goal is to maintain the system functionality at the desired level. On the other hand, quantification of resilience based on this definition, which is application and circumstance specific, will be more convenient and can be integrated into engineering practices (discussed below). The suggested definition can be adopted to different types of engineered systems, such as transportation or water distribution systems.

3.2.2 Quantification of Resilience

Resilience of a demand-side system such as community scale integrated energy systems (IES) can be characterized by its performance when stressed by internal or external *disruptions*. The term *Interruption*, then, refers to the system inability to deliver its functional service(s) during the disruption and afterwards. In this study, we have only considered the functionality losses and assumed that the damage costs and recovery costs are zero. Figure 3-1 schematically illustrates performance of a system when undergoing a disruption. Curve (1-3) represents the desired performance level identified by demand(s) provided by the system, while curve (1-2-3) shows the actual system performance due to the disruption. Let the time interval $t_0 \leq t \leq t_0 + T_{DP}$ be the time of the disruption occurrence which essentially depends on nature of the event and can range from momentary ones, such as electric grid voltage drop, to long-lasting ones, like hurricanes and floods. Curve (1-2) shows how the system response to the disruption during this time; functional services loss rate might be slower at the beginning due to robustness of the system components. Curve (2-3) illustrates how the system bounces back to its desired state after a partial failure; depending on the disruption and the system characteristics, complete failure may occur, as illustrated by curve (2´-3´), and all functional services might be lost. The time interval $t_0 \leq t \leq t_0 + T_{IP}$ represents the interruption period during which the system cannot perform at its desired level. Note that the interruption period can be the same as disruption period meaning that the system is able to perform at the desired level right after the disruption has passed. At any moment during the interruption period, difference between the desired performance level and the actual performance identifies system *functional service loss*, denoted by $f_{loss}(t)$. Therefore, the shaded area in Figure 3-1 represents total functional service losses due to the disruption:

$$FL = \int_{t_0}^{t_0+T_{IP}} [f_{desired}(t) - f_{actual}(t)].dt = \int_{t_0}^{t_0+T_{IP}} f_{loss}(t).dt \tag{3-1}$$

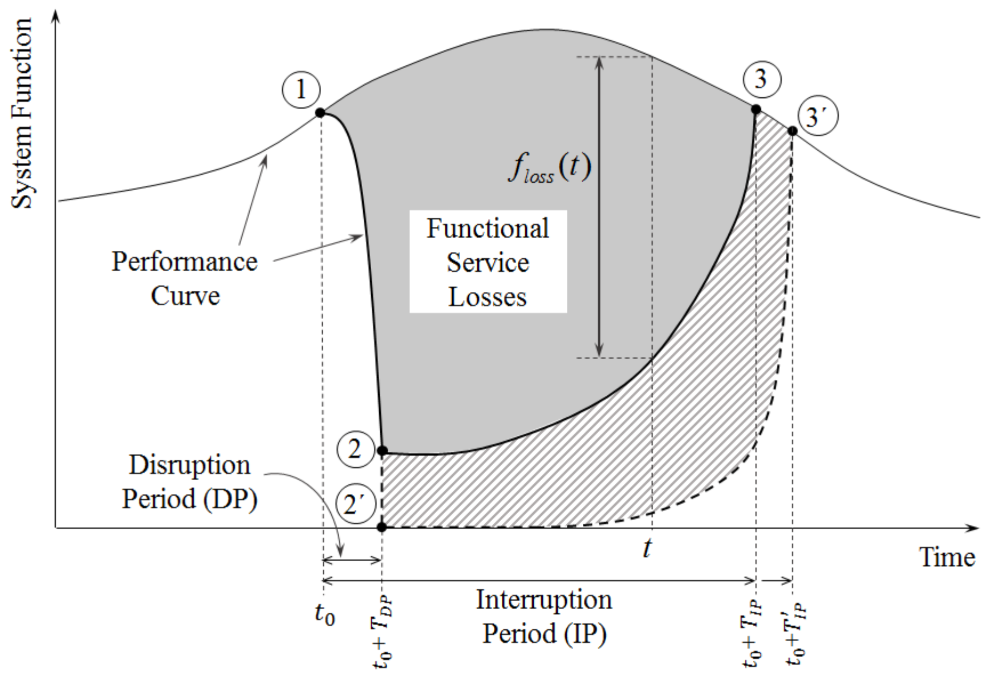

Figure 3-1- Schematic of functionality and performance curves of an interrupted system under partial (curve 1-2-3) and complete failure (1-2´-3´); interruption period is assumed to be longer in the case of complete failure

Ideally, a resilient system would meet its performance targets during the entire interruption period. Two attributes characterize this attribute: (a) preparedness before the disruption, and (b) agility in recovery after the disruption. However, we argue that not all kinds of interruptions require a recover period after the disruption is passed. For instance, if performance of a manufacturing unit is interrupted due to “lack of raw material” (disruption), it can start delivering its service as soon as the disruption is over. In this case, disruption and interruption periods are the same and there is no recovery process as such. Therefore, this analysis quantifies resilience of engineered system based upon the system performance during the interruption period, characterized by functional service losses, rather than solely based on specific attributes or metrics (as in most of the published literature).

A large number of disruptions can be identified for a particular system and it would be impossible to analyze the system resilience in terms of all such disruptions. Instead, for any system with given number of the system components, we can identify a finite number of failure modes. Regardless of cause of failures, i.e. the disruptions, analyzing effects of failures on system performance would be of great value. Therefore, **in this study we focus on effects of system components failures rather than the inherent cause of the failure**. Hence, a resilient system should be able to minimize losses in delivering its services, for any possible failure mode, and during all operational temporal periods. This can be represented as a three-dimensional matrix:

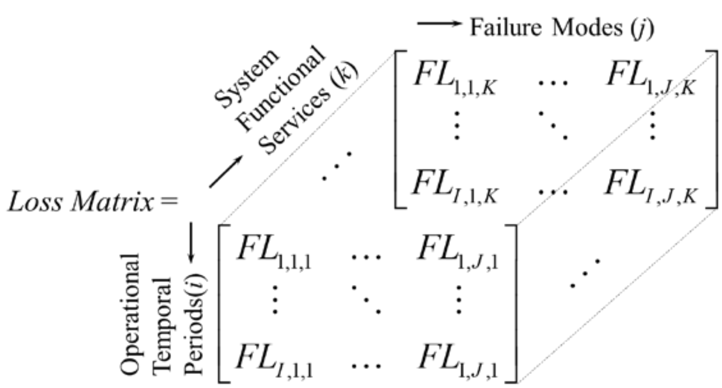

(3-2)

where arrays are service losses (each identified by Eq. 3-1 and shaded area in Figure 3-1), *j* represent various failure modes correspond to failure of system components, *k* identifies system functional services ($1 \leq k$), and *i* shows various operational temporal periods impacting the resilience of the system. Operational temporal periods may represent temporal variations in the system operation and are meant to reflect extreme cases such as maximum demands in various seasons of the year. Hereafter, combinations of failure modes and operational temporal periods are referred to as *scenarios*.

Analyzing and studying a three-dimensional matrix would be inconvenient, especially for large systems with numerous many components and failure modes. We, therefore, suggest assigning monetary penalty costs to functional service losses and thereby reducing the matrix order to two. To do so, at any given *i* and *j*, i.e. for a given scenario, we estimate total imposed costs due to functional service losses and non-optimal system operations as:

$$IC_{i,j}|f_j = \left[OC_{i,j} + \sum_{k=1}^{K}\left(FL_{i,j,k} \times PC_{i,k}\right)\right] - OC_{i\_desired} \tag{3-3}$$

where $IC_{i,j}|f_j$ denotes the imposed costs due to failure mode *j*, $OC_{i,j}$ is the operational costs during failure mode *j* and time period *i*, *K* is the total number of system functional services, and $PC_{i,k}$ represents the penalty costs associated with one unit of *k* functional service loss during time period *i*. Further, we have assumed that the penalty costs do not vary based on the failure modes, but may vary depending on the time period. For instance, penalty costs of unmet electrical loads (in $/unmet kWh) in a commercial unit are independent of why the system is unable to meet the loads (i.e. the failure mode) but may vary throughout the day depending on criticality of electrical loads during different hours of the day. $OC_{i\_desired}$ is the operational cost for uninterrupted system running optimally during time period *i*. More detailed discussions on identification of failure modes and calculation of imposed costs are provided below. Note that repair and replacement recovery costs of failed or damaged systems can be included in estimating the imposed costs in real-case applications. Also, more complex penalty cost functions can be used to estimate the imposed costs but linear penalty cost functions were used in this study.

Using Eq. 3-3, the three-dimensional *Loss Matrix* can be reduced to a two-dimensional matrix called "*Consequence Matrix*" which includes the imposed monetary costs associated with different scenarios:

$$Consequence\ Matrix = \begin{bmatrix} IC_{1,1} & \cdots & IC_{1,J} \\ \vdots & \ddots & \vdots \\ IC_{I,1} & \cdots & IC_{I,J} \end{bmatrix} \tag{3-4}$$

Therefore, resilience of the system can be characterized by the *Consequence Matrix* containing total monetary costs incurred to the system stakeholders (users, owners, etc.) under different scenarios. Such failures could range from random failure of the system components, to deliberate attacks, to personnel mistakes. In any case, one or multiple system components would fail whereby functionality of the system is compromised if the system is not fully resilient. Failing to deliver the functional services at the desired level may cause considerable damages to assets, products, or even to reputation of the provider. Such damages can be often expressed in monetary penalty costs. For instance, according to Hamachi LaCommare and Eto, economic costs associated with power interruption to the U.S electricity customers is estimated to be about $80 billion annually [75].

Imposed costs can be used to develop a quantitative resilience index. Since resilience is a positive attribute, higher numbers should reflect better performance while higher imposed costs ought to represent poorer resilience in dealing with disruptions. Therefore, in this analysis, the resilience index is defined pertinent to each scenario as:

$$Re_{i,j} = \frac{IC_i^{Max} - IC_{i,j}}{IC_i^{Max}} \quad (3\text{-}5)$$

where IC_i^{Max} is the maximum possible imposed costs in each scenario, i.e. if all functional services during operational temporal period *i* are lost. Figure 3-2 schematically illustrates the resilience index as $\left({}^{Shaded\ Area}/_{Hatched\ Area}\right)$. Therefore, resilience index ranges between 0 and 1, and corresponds to the worst and best level of resilience respectively. *Re* = 0 reflects the situation that system would not be able to deliver any of its functional services, and *Re* =1 indicates that functionality of the system would not be interrupted at all.

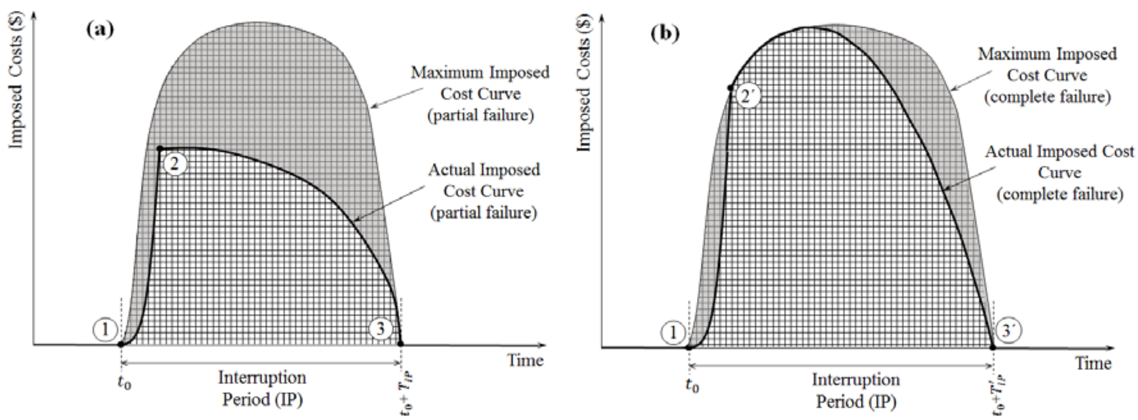

Figure 3-2- Schematic of the imposed costs curves of an interrupted system under (a) partial failure (curve 1-2-3) and (b) complete failure (1-2´-3´)

The *Resilience Matrix* which includes resilience indices for all identified scenarios can be represented as:

$$Resilience\ Matrix = \begin{bmatrix} \frac{IC_1^{Max} - IC_{1,1}}{IC_1^{Max}} & \cdots & \frac{IC_1^{Max} - IC_{1,J}}{IC_1^{Max}} \\ \vdots & \ddots & \vdots \\ \frac{IC_I^{Max} - IC_{I,1}}{IC_I^{Max}} & \cdots & \frac{IC_I^{Max} - IC_{I,J}}{IC_I^{Max}} \end{bmatrix} = \begin{bmatrix} Re_{1,1} & \cdots & Re_{1,J} \\ \vdots & \ddots & \vdots \\ Re_{I,1} & \cdots & Re_{I,J} \end{bmatrix} \quad (3\text{-}6)$$

Note that the proposed methodology is a performance-based approach. Expressing resilience of the system in monetary terms will enable planners and designers to perform cost-effectiveness analysis of various resilience enhancement options more conveniently.

3.2.2.1 Failure Modes

In this study, disruptions are defined based on failure of individual system components regardless of the causes and type of events which caused them. It should be noted that while cause of failures for various system components are not explicitly involved in the analysis, investigating causes of various components failures would be of great value in reducing failure risks. This will improve *predictive* and *adaptive* performance of the system in order to reduce the probability of failures, and thereby enhance resilience of the system. In addition, enhancing *robustness* of individual components against prevailing disruptions can improve resilience of the whole system.

Failure of any set of system components can be considered as a system failure mode. Total number of single-component failures disruption scenarios can be as large as number of system components. Since system complexity is often defined as number of components and their connections, the proposed framework also accounts for *complexity* of the system considered as an important factor affecting system resilience.

This study is more focused on single-component failures in order to identify the critical components of the system and the level of functionality losses. This should not be confused with "cascading failures" which are considered in this analysis through system performance simulation during different failure modes; cascading failure (or sometimes referred to as ripple effects) occurs when failure of one component propagates to other components of the system and causes additional failures. In this analysis, cascading effects are modeled. The case of multiple-components failures is left for future extensions of this study as proper sampling methods and prior domain knowledge regarding simultaneous failures, especially for systems will large number of components, is required.

3.2.2.2 Imposed Costs Calculation

Imposed costs due to system failures would have many different aspects and may vary depending on type of failure, type of undelivered functions, and failure duration. The imposed costs are those forced on the system stakeholders due to disruptions and ought to be distinguished from operational costs of the system during normal operations.

In order to estimate losses in functional services, the investigated system has to be modeled at the appropriate granularity and fidelity levels. The system model should be able to realistically reflect behavior of the system during normal operation, as well as during each failure mode. Network systems modeling, also known as graph models, can be used to simulate the interactions between various components within the system and with upstream systems.

Performance of engineered systems are constrained by economic, physical, and operational limitations which can be easily formulated and incorporated into an optimization model reflective of how the system *can* and *ought to* perform. Applying physical and practical constraints requires background knowledge of the system, and relatively detailed component and interaction models are needed. The objective of the optimization model will reflect desired performance of the system which can be minimum operational costs, maximum revenue, etc. Defining the resilience index in terms of monetary costs enables us to formulate the objective function of the optimization model as minimum imposed costs for each failure mode during each operational temporal period. Since the penalty costs associated with functional service losses are included in the imposed costs, the optimization model will set the system status, i.e. load of different components, such that those losses are minimal. Therefore, the system will adopt and actively respond to each failure. Further discussions and mathematical formulations are provided in section 3.3.

3.2.2.3 Penalty Costs

The costs imposed to the stakeholders, due to inability to deliver functional services, damages to the system, and non-optimal operation are used to quantify the resilience index. This would essentially depend on type of products and/or services provided by the system and the assigned monetary values to losses in delivery of those services. One example can be economic values of uninterrupted electricity services which can be estimated through various perspectives and methods [76]; these methods include: (i) *surveying* customers to assign dollar values to the costs that might incurred during an outage. This can be direct costs such as loss of production in an industrial unit, for which market prices are available, or contingent costs for services with no market value. In the latter case, “willingness to accept” or “willingness to pay” concepts are often used in order to monetize the damages. (ii) *Proxy methods* through which cost of the outage is evaluated by an observable behavior such as the amount of money industrial customers would invest on back-up generators to prevent loss of functional services and damages due to electric grid failures. Such back-up systems are usually sized based on the critical functions (critical functions/outputs are those that will impose huge cost to the stakeholders if interrupted) such as life safety loads in a health care hospital. Further discussions on critical loads can be found in "critical loads securing" literature (such as studies by Pipattanasomporn et al. [77] and by Sujil et al. [78]).

3.3 System Modeling and Simulation

To estimate the system functional service losses due to a disruptive event, i.e. to identify how failure of each individual system component affects the whole system functionality, a realistic model of the entire system with proper level of fidelity is required. Scope and purpose of the analysis identifies how detailed such a system model should be. As stated earlier, we suggest the use of optimization model of the system as it provides several advantages [69]. Such models not only are able to capture topological features of the system, i.e. number of system components and their interconnections, but also, they account for physical and operational limitations through model constraints. With inclusion of penalty costs (due to undelivered functional services) in the objective function of the optimization model, *adaptation* would be an in-built capability of the system to respond to various failure modes. Additionally, prioritizing different functional services of the system can be easily accomplished by assigning proper penalty costs to undelivered services proportional to their criticality. This is one of the unique features of the current study.

The proposed resiliency assessment methodology is illustrated for an integrated energy system (IES) shown in Figure 3-3. The system includes various types of on-site power generation systems, such as combined heat and power (CHP) and solar photovoltaics (PV), electrical energy storage systems, and heating and cooling equipment. The energy system loads, i.e. heating, cooling, and electrical loads, are classified as critical and noncritical loads. This classification will help in prioritizing various types of services and to treat them differently when maximizing system resilience. Loads classification depends on type of the system and should be specified by the stakeholders. On the other hand, multiple number of equipment of each type are usually installed in order to provide redundancy and also to achieve more efficient performance. The corresponding network representation of the IES is shown in Figure 3-4. System components are shown as nodes and linked through vectors or edges. Depending on type of the system, these vectors can be electric transmission lines, pipelines, roads, etc.

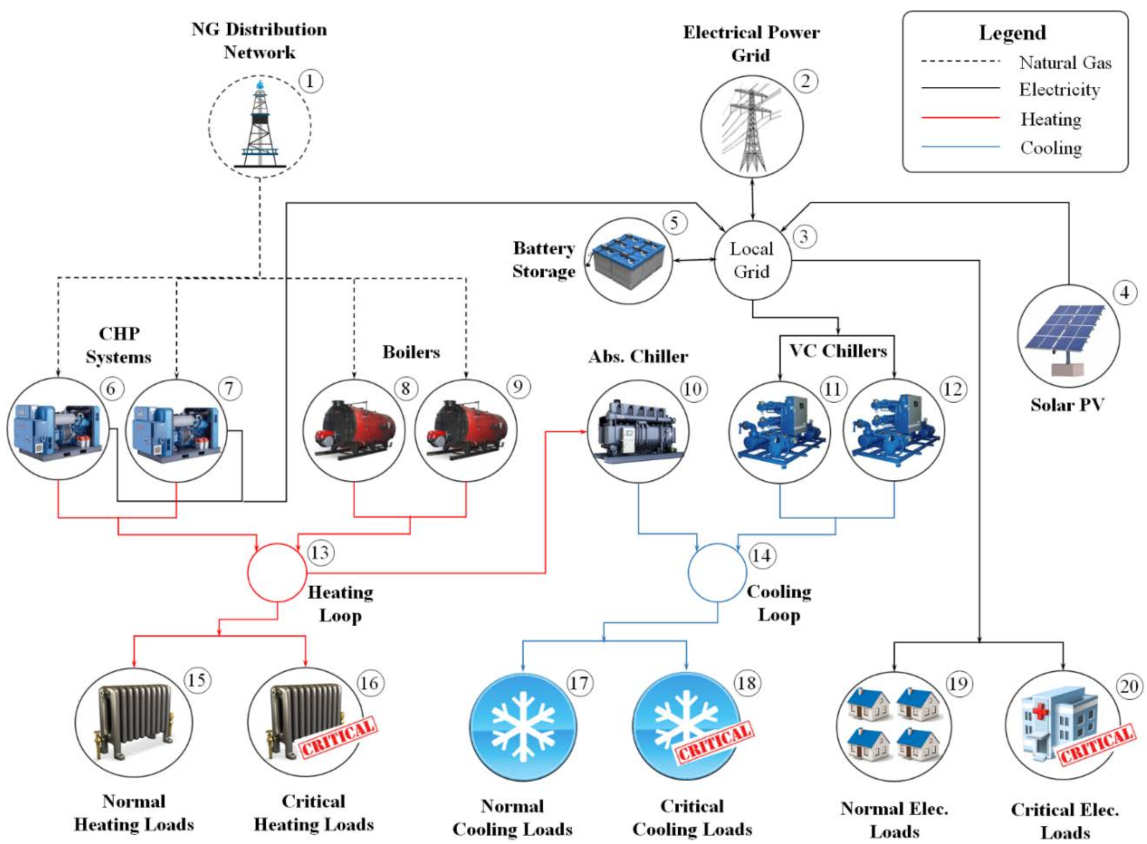

Figure 3-3- A typical integrated energy system diagram which includes utility electricity and Natural Gas inputs, on-site power generation, heating and cooling equipment, and the facility loads.

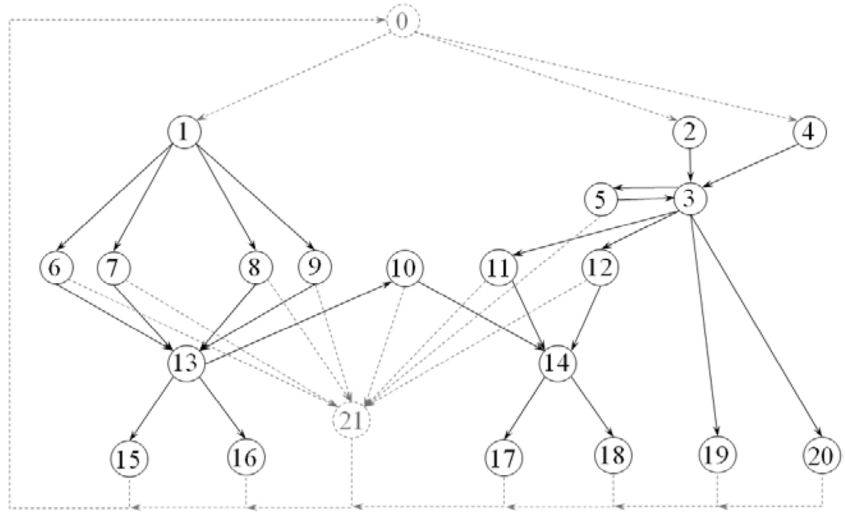

Figure 3-4- Network representation of the IES shown in Figure 3-3

Figure 3-4 illustrates the network model of the IES. Node 0 and node 21 are imaginary nodes added to the network model to fulfill the conservation laws for the energy system network. Node 0 represents total energy enters the system and node 21 is an energy sink which captures all energy losses from system components. Component performance (or efficiency) models identify the lost portion of the input energy to that component. Various linear (constant efficiency) and non-linear (variable efficiency based on the system part-load ratio) models for each component type can be found in the literature (see [79,80] for more detailed discussions on component models and control optimization of integrated energy systems). Segmented-linear models were used in this study in order to reduce the computational burdens while accounting for non-linear nature of efficiency performance of these components. The developed optimization models have been validated by independent evaluations with two other research groups [81]. By connecting all the system outputs and the sink node (node #21) to the source node (node #0), the conservation law for the entire system will be fulfilled.

Figure 3-4 is the connected directed graph for the IES assumed in Figure 3-3. The network shows energy flows between system components. In this case, the optimization model objective function can be defined as:

$$\min \left\{OC_{i,j} + \left(\sum_{k=1}^{K} FL_{i,j,k} \times PC_{i,k}\right)\right\} \tag{3-7}$$

This optimization model is subject to physical and operational constraints. Interconnections among system components are captured by conservation laws as:

$$\sum_p x_{pq} - \sum_r x_{qr} = 0 \qquad for \qquad q = 1,2, \ldots, N \tag{3-8}$$

where x_{pq} represents flows enter the node q and x_{qr} represents flows leave the node q and N shows total number of nodes (i.e. system components). Eq. 3-8 can be expressed in the matrix form as:

$$[A]_{N\times M}[X]_{M\times 1} = 0 \tag{3-9}$$

where matrix A is the node-edge incidence matrix, i.e. rows represents nodes and columns represents edges and entries are -1 or +1 or 0 (refer to a graph theory textbook such as [82] for further details). The matrix X arrays, i.e. x_{pq}s are flows (energy flows in this case) from node p to node q (p,q=1,2,…,N) and M denotes total number of edges (connections) in the graph. Depending on type of the system, other operational and physical constraints should also be included in the optimization model. Detailed discussions on the IES optimization model constraints can be found in [79,80].

When IES are analyzed, functional service losses would involve unmet heating, cooling, and electrical loads (both normal and critical). As discussed earlier, proper penalty cost values should be assigned to unmet loads (in Dollar per unmet MJ) reflective of criticality of loads. The optimization model, then, minimizes the operational and penalty costs during each scenario (recall that each scenario is a combination of a failure mode happening during an operational temporal period). For instance, one failure mode can be electric grid failure; depending on the facility loads at each operational temporal period, on-site power generation components, such as the CHP system and the solar PVs might not be able to entirely meet the loads. Therefore, the optimization model will prioritize different system functions based on the assigned penalty costs and will try to cover the more critical ones first such that the penalty costs are minimum.

The operational costs, i.e. electricity and fuel costs, should also be determined from the optimization model, modified to treat the conditional case where one or more nodes and/or one or more links are broken. Under such cases, the needed services can be met by operating the numerous equipment differently. For instance, when the electric grid fails, cooling loads can be met by electric chillers fed by on-site generated power or by the absorption chiller which can use the heat generated by the boiler or recovered from the CHP system. The optimization model identifies which alternative would be more economical. Note that the assigned penalty costs to unmet loads should be larger than operational costs otherwise the optimization model would choose not to meet the loads in order to minimize the objective function.

The flowchart depicted in Figure 3-5 summarizes all the steps in the proposed resilience assessment methodology.

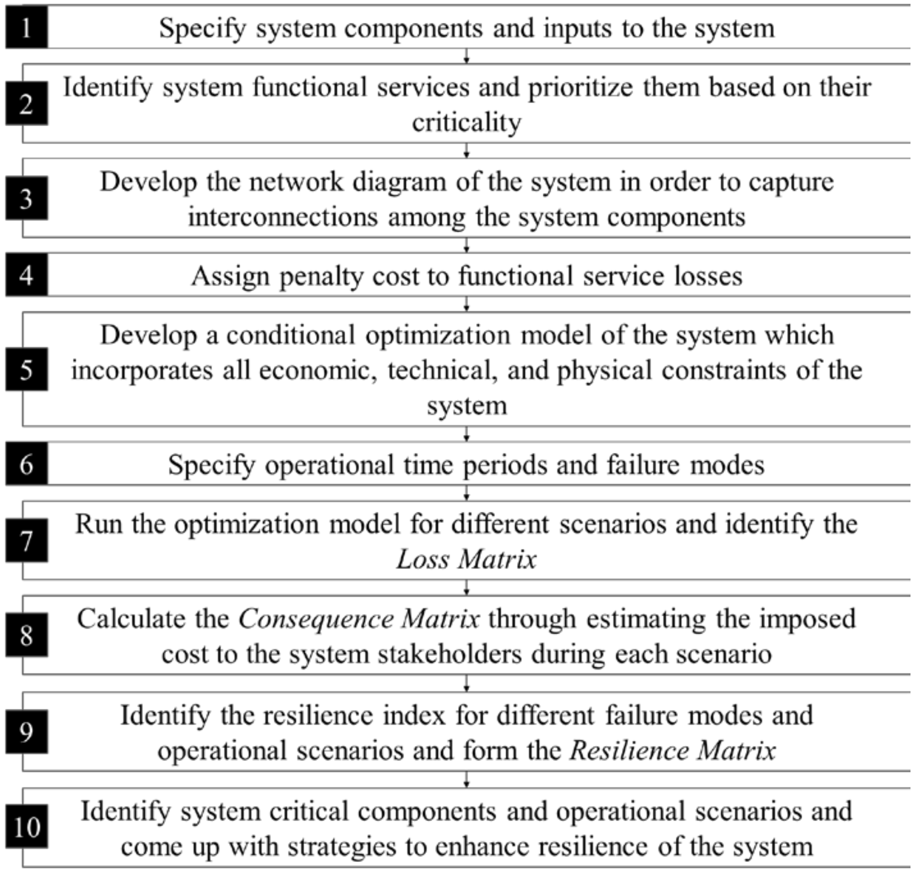

Figure 3-5- Flowchart illustrating the various steps of the proposed resilience assessment framework

3.4 Case Study

The integrated energy system shown in Figure 3-3 is assumed in order to illustrate the capabilities of the developed framework. A large office building with 5,500 m^2 floor area located in Boston, MA is assumed whose IES consists of two CHP systems, two boilers, two vapor compression (VC) chillers, and one absorption chiller (Table 3-1) [79,80]. The baseline case does not include solar PVs and electrical battery storage systems.

Table 3-1- Equipment specifications for IES case study

	Prime Mover	Boilers	VC Chiller	Abs. Chiller
Quantity	1 (reciprocating engine) + 1 (turbine)	2 (identical)	2 (identical)	1
Capacity (unit)	788+242 (kW)	7063.7 MJ/h	600 Ton	155 Ton

In this case study, four operational temporal periods have been selected representative of various seasonal and diurnal operational conditions of the system. The Summer and Winter design days were selected to be July 24th and February 2nd respectively. In addition, six system functional services have been considered in the current study as specified in Table 3-2. Penalty costs associated with critical and noncritical electrical unmet loads were taken from prior research which assigned monetary costs to electric utilities service reliability for different types of customers across the U.S. [83]. However, we could not find similar penalty costs for heating and cooling unmet loads; therefore, the values listed in Table 3-2 are assumed only for the purpose of this analysis. Note that these penalty costs are case-specific and the best practice would be to conduct surveys and seek system stakeholders participation to decide on the operational temporal scenarios, load classifications, and the assigned penalty costs.

Table 3-2- Case study operational temporal periods, system functions, and assigned penalty costs

Operational Temporal Periods	IES Functional Services					
	Noncritical Elec. ($/kWh)	Critical Elec. ($/kWh)	Noncritical Heating ($/GJ)	Critical Heating ($/GJ)	Noncritical Cooling ($/GJ)	Critical Cooling ($/GJ)
1- Summer-Day (6AM-5PM)	20	200	50	500	100	1000
2- Summer-Night (6PM-5AM)	10	200	25	500	50	1000
3- Winter-Day (6AM-5PM)	20	200	50	500	100	1000
4- Winter-Night (6PM-5AM)	10	200	25	500	50	1000

Table 3-3 summarizes hourly critical and noncritical loads of the studied IES averaged during the specified time interval of each operational temporal periods (these were determined by a detailed hourly building energy simulation program described in [25]). Note that the case study is conducted on an hourly basis due to unavailability of data on failure durations for most of the failure modes and large uncertainties associated with those for which data could be found (e.g. power grid failure).

Table 3-3- Assumed critical and noncritical loads of the case study energy system

Operational Temporal Periods	Hourly Average Loads					
	Noncritical Elec. (kWh)	Critical Elec. (kWh)	Noncritical Heating (GJ)	Critical Heating (GJ)	Noncritical Cooling (GJ)	Critical Cooling (GJ)
1- Summer-Day	1480	295	1.4	0.3	9.7	1.9
2- Summer-Night	530	106	1.0	0.2	4.2	0.9
3- Winter-Day	1482	296	6.8	1.4	3.5	0.7
4- Winter-Night	650	130	4.3	0.9	1.8	0.4

Ten specific failure modes were considered in this analysis: 1- electric power grid failure; 2- natural gas distribution grid failure; 3- reciprocating engine (prime mover) failure; 4- turbine (prime mover) failure; 5- both prime movers failure; 6- one boiler failure; 7- both boilers failure; 8- one vapor compression chiller (VC) failure; 9- both VCs failure; and 10- absorption (Abs.) chiller failure. The IES was simulated through each of these failure modes and deficiencies in desired functional services were evaluated for all scenarios.

3.5 Results and Discussion

3.5.1 Baseline Case

The *Loss Matrix* (Eq. 3-2) is generated for this case study as a 4×6×10 matrix (shown in Figure 3-6); each array identifies unmet loads (in GJ) due to one failure mode and during one operational temporal period.

6- Critical Cooling Loads

	1- Elec. Grid Failure	2- NG Grid Failure	3- Recip. Failure	4- Turbine Failure	5- Both PMs Failure	6- One Boiler Failure	7- Both Boilers Failure	8- One VC Failure	9- Both VCs Failure	10- Abs. Failure
1- Summer Day	0.1	0.0	0.0	0.0	0.0	0.0	0.0	0.0	0.1	0.0
2- Summer Night	0.0	0.0	0.0	0.0	0.0	0.0	0.0	0.0	0.0	0.0
3- Winter Day	0.0	0.0	0.0	0.0	0.0	0.0	0.0	0.0	0.0	0.0
4- Winter Night	0.0	0.0	0.0	0.0	0.0	0.0	0.0	0.0	0.0	0.0

5- Noncritical Cooling Loads

	1- Elec. Grid Failure	2- NG Grid Failure	3- Recip. Failure	4- Turbine Failure	5- Both PMs Failure	6- One Boiler Failure	7- Both Boilers Failure	8- One VC Failure	9- Both VCs Failure	10- Abs. Failure
1- Summer Day	10.2	0.0	0.0	0.0	0.0	0.0	0.0	2.7	10.2	0.0
2- Summer Night	0.0	0.0	0.0	0.0	0.0	0.0	0.0	0.0	3.4	0.0
3- Winter Day	2.5	0.0	0.0	0.0	0.0	0.0	0.0	0.0	2.5	0.0
4- Winter Night	0.0	0.0	0.0	0.0	0.0	0.0	0.0	0.0	0.3	0.0

4- Critical Heating Loads

	1- Elec. Grid Failure	2- NG Grid Failure	3- Recip. Failure	4- Turbine Failure	5- Both PMs Failure	6- One Boiler Failure	7- Both Boilers Failure	8- One VC Failure	9- Both VCs Failure	10- Abs. Failure
1- Summer Day	0.0	0.3	0.0	0.0	0.0	0.0	0.0	0.0	0.0	0.0
2- Summer Night	0.0	0.2	0.0	0.0	0.0	0.0	0.0	0.0	0.0	0.0
3- Winter Day	0.0	1.4	0.0	0.0	0.0	0.0	0.0	0.0	0.0	0.0
4- Winter Night	0.0	0.9	0.0	0.0	0.0	0.0	0.0	0.0	0.0	0.0

3- Noncritical Heating Loads

	1- Elec. Grid Failure	2- NG Grid Failure	3- Recip. Failure	4- Turbine Failure	5- Both PMs Failure	6- One Boiler Failure	7- Both Boilers Failure	8- One VC Failure	9- Both VCs Failure	10- Abs. Failure
1- Summer Day	0.0	1.4	0.1	0.0	0.0	0.0	0.0	0.0	0.0	0.0
2- Summer Night	0.0	1.0	0.0	0.0	0.0	0.0	0.0	0.0	0.0	0.0
3- Winter Day	0.0	7.1	0.0	0.0	0.0	0.0	3.0	0.0	0.0	0.0
4- Winter Night	0.0	4.5	0.0	0.0	0.0	0.0	0.0	0.2	0.0	0.0

2- Critical Elec. Loads

	1- Elec. Grid Failure	2- NG Grid Failure	3- Recip. Failure	4- Turbine Failure	5- Both PMs Failure	6- One Boiler Failure	7- Both Boilers Failure	8- One VC Failure	9- Both VCs Failure	10- Abs. Failure
1- Summer Day	0.0	0.0	0.0	0.0	0.0	0.0	0.0	0.0	0.0	0.0
2- Summer Night	0.0	0.0	0.0	0.0	0.0	0.0	0.0	0.0	0.0	0.0
3- Winter Day	0.0	0.0	0.0	0.0	0.0	0.0	0.0	0.0	0.0	0.0
4- Winter Night	0.0	0.0	0.0	0.0	0.0	0.0	0.0	0.0	0.0	0.0

1- Noncritical Elec. Loads

	1- Elec. Grid Failure	2- NG Grid Failure	3- Recip. Failure	4- Turbine Failure	5- Both PMs Failure	6- One Boiler Failure	7- Both Boilers Failure	8- One VC Failure	9- Both VCs Failure	10- Abs. Failure
1- Summer Day	2.68	0.0	0.0	0.0	0.0	0.0	0.0	0.0	0.0	0.0
2- Summer Night	0.0	0.0	0.0	0.0	0.0	0.0	0.0	0.0	0.0	0.0
3- Winter Day	2.69	0.0	0.0	0.0	0.0	0.0	0.0	0.0	0.0	0.0
4- Winter Night	0.0	0.0	0.0	0.0	0.0	0.0	0.0	0.0	0.0	0.0

Figure 3-6- Loss Matrix associated with the case study IES. Functional service losses are in GJ/h.

Zero values in the loss matrix imply that the corresponding load or service is being fully met. It can be seen that critical electrical loads are all met during all scenarios. Using an optimization model of the system along with proper penalty cost values enable the system to prioritize different functionalities based on their criticality and manage available sources to first satisfy more critical ones. As noted from the Loss Matrix, none of the unmet critical loads are greater than noncritical ones for any given scenario which identifies that the model is capable of prioritizing different tasks based on their criticality.

Consequence Matrix for the investigated IES is shown in Figure 3-7. Using Eq. 3-3 and the penalty cost values given in Table 3-2, imposed costs were calculated for each failure mode and operational temporal period. It is obvious from the results that the “Electric Grid Failure” mode would cause the highest imposed costs mainly due to high electrical loads, specifically during the “Summer Day” and “Winter Day” operational temporal periods. The “NG Grid Failure” mode would be the next critical failure mode followed by the “Both VC Chillers Failure” mode which would impose penalty costs due to unmet cooling loads during the “Summer Day” operational temporal period. It is worth mentioning that failure modes 3, 4, 5, and 10 would not impose any penalty costs, and all the imposed penalty costs are due to non-optimal performance of the IES. All other failure modes result in some amount of penalty costs. Comparing failure mode 6 with failure mode 7, and failure mode 8 with 9, demonstrate that the provided redundancy can reduce the unmet loads due to failure of the equipment thereby improves resilience of the IES.

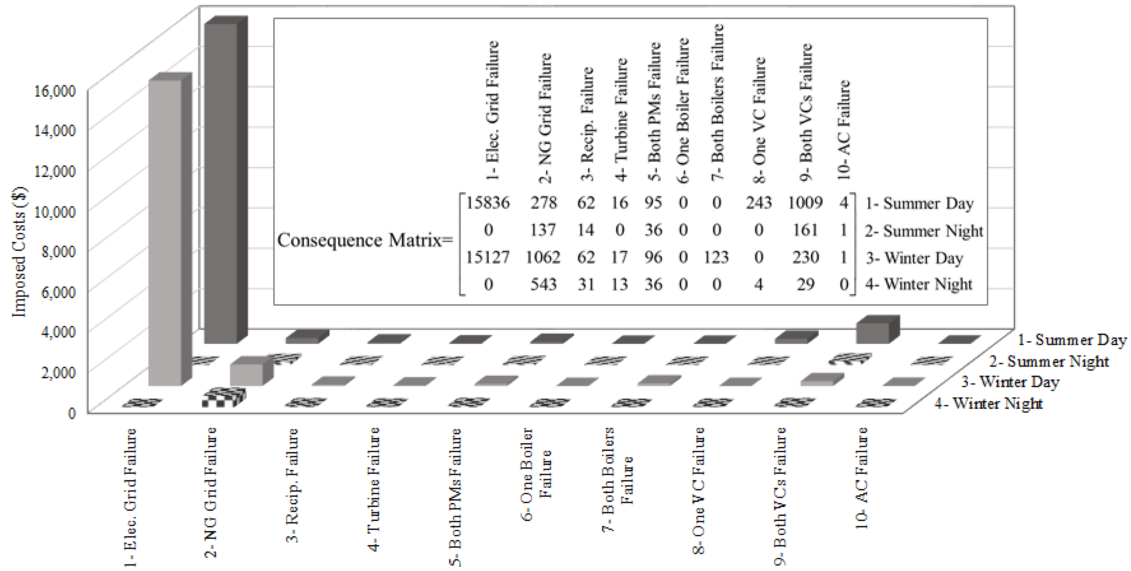

Figure 3-7- Consequence Matrix for the case study IES

Finally, the values of the *Resilience Matrix,* calculated according to Eq. 3-5 and Eq. 3-6 are shown in Figure 3-8. Recall that Re=0 implies total loss in functional services and that Re = 1 implies no loss in delivered services.

$$
\begin{array}{cccccccccccl}
 & \text{1- Elec. Grid Failure} & \text{2- NG Grid Failure} & \text{3- Recip. Failure} & \text{4- Turbine Failure} & \text{5- Both PMs Failure} & \text{6- One Boiler Failure} & \text{7- Both Boilers Failure} & \text{8- One VC Failure} & \text{9- Both VCs Failure} & \text{10- AC Failure} & \\
\textit{Resilience Matrix} = & \left[\begin{array}{c} 0.828 \\ 1 \\ 0.835 \\ 1 \end{array}\right. & \begin{array}{c} 0.997 \\ 0.999 \\ 0.988 \\ 0.994 \end{array} & \begin{array}{c} 0.999 \\ 1 \\ 0.999 \\ 1 \end{array} & \begin{array}{c} 1 \\ 1 \\ 1 \\ 1 \end{array} & \begin{array}{c} 0.999 \\ 1 \\ 0.999 \\ 1 \end{array} & \begin{array}{c} 1 \\ 1 \\ 1 \\ 1 \end{array} & \begin{array}{c} 1 \\ 1 \\ 0.999 \\ 1 \end{array} & \begin{array}{c} 0.997 \\ 1 \\ 1 \\ 1 \end{array} & \begin{array}{c} 0.989 \\ 0.998 \\ 0.997 \\ 1 \end{array} & \left.\begin{array}{c} 1 \\ 1 \\ 1 \\ 1 \end{array}\right] & \begin{array}{l} \text{1- Summer Day} \\ \text{2- Summer Night} \\ \text{3- Winter Day} \\ \text{4- Winter Night} \end{array}
\end{array}
$$

Figure 3-8- Resilience Matrix for the case study IES for different failure modes and operational temporal periods

As expected, resilience indices correspond to “electric Grid Failure” during “Summer Day” and “Winter Day” are the lowest amongst all investigated scenarios. We can conclude that resilience improvement strategies should be focused on strengthening against these scenarios. On the other hand, natural gas grid distribution network is more reliable compared to electric grids and other forms of energy transport systems mostly because it is underground [84].

3.5.2 Resilience Improvement Measures

Since the "Electric Grid Failure" mode is found to be by far the most critical one, it is reasonable to focus on improving the system resilience against this failure mode. Therefore, two improvement strategies, called Resilience Improvement Measures (RIM), were considered: RIM1: adding a solar PV system; and RIM2: adding an electrical battery storage. The PV system and the battery system are sized such that the initial costs are equal for both RIMs. First, a 700-kW PV system was modeled using PVWatts calculator developed by NREL [85] (standard panel type, fixed mount with 42° tilt angle equal to the location latitude); the PV system capacity was selected such that it can cover 30% of the peak total electrical loads during the Summer design day (July 24th); then, the initial cost of the PV system was calculated based on $3/Watt (according to [86]) which was found to be around $2 million. Battery system capacity, calculated based on similar initial investment ($2 million), was found to be 7000 kWh (battery price was assumed to be $300/kWh [87]). We assumed that 10% of battery charge is always available for emergency situations, such as sudden grid failure.

It should be noted that solar PVs and battery storage systems are reliable systems. According to Vazquez and Roy-Stolle, solar PVs failure rates are in the order of 10^{-3} failures per year [88]. Reliability of battery storage systems drops sharply after certain number of cycles which depends on storage system configuration and management strategies [89]; before reaching to such point, battery systems are reliable if sized and maintained properly. On the other hand, failure of the PV or the battery components would degrade the whole system performance to the baseline case. Therefore, PV and battery storage failure modes were not considered for the improved IES. In general, adding a new component to the baseline case should be considered by defining an additional failure mode.

Figure 3-9 assembles the results of the constrained optimization for unmet noncritical electrical loads for the three cases. Both the RIMs have reduced the unmet loads for the two “Summer Day” and “Winter Day” operational temporal periods with battery option being more effective. However, for the two night periods, there is no unmet loads in all three instances. The uncertainty bands shown for RIM1 reflects the variability of the PV system output during each operational temporal period; the upper limit corresponds to zero PV output (say due to overcast sky) and the lower limit is when the PV system generates at its maximum capacity during that operational temporal period. Such variability is a drawback of PV systems, or any other non-dispatchable power generation technology, with regards to resilience performance. No critical electrical load is left unmet in all cases (i.e. the baseline as well as the two improved cases) suggesting that on-site power generation (CHP system) has improved system resilience during “Electric Grid Failure” mode; such capability is often referred to as *self-sufficiency* or *adaptability*.

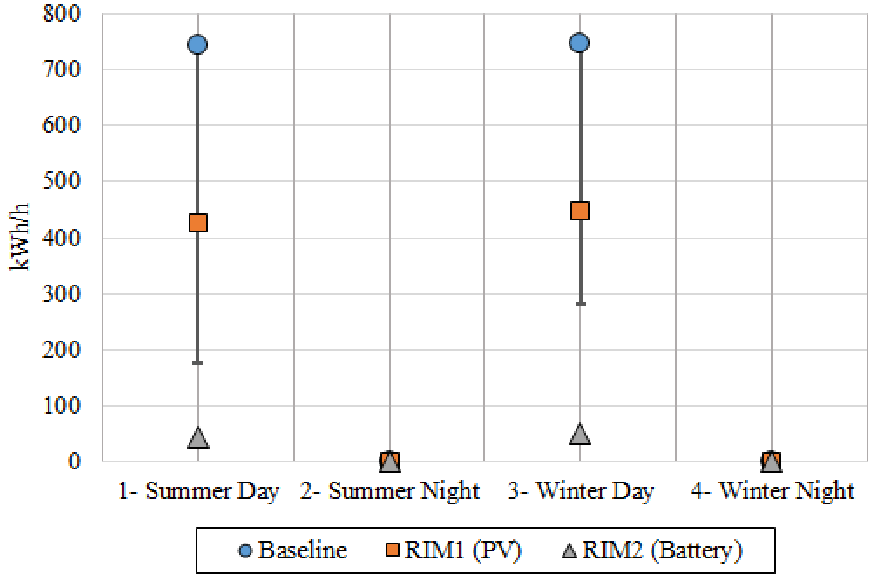

Figure 3-9- Unmet noncritical electrical loads comparison along with uncertainty bands associated with PV outputs

Results of the first RIM, i.e. solar PV implementation, corresponds to electric grid failure are:

$$Consequence\ Matrix, RIM1 = \begin{bmatrix} 8566 \\ 0 \\ 10038 \\ 0 \end{bmatrix}, Resilience\ Matrix, RIM1 = \begin{bmatrix} 0.907 \\ 1 \\ 0.891 \\ 1 \end{bmatrix}$$

and for the second RIM:

$$Consequence\ Matrix, RIM2 = \begin{bmatrix} 1906 \\ 0 \\ 1197 \\ 0 \end{bmatrix}, Resilience\ Matrix, RIM2 = \begin{bmatrix} 0.979 \\ 1 \\ 0.987 \\ 1 \end{bmatrix}$$

RIM2 can improve the resilience index of the system by 18.1% for both “Summer Day” and “Winter Day” periods while RIM1 improves the system resilience by 9.5% during the “Summer Day” and by 6.7% during the “Winter Day”. Thus, we conclude that battery storage can result it much lower imposed costs and higher resilience indices. Therefore, from the resilience standpoint, having a battery storage would be a better option compared to the PV system. In addition, PV system output is stochastic and may not be available during the grid failure mode should it be cloudy. Thus, we would conclude that battery storage system has a better design value in term of enhancing the IES resilience. Other types if RIMs can be evaluated in a similar fashion.

In dealing with electric grid outages, frequency and duration of outages, which varies considerably by country and region, would be decisive factors. Such statistics are usually collected, tracked, and published by federal and governmental authorities. American Public Power Association (APPA) has published grid reliability data for various U.S. regions [90]. Customer Average Interruption Duration Index (CAIDI), reported in minutes, and System Average Frequency Interruption Index (SAIFI), reported in number of occurrences per annum, are particularly helpful regarding end-use energy systems. The large office building studied here is located in Boston, MA, in the APPA region 8 for which the CAIDI is 65 minutes and the SAIFI is 0.51 (almost once in two years with average during around one hour). This information can be used to assess the real value of the resilience improvement measures over the lifecycle of the energy system. For instance, according to SAIFI of the given location, 12 outages are expected during lifespan of the PV system (assumed to be 25 years). Note that APPA region 8 has one of the most reliable electric grids in the U.S, and thus, resilience improvements measure would be more significant in other regions. For example, the SAIFI for region 3 is 1.63 and therefore 41 outages would be expected during the 25-year horizon. Average interruption duration is also higher in region 3 (191.25 minutes); resilience improvements would be crucial in such regions.

3.6 Summary and Future Work

Sustainable and resilient infrastructure systems are critical to achieve sustainable development under normal conditions, and in confronting extreme events and disasters.

Improving infrastructure systems resilience, as a crucial attribute of sustainable systems, is thus an area of research which has gained considerable momentum in recent years. Developing quantitative resilience assessment methods in support of decision-analysis regarding operation, design, and retrofitting resilient engineered systems would be one of the first steps towards this goal.

In this study, resilience is regarded as an umbrella term which covers several concepts including reliability, robustness, adaptability, self-sufficiency, etc. A new simple and comprehensive definition is proposed for resilience of engineered systems which can be adopted to different types of systems and captures different operational and structural resilience characteristics. This paper proposed a mathematical resilience assessment framework for multi-functional demand-side engineered systems. Through modeling and constrained optimization of system response to potential internal and external failures, the proposed methodology allows resilience to be quantified in terms of functional loss and monetary costs arising from loss in services which the system is designed to deliver. A three-dimensional matrix, called *Loss Matrix,* is introduced which represents undelivered system services under different scenarios, i.e. combination of the specified failure modes during different operational temporal periods (such as different diurnal and seasonal periods of the year). By assigning monetary cost penalties to different service losses for different temporal periods, the three-dimension loss matrix can be reframed into a two-dimensional *Consequence Matrix* where individual elements represent the imposed penalty costs to the system stakeholders due to undelivered services and/or non-optimal system performance under different scenarios. Normalizing the individual elements results into the *Resilience Matrix* of the system whose elements range between 0 and 1, with 0 denoting total loss in all functional services and 1 denoting no loss under the corresponding scenario.

The developed methodology was applied to assess resilience of an integrated energy system of a large office building, composed of on-site power generation, electricity and natural gas inputs from utility, and heating and cooling equipment serve to satisfy critical and noncritical electrical, heating, and cooling loads (i.e., six end-use services in all). Performance of the IES case study was simulated during four operational temporal periods and 10 failure modes using a constrained optimization model capable of capturing economic, physical, and practical limitations. Critical components of the IES were identified as those whose failure causes greatest imposed costs, and two resilience improvement measures, i.e. adding solar PV system and adding electrical battery storage, were evaluated. Results showed that adding battery storage system would be a more effective strategy to improve IES resilience.

The proposed resilience assessment framework offers several advantages compared to the existing ones: (i) through a constraint optimization model of the system, the system performance during disruption can be realistically modeled accounting for physical, economic, and operational limitations; such models are usually available for operational control and optimization and can be modified to include penalty costs and possible failure scenarios to be used for resilience assessment purposes; (ii) the developed framework can be implemented for different types of engineered systems and is able, and meant to, handle multi-functional systems; (iii) quantification of resilience performance in monetary terms facilitates resilience considerations to be incorporated in cost-effectiveness analyses; (iv) it directly targets system performance when confronted a disruption, rather than focusing on system characteristics, e.g. faster recovery, which may or may not improve the system respond to the disruption.

Note that assigning penalty costs ought to be based on the condition and type of building/facility and ranges from “loss in personnel productivity” to “loss of lives”. For instance, in a residential building located in an extreme cold weather, heating loads are more critical as residents may lose their lives in the absence of heat supplies; in this case, different, and potentially very high, penalty costs would be assigned to the critical heating loads. Value of Statistical Life (VSL), which is an economic value used to quantify the benefit of avoiding fatalities, can be used to estimate the associated penalty costs to the critical heating loads.

Assumptions and limitations of the proposed resilience assessment framework includes:

- Physical damages and recovery paths are considered in this analysis.
- Duration of failures in the analyzed case study are assumed to be one hour due to lack of information regarding typical duration of different failure modes.
- Constant penalty costs are assumed in this analysis while more complex, and potentially non-linear penalty costs functions will be considered in future extensions of this study.

The methodology proposed in this paper can be extended/improved in a number of ways: (i) more subtle consideration of the criticality of loads (rather than simply considering them as critical and non-critical) and expressing associated service loss penalties as a non-linear function with relevant uncertainties stated as, say fuzzy numbers, (ii) extending the current methodology which is limited to events that cause little or no physical damage to more extreme events including disasters, (iii) including frequency of occurrences of different failure modes and their duration which is important for resilience-enhancing investment.

Chapter 4 – Performance-Based Sustainability Assessment of Integrated Energy Systems

Abstract

One of the key infrastructures of any community or facility is the energy system which consists of utility power plants, distributed generation technologies, and building heating and cooling systems. In general, there are two dimensions to “sustainability” as it applies to an engineered system. It needs to be designed, operated, managed, and supported in such a manner that its environmental impacts and costs are minimal (energy efficient design and operation), and also be designed and configured in such a way that it is robust to extreme disruptions and shocks posed by natural, manmade, or random events (resilience). These somewhat conflicting attributes call for a multi-criteria analysis framework. This paper proposes such an assessment framework for community energy systems involving location and circumstance-specific sustainability indices that monetize the economic, environmental and resiliency characteristics throughout the lifecycle of the system components. The proposed framework, thus, allows translating sustainability goals into engineering practices and is applicable to: (i) design of new energy systems, (ii) assessing performance of an existing system, (iii) day-to-day scheduling and operation of the energy systems, and (iv) future growth planning. A new type of diagram called “Sustainability Compass” is also proposed which allows decision-makers to visually track the direction and magnitude of changes in the individual sustainability indices of different energy scenarios which can then be more easily communicated to various stakeholders. The proposed methodology and the usefulness of the Sustainability Compass diagram have been illustrated using end-use monitored data for a whole year of operation of a university campus energy system in order to evaluate five alternative

energy development scenarios involving a combined heat and power system and solar photovoltaic systems with different penetration levels.

4.1 Introduction and Background

Based on EIA (Energy Information Administration) [4], buildings account for 40% of the U.S. primary energy use, over 70% of the electricity use and 40% of carbon emissions. Emissions associated with residential and commercial sectors, known as the "building sector", are dominated by indirect emissions of electrical power generation [46]. Therefore, sustainable development of energy infrastructure should explicitly include generation, transmission, and consumption sectors, or in other words the whole life cycle of the building stock. In order to achieve this goal, one should be able to characterize sustainability of energy systems which includes social, environmental, and economic values and burdens known as the triple bottom line (TBL).

4.1.1 Overview of Sustainability Assessment

Many researchers have conducted sustainability assessment studies on various power generation technologies in order to provide insight and compare sustainable performance of such technologies and to examine development potentials in power sectors. They have adopted different sustainability criteria and indicators pertinent to type and scale of the system/technology. Most commonly, TBL impacts of energy systems have been investigated using different indicators (sometimes known as metrics) which are normalized and weighted to determine a composite score. Additionally, it is crucial to assess sustainability of energy systems and technologies in a bigger picture and throughout the system lifecycle.

Although TBL is often regarded as main sustainability criteria, other criteria might as well be integrated into sustainability assessment framework depending on the system type, scope, and scale of the assessment. There are two dimensions to “sustainability” as it applies to an energy system. It needs to be: (a) designed, operated, managed, and supported in such a manner that its environmental impacts and costs are minimal- this is the concept of energy efficient design and operation; and (b) designed such that it is robust to disruptions and shocks posed by natural, manmade, or random events and, if possible, can dynamically transform and adapt, and be able to recover and deal with the aftermaths; these capabilities are generally referred to as resilience. Both design objectives (a) and (b) are to some extent contradictory. Energy efficient design requires that little (to no) redundancies be built into the system <u>contrary to what is usually followed to make energy systems resilient</u>. Increased complexity of urban infrastructure systems on one hand, and more severe and more frequent natural disasters due to global climate change on the other hand, have forced researchers to explicitly consider resilience in or along with sustainability assessment of infrastructures.

Social dimensions of energy systems have been rarely included in technical studies as a separate aspect, but have been combined in some manner with multi-criteria sustainability assessment studies. Kowalski et al. [91] considered social cohesion, employment, effect on public spending, import independency, social justice, and security of supply as social characteristics of four renewable energy scenarios along with cost and environmental impacts. Atilgan and Azapagic [92] also accounted for employment, worker safety and energy security of various power production facilities of Turkey. Moslehi and Arababadi [19] conducted a life cycle sustainability assessment of broad implementation of solar PVs at local scale accounting for safety and accountability of energy systems as social sustainability metrics.

Three general methods can be found in the literature regarding developing and quantifying sustainability indices for energy systems:

(a) Most of the existing sustainability assessment systems use weight factors to capture preferences among sustainability indicators (such as [93–95]). Since many different weighting methods exists generally relying on value judgments about relative importance of indicators, the analysis results are somewhat arbitrary and the decision analysis process may be affected by the selected weighting method.

(b) To overcome such issues, many studies (such as [96]) present the midpoint sustainability assessment results separately for each sustainability indicator in its actual unit normalized against the selected functional unit (say ton CO_2/ MWh), rather than combine the impacts into one sustainability index. While this type of analysis provides valuable insight into potentials and limitations of energy systems in support of national and regional scale energy development and transition policies, it may not be suitable for decision analysis, in that, no single system/technology would have superior attributes in all indicators. For instance, one system may have lower CO_2 emissions while another may emit lower SO_x emissions.

(c) Another methodology includes ranking different alternatives based on each indicator and scale impacts (usually between 0 and 1) relative to the worst and the best alternatives (such as [97–102]). Disadvantage of this method is that the relative importance of different metrics will be improperly captured. Such an approach was the basis of a study by Phillips [103] who performed a sustainability assessment on large-scale solar photovoltaic solar power plants by converting qualitative-based results of the study conducted by Turney and Fthenakis [104] into quantitative indices through assigning relative scores to various sustainability indicators. There is not enough published studies supporting the reasoning behind the allocation of scores [105]. Further, the scoring systems does not account for uncertainty or variability in the perception of metrics [105].

We have expanded on this approach by combining and aggregating different indicators in each sustainability criteria which relies on monetary external/penalty costs estimated based on surveys and statistical analysis; this allows proper accounting for the relative importance of different metrics within each sustainability criteria.

One common way to quantify burdens of energy systems on the environment and society is through assigning price tags to them, referred to as external costs. Many researchers have used this method to come up with a single environmental sustainability index for national and utility scale power generation technologies; Hohmeyer [6]conducted one of the very first studies on external costs of fossil fuels power generation in 1988, using pollutant damage costs estimated by Wicke [7]. Roth et al. [106] evaluated and incorporated external costs of different power generation technologies at national scale to evaluate future development strategies in Switzerland. Rabl and Spadaro [9] performed a life cycle assessment to evaluate the power generation externalities throughout the lifecycle of various power generation technologies in Europe. This quantification method, which is adopted in the current study, provides several advantages compared to the review scoring and normalization methods; (i) presenting results in monetary costs would attract more public attention and reflects the actual burdens on the society; and (ii) relative importance of different environmental impacts is reflected in the assigned monetary damages; e.g. monetary costs associated with emission of one ton of CO_2 and one ton of SO_x reflects the relative impacts they might have on the environment and people health. Additionally, as proposed in this study, developing sustainability indices in terms of monetary costs facilitates effective incorporation of sustainability goals into cost-effective design and operation of energy systems.

4.1.2 Sustainability Assessment at National or Regional Scale

Great deal of effort has been devoted to assessing sustainability of energy infrastructure at national scale for policy development purposes. Begic and Afgan [107] conducted a multi-criteria sustainability assessment on various power generation technologies, including renewable and non-renewable technologies in Bosnia using non-numeric, non-exact, and non-complete information. They considered four sustainability criteria: resources, environment, economic, and social, with each including multiple indicator aggregated through applying weight factors. In order to compare the overall sustainability performance of various systems, they defined two cases where different sustainability criteria are prioritized based on assumed relative importance. Karger and Hennings [108] investigated the advantages and disadvantages of distributed electricity generation for Germany through sustainability assessment of four specified future scenarios regarding power generation decentralization. Through interviews with 11 representatives with different backgrounds, they compiled sustainability criteria classified into environmental protection, health protection, security of supply, economic aspects, and social aspects each involving detailed indicators. Based on expert judgments, they found that decentralization has positive effects on “CO_2 emissions” while “conservation of materials” will be negatively affected. Impacts of decentralization on “security of supply” is characterized by number of contradictory factors and large uncertainties. Schlor et al. [109] developed two indices, index of sustainable development (ISUD) and standardized sustainability index (SSEI) in order to identify the degree to which sustainability is achieved according to the sustainability goals set by the German government. Dapkus and Streimikiene [110] conducted a sustainability assessment on various power generation technologies in order to identify most sustainable development paths in the EU. Using a multi-criteria decision method called MULTIMOORA, they found that solar and hydro power systems are the most sustainable technologies followed by wood CHP (combined heat and power) systems and wind energy. Santoyo-Castelazo and Azapagic [93] assessed sustainability of eleven future electricity supply scenarios in Mexico considering environmental, economic, and social sustainability dimensions.

4.1.3 Sustainability Assessment at Community Scale

Rather than regional and national scales, it is easier to tackle these sustainability concerns in the narrower context of communities (campuses, neighborhoods, etc.), where considerable work has already been done and which have a well-defined central authority whereby policy decisions regarding social practices and engineering systems are easier to implement. At point of use, community-scale energy systems are crucial in achieving sustainable development due to involvement of end-use consumers on one hand [3], and their large contribution in the world’s energy use and GHG emissions on the other hand (according to [4] in 2017, 40% of total U.S. energy consumption was from residential and commercial buildings).

There are few published work on sustainability assessment of community-scale energy systems. Lo Prete et al. [111] developed a framework for quantitative sustainability and reliability assessment of different power generation scenarios at regional scale in European electricity market. Results of their analysis suggest that the power network which includes fossil-fueled microgrid and a price on CO_2 emissions yields the highest sustainability index which is comprised of environmental, economic, technical, and reliability sub-indices. Safaei et al. [112] proposed a life-cycle model to estimate cost and environmental impacts of three different cogeneration and solar technologies in buildings. They found that specific design and operation strategies have to be adopted for distributed power generation systems in order to meet the cost and environmental impacts reduction goals.

4.1.4 Objectives

The objective of this paper is to propose a multi-criteria sustainability assessment framework which: (i) captures the two important dimensions of sustainability (i.e., minimal impact on the environment via efficient performance and resilience) pertinent to end-use energy systems at community scale, (ii) allows presenting the results so that trade-offs and system impacts are clear and well defined in order for stakeholders to participate and make informed decisions. The framework and indices proposed will be useful for a variety of sustainability-relevant tasks: (i) for sustainability-conscious design of new energy systems, (ii) for assessing performance of an existing system, (iii) for day-to-day scheduling and operation of the energy systems, and (iv) for development and planning for future growth.

4.2 Quantification and Benchmarking

We propose a performance-based sustainability assessment framework for benchmarking and evaluating different kinds of energy systems at the community scale. This framework would be akin to energy benchmarking of individual buildings meant to compare and rank measured energy performance of a particular building against a distribution of similar buildings. The benchmarking index commonly used is the Energy Use Intensity (EUI), in units of kWh/sqft.yr or Btu/sqft.yr.

4.2.1 Economic/Cost Index

Life Cycle Cost analysis is a financial approach which helps decision makers identify the most cost-effective measure among competing alternatives. Costs associated with a particular product or service can be divided into capital costs, consumption costs, and O&M (operation and maintenance) costs. In the case of energy systems, capital costs include procurement of new equipment and systems while consumption costs refer to purchase of electricity (actual electricity costs and demand charge rates and incentives and rebates) and natural gas from utility providers. Other direct costs of the energy system might be considered based on the scope and goal of the analysis.

We propose a normalized economic index called Energy Costs Intensity (*EnCI*), which is the sum of annualized initial costs of different energy system components, annual consumption costs, and O&M costs normalized per unit area of the building/facility served by the energy system. The *EnCI* index, expressed in $/m^2/year, provides multiple advantages compared to the existing energy metrics (such as EUI index): first, in addition to the energy consumption, the *EnCI* index includes the energy related capital, consumption costs (and the temporal variations in rate structures), and

O&M costs. Further, it accounts for the demand charges which are usually a big portion of the energy bills for commercial and industrial facilities. For instance, implementing a peak-load shifting strategy has no impact on the EUI, while *EnCI* can capture such effects.

4.2.2 Environmental Impacts Index

Environmental and health impacts are often very decisive sustainability criteria. Environmental impacts of any product or service can be evaluated and quantified through a life cycle assessment (LCA). An extensive LCA is required to estimate emissions and the associated environmental and health burdens of end-use energy systems as numerous processes and infrastructure are involved (refer to Chapter 2 for more details).

We propose an environmental sustainability index called External Costs Intensity (*ExCI*) which is the monetized locations-specific environmental and health impacts of the energy system imposed to the society normalized against unit area of the building/facility served by the energy system. The *ExCI* index, represented in $/m^2/year, involves all lifecycle stages of any source and system required to meet the electrical, heating and cooling energy needs of the community.

External cost approach, i.e. the monetized adverse health and environmental impacts, was used to quantify the environmental and health impacts associated with various components of the energy system throughout their lifecycle. The proposed methodology for evaluating the environmental and health impacts of the end-use energy systems is specific to the location of the facility and accounts for regional power generation energy portfolio mix which is necessary due to two main reasons: (a) power generation fuel mix and thereby the associated environmental and health impacts vary drastically across the U.S. (b) features of the environment which receives the pollution, including climatic conditions and population density, identify how and at what level the impacts would be [95]. Note also that one of the drawbacks of relying on EUI is that it cannot reflect the quality of the energy being used for the building while the *ExCI* index, along with the *EnCI* index, reflect both quantity and quality of the consumed energy.

4.2.3 Resilience Index

A new performance-based method for characterizing and assessing resilience of multi-functional engineered systems has been proposed by the authors (Chapter 3). The proposed methodology quantifies resilience of the system based upon loss in the services which the system is designed to deliver.

The area-normalized costs imposed to the system stakeholders due to loss of functionality over a certain period of time (say, one year), is considered as the resilience cost intensity, *ReCI*, represented in $\$/m^2$/year. This index would essentially depend on types of services provided by the community and represent the imposed penalty costs to the system stakeholders due to undelivered services and/or non-optimal system performance. The index is also location specific due to type, frequency, severity and duration of extreme events vary from one region to another.

Resilience assessment also has to be location and case specific since the type and frequency of occurrence of disruptions may vary from place to place; for instance, electric grid reliability statistics confirms that outages are more frequent and last longer in some regions.

4.2.4 Representation of Results- Sustainability Compass Diagram

Analyzing alternative scenarios and identifying their sustainability status allow decision-makers to ascertain whether one scenario is more sustainable than another. Our framework involves characterizing the sustainability of energy systems by three indices, namely *EnCI*, *ExCI*, and *ReCI*. Mapping different scenarios on a plot will enhance comprehension since people can interpret visual results more easily. The Sustainability Compass diagram proposed is illustrated in Figure 4-1. Any point on the compass represents a system status reflecting two joint sustainability attributes of the system. The Sustainability Compass can also be used to identify whether a particular strategy or modification will improve sustainability of the system compared to the baseline case.

The results can be represented in two different ways:

(a) if the system stakeholders only want to evaluate the system sustainability during normal operation, then the two indices *EnCI* and *ExCI* are the appropriate ones to consider (Figure 4-1-a).

(b) if resilience attributes, i.e. the system performance in dealing with disruptions, have to be assessed, then *EnCI and ReCI* are more appropriate (Figure 4-1-b) since maintaining/restoring system functionality is more critical than minimizing the environmental impact of the system during the relatively short interruption period.

In the imaginary case shown in Figure 4-1, the change from point A (represent the baseline status of the system) to point B (after implementation of a particular modification) suggests that the economic and resilience performance of the system are improved (i.e. lower *EnCI* and *ReCI* indices) but at the expense of the environmental impacts (i.e. higher *ExCI* index). Thus, the Sustainability Compass not only shows the direction and magnitude of the change in each sustainability criterion, it also helps in identifying the potential tradeoffs among different sustainability indices. Ideally, we would like that point B to fall in the lower left quadrant of the compass.

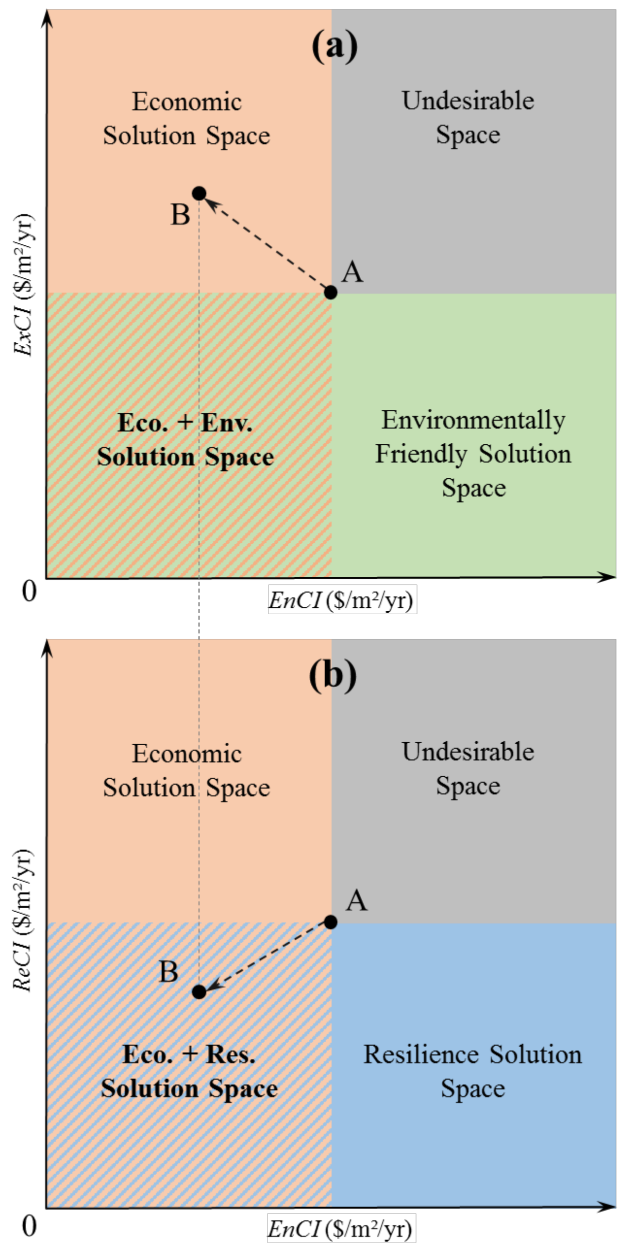

Figure 4-1- Sustainability Compass allows visualizing the magnitude and direction of change in the sustainability status of an energy system/community when system changes are made

4.2.5 Sustainability Assessment Framework

The overall sustainability assessment framework proposed in this study (Figure 4-2) starts by **defining the goals and scope** of the analysis. **System modifications** (or scenarios that are technically feasible options) should then be defined and documented based on the goals. These scenarios can be design/development alternatives at the early stages of a project, scheduling/operating options, or even the implementation of different EEMs (Energy Efficiency Measures) or ECMs (Energy Conservation Measures).

The next step is **data collection**; for an existing energy system monitored data can be used, failing which it can be generated by system simulation. The data requirements (length, frequency, accuracy, level of granularity) would depend on the scope of the analysis. Energy modeling should also allow for predicting system performance when different scenarios are being evaluated. Also, time scale of the monitored or simulated data would depend on the specific scenario being evaluated; for example, 15-minute data might be necessary for electric demand charge calculations while seasonal/annual estimations would be adequate for future growth evaluations. Energy consumption of the on-site facilities (such as chillers, boilers, etc.) operated to meet the energy demands need to be considered. For each system and at each time step, the environmental impacts, including direct emissions and fuel/electricity consumption along with associated costs, i.e. operational, maintenance, and capital costs have to be calculated and aggregated in order to reflect overall system behavior.

The next step is to calculate the sustainability indices by conducting the Life Cycle Assessment (LCA), Life Cycle Costing (LCC), during normal operation conditions as well as analyzing the resilience performance of the energy system under disruptions. The sustainability indicators, i.e. environmental, economic, and resilience performance indices, will be mapped on the Sustainability Compass in order to facilitate the decision-making process. Stakeholders might assign membership functions to different indices using fuzzy logic framework in order to either magnify or lessen the importance of a particular index. They could also assign penalty costs to the system functionality losses based on the time of interruption, type of lost functionalities, and number of people affected.

In this study, stakeholder preferences are viewed as reflective of the social dimension of sustainability of the community energy systems. Health effects of the systems (also part of social impacts) are included in the LCA analysis while other social metrics such as social justice, equity, employment, human rights, etc., have not been included here. Health effects of the systems, which can be considered as part of social impacts, are included in the LCA of the energy system.

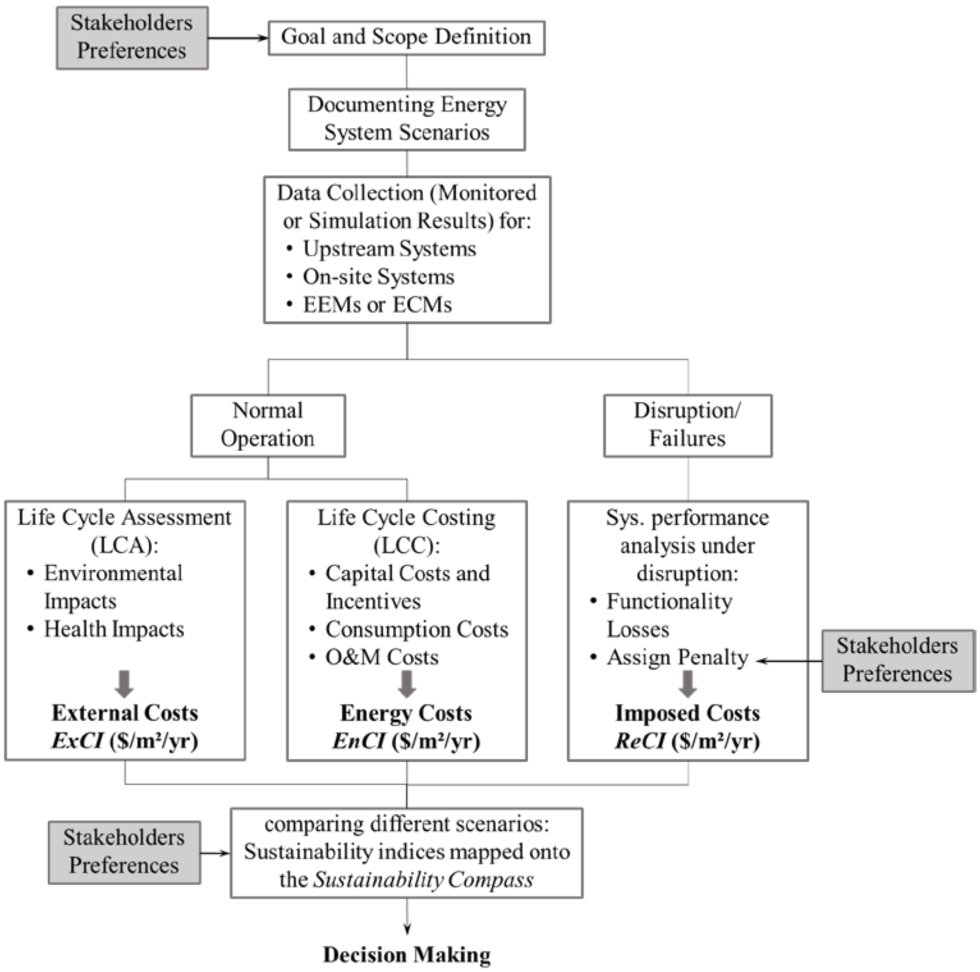

Figure 4-2- Flowchart of the sustainability assessment framework proposed

4.3 Case Study

4.3.1 Energy System Description

The proposed methodology described above has been applied to the integrated energy system (IES) of a university campus with more than 280 buildings located in Arizona, U.S.A. The entire energy system is extensively instrumented by an Energy Information System which collects and stores end-use data from various systems at 15-minute time intervals. The overall energy demand of the campus is met through a variety of sources ranging from electricity purchases from a local power company to solar PV systems installed on several campus buildings and parking lots, as well as a CHP plant consisting of a 7-MW gas turbine and a 2-MW steam turbine. The cooling plant comprises of 10 centrifugal chillers each of capacity 2,000 Tons (one refrigeration Ton is 3.517 kW or 12,000 Btu/h), and 6 chilled water TES (Thermal Energy Storage) tanks each having a capacity of one million gallons of water. Solar panels are mostly polycrystalline and are either stationary or one-axis trackers. Whole year of hourly monitored data on electricity and natural gas consumption has been used in this analysis.

4.3.2 Development/Design Scenarios

Six design/development scenarios were considered in order to illustrate how the proposed sustainability assessment method can be used to quantify and compare different alternatives from the sustainability standpoint. Scenarios were constructed based on different penetration level of solar PVs and capacity of the CHP system as listed in Table 4-1. Scenario A, which serves as the baseline, does not include any on-site power generation, and therefore all electrical loads (including cooling loads) are fed by the utility grid. In scenario B, a 9-MW CHP system (a 7-MW gas turbine plus a 2-MW steam turbine) were added to the baseline energy system. Scenario C considers the implementation of on-site solar PVs; a 6.85 MW solar PV was added to the baseline system and sized such that the initial costs are equal to that for the CHP system used in scenario B. Scenario D considers higher levels of solar power penetration by introducing a 13.7 MW solar PV system to the baseline system and scenario E includes both PV and CHP systems used in scenario B and scenario C. Note that scenario D and scenario E would have equal initial capital costs before the incentives are applied. Scenario F includes three 2 MW diesel generators which are to be operated only under emergency conditions.

Table 4-1- Specification of the baseline energy system (scenario A) and five alternative scenarios evaluated

Scenarios	Solar PV	CHP	Diesel Generator	notes
A	-	-	-	Baseline (no on-site power generation)
B	-	9 MW*	-	Addition of CHP system
C	6.85 MW	-	-	Lower solar penetration
D	13.7 MW	-	-	Higher solar penetration
E	6.85 MW	9 MW*	-	Lower solar penetration with CHP
F	-	-	3 x 2000 kW	Traditional stand-by generator

**7MW gas turbine + 2MW steam turbine*

4.3.3 Results and Discussions

4.3.3.1 Cost Analysis Results

Evaluation of the economic performance of the campus energy system involved conducting a LCC analysis which takes into account the energy consumption costs, including purchasing electricity and natural gas from the utility companies, demand charges, O&M costs, and annualized initial costs considering incentives. Table 4-2 summarizes the input data assumed for this LCC analysis for on-site generation systems, i.e. the solar PVs and the CHP system. Following [41], discount rate is taken to be 2%.

Table 4-2- Financial input data

System	Lifespan	Initial Cost	Incentives	O&M Costs
CHP	25 years [113]	$1000/kW (gas turbine) $1300/kW (steam turbine) [114]	500 $/kW [114]	40 $/kW/yr [113]
Solar PV	25 years	$1.62/W installed* [86]	30% Federal tax credit [115] plus 10% state tax credit [116]	$14/kW/yr [86]
Diesel Gen.	25 years	$1000/kW [117]	-	$3.6/kW/yr [118]

** this includes module, inverter, balance of system (BOS), install labor, tax and overhead costs*

Electrical energy and demand charge tariffs are assembled in Table 4-3. Natural gas price fluctuates from a low of $7.21/GJ in December to a high of $9.88/GJ in June; however, we have assumed an annual average of $8.54/GJ.

Table 4-3- Electrical and demand charge rates

	Electrical Energy ($/kWh)	Demand Charge ($/kW)
On-peak	0.04483	19.229
Off-peak	0.0355	2.974

First, a cashflow analysis was conducted for the different scenarios. Savings due to lower consumption costs and lower demand charges are calculated and cumulated to estimate the payback time for the different scenarios. It was found that, after 25 years, the cumulative savings from scenario B and C are $16.3 million and $11.1 million respectively; therefore, the CHP system has better economic performance compared to the PV system as its payback time is shorter and total saving over its lifespan are larger. Comparing scenario D and E, which have equal initial costs, also confirms that the CHP system has better economic performance than the PV system mainly due to higher capacity factor. In addition, CHP systems are dispatchable and can be run at different part-loads depending on the campus energy needs and the electricity rate structures.

Regular costs of the energy system include, electricity costs, fuel costs, demand charges, and operational and maintenance costs. Results of our financial analysis reveal that the demand costs are very significant, while additional O&M costs due to adding new systems are negligible compared to other costs (see Figure 4-3). In scenarios B and E, annual fuel costs are higher than the demand charges due to NG-fired on-site power generation. For scenarios C and D, the introduction of solar PV systems has reduced both energy costs and demand charges with the later saving being slightly greater.

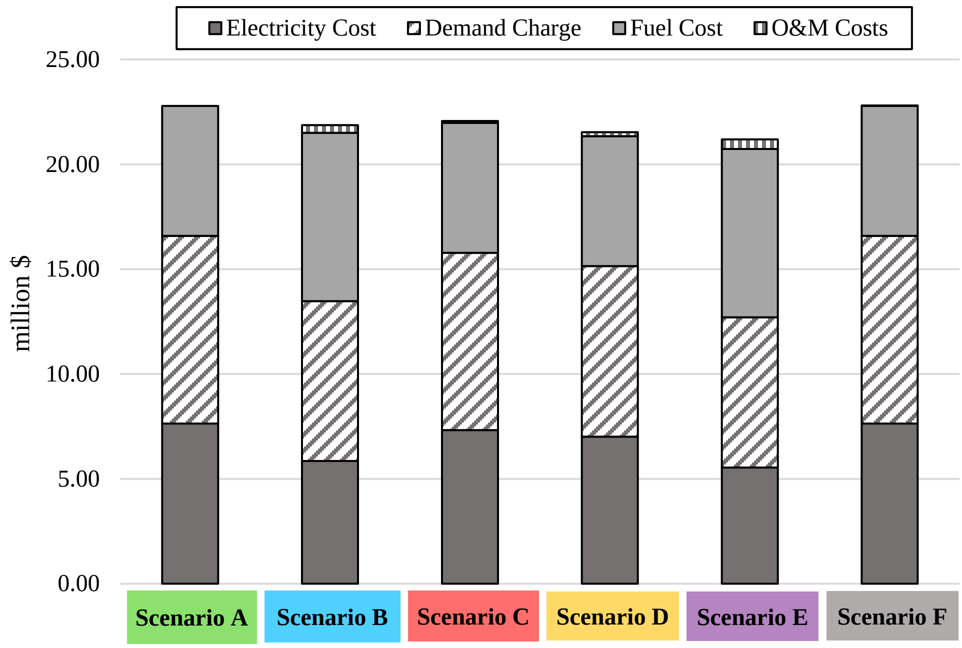

Figure 4-3- Contribution of different types of costs to annual costs

The *EnCI* index (Figure 4-4-a) has been compared across the different scenarios along with the payback periods (Figure 4-4-b). Comparison between scenario B and scenario C results confirms that the CHP system has a payback period of 7.2 years while it takes around 9.4 years for solar PVs to pay off the capital investment in scenario C. Scenario D with an installed PV system double that of scenario C results in longer payback time around 10.6 years. The payback period for scenario E is found to be 8.3 years. It can be seen that all scenarios improve *EnCI* indices compared to the baseline case (scenario A) except for scenario F which does not provide any savings in normal conditions; scenario E has the best *EnCI* index among the analyzed scenarios. The *EnCI* index includes a variety of costs including initial capital costs, consumption costs, operation and maintenance costs, and incentives, and therefore offers a comprehensive comparison among the competing alternatives.

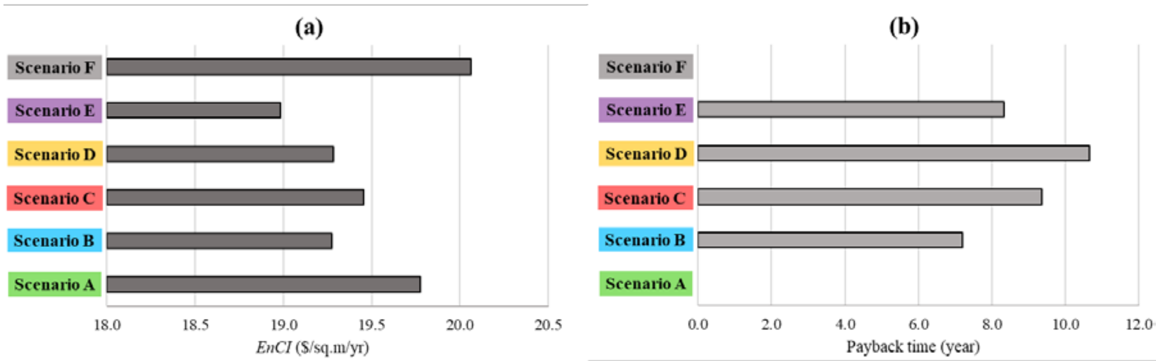

Figure 4-4- EnCI index and payback time of different scenarios, no pay-back time is calculated for scenario F since the emergency diesel generators does not provide any saving during normal operation

4.3.3.2 Environmental Impacts Analysis Results

Chapter 2 reported on location-specific environmental impacts of power generation at utility scale in the AZNM eGRID sub-region where the university campus is located. Temporal variations in the emission factors due to change in the utility power generation fuel mix are included as are the environmental costs of on-site CHP and boilers operation and manufacturing, transportation, operation and maintenance of the PV systems.

The *ExCI* indices for the different energy scenarios along with the contribution of purchased electricity, the natural gas burnt in the CHP system and boilers, and the PV systems, are shown in Figure 4-5. The implementation of the CHP system results in higher environmental impacts although boilers loads and amount of purchased electricity are reduced (see Figure 4-5-a). As shown by the results of scenario C and scenario, solar PV systems can reduce the environmental impacts of the campus energy system. Combination of solar PV and the CHP systems (scenario E) can also slightly improve the performance of the energy system with regards to environmental burdens. In addition, the impacts associated with the solar PVs lifecycle were found to be insignificant compared to purchased utility electricity and fuels. Our environmental impacts assessment (using ecoinvent database [50]) confirms that impacts associated with the diesel generators manufacturing are negligible relative to those from purchased electricity and NG given the amount of purchased electricity, and therefore scenario A and F would have equal environmental and health impacts.

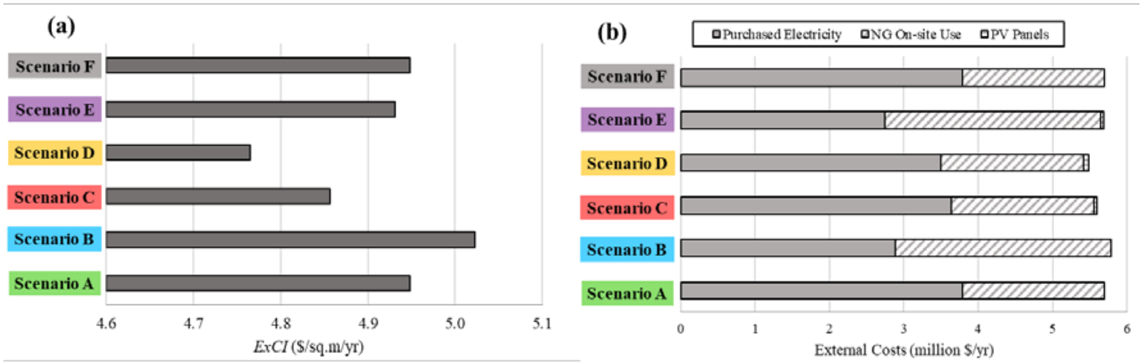

Figure 4-5- ExCI indices and total annual external costs associated with different sources

The energy system in Scenario B imposes $2.1 million additional externalities (compared to the baseline) to the society over the system lifetime while scenario C and scenario D reduces total externalities by $2.6 million and $5.3 million respectively. Implementing both PV and CHP system in scenario E would result in minor reduction of $0.5 million over the 25-year horizon. Note that with the same initial investments, savings on external costs from the solar PV system are higher than the increase in externalities from the CHP system.

4.3.3.3 Resilience Assessment Results

A resilience assessment framework which characterizes and quantifies resilience of an end-use energy system based upon the unmet electrical, heating, and cooling loads was proposed in Chapter 3. The resilience cost intensity captures the cost that the system stakeholders would incur due to functionality losses due to interrupted services. In this case study, we have used historical hourly data obtained from the campus energy information system (EIS), in order to assess resilience performance of the developed scenarios. Total electrical loads (including the cooling loads) were collected separately for Summer Days, Summer Nights, Non-summer Days, and Non-Summer Nights, as different operational temporal periods, to reflect variability in the campus loads and in the solar PVs output. We assumed that critical safety and sensitive laboratory loads are 20% of total electrical loads. Since the developed scenarios focuses on electrical energy systems, we have opted not to include heating loads in our resilience analysis. On the other hand, natural grid distribution network is more reliable compared to electric grids and other forms of energy transportations as it is underground [84]. Therefore, the campus energy system ought to be more resilient against electric grid failure since it is the more critical failure mode. Failure of other on-site power generating systems, i.e. PVs and the CHP systems, will not leave any electrical loads unmet as the grid utility can feed the campus.

Duration and frequency of failures over the timeframe of the study affects the costs imposed on the system stakeholders. Such statistics are available for electric grid failures across the U.S. for different APPA (American Public Power Association) regions as CAIDI (Customer Average Interruption Duration Index) and SAIFI (System Average Frequency Interruption Index) [90]. CAIDI is reported as average length of outages (in minutes) that a customer would experience in a year while SAIFI describes the frequency of sustained outages experienced by customers in one year [75]. The campus studied here is located in the state of Arizona (APPA region 6) for which the CAIDI is 106.8 minutes and the SAIFI is 1.36. Table 4-4 assembles the campus critical and non-critical electrical loads along with the penalty costs assigned to unmet loads estimated based on a study conducted by Lawrence Berkley National Laboratory (LBNL) on value of the electric utility service reliability for different types of customers [119].

Table 4-4- Penalty costs of unmet critical and non-critical electrical loads

	Non-Critical Elec. Loads (kWh)			Critical Elec. Loads (kWh)			Assigned Penalty Costs ($/kWh)	
	min	Average	Max	min	Average	Max	Non-critical	Critical
Summer* Days**	13,098	20,629	25,442	3,275	5,157	6,360	30	200
Summer Nights	11,269	16,760	21,676	2,817	4,190	5,419	15	200
Non-Summer Days	3,442	18,752	23,992	860	4,688	5,998	20	200
Non-Summer Nights	3,439	15,422	19,506	860	3,856	4,876	10	200

* May through October

** 7AM to 7PM

Since electrical loads vary by time of the day and throughout the year, the imposed penalty costs were calculated for grid failure were they to occur during different operational temporal periods and lasting for 106 minutes. In scenario A, for which the resilience assessment results are depicted in Figure 4-6, all critical and non-critical electrical loads will be unmet since there is no on-site power generation. Figure 4-6 shows the imposed costs if electric grid failure occurs during any of the operational temporal periods. The depicted error bars in the imposed costs are due to the variations in the campus loads (minimum and maximum loads are given in Table 4-4 for critical and non-critical loads during different operational temporal periods). For instance, if the power grid fails during a Summer day, the average imposed costs (from both critical and non-critical loads) would be around $4 million ranging from the low of $2.5 million to the high of $4.9 million.

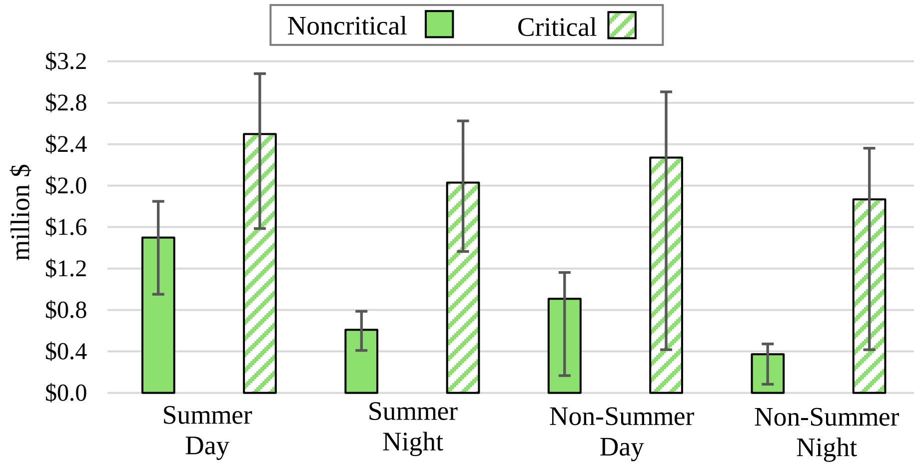

Figure 4-6- Scenario A (baseline), imposed costs due to unmet critical and non-critical electrical loads during electric grid failure. The error bands correspond to minimum and maximum loads during the respective seasons

In scenario B, a 9-MW CHP system was added to the baseline case. Since the gas turbine prime movers have fast ramping rates, we assumed that the CHP system will attain its maximum capacity very quickly once started in case of electric grid failure. It is obvious that the imposed costs (Figure 4-7) are considerably lower in scenario B as none of the critical loads are unmet. We found that the CHP system is able to meet a portion of the non-critical loads as well.

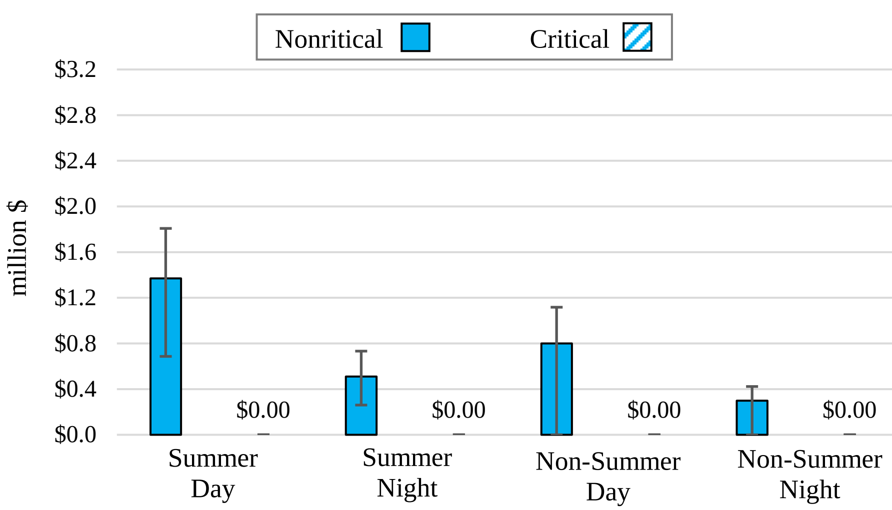

Figure 4-7- Scenario B (9MW CHP), imposed costs due to unmet critical and non-critical electrical loads during electric grid failure

Scenarios C, D, and E involve different penetration level of solar PV systems. Since the PV system output depends on the weather condition, three different conditions, namely overcast, partly sunny, and sunny, were considered so as to capture the variability in the PV output. Results of scenario C resilience assessment (Figure 4-8) indicate that the 6.8 MW solar PV cannot cover all the critical loads even if the weather conditions are favorable (sunny) unless critical loads are at their minimum levels. Since priority will be given to meet the critical loads, non-critical loads will not be covered before all critical loads are met; this can be achieved through optimal control of the energy system which incorporates the assigned penalty cost to the functionality losses (see Chapter 3). If a failure occurs during a Non-Summer sunny day during a period when the loads are at their minimum level, the solar PV system will be able to meet both critical and non-critical loads.

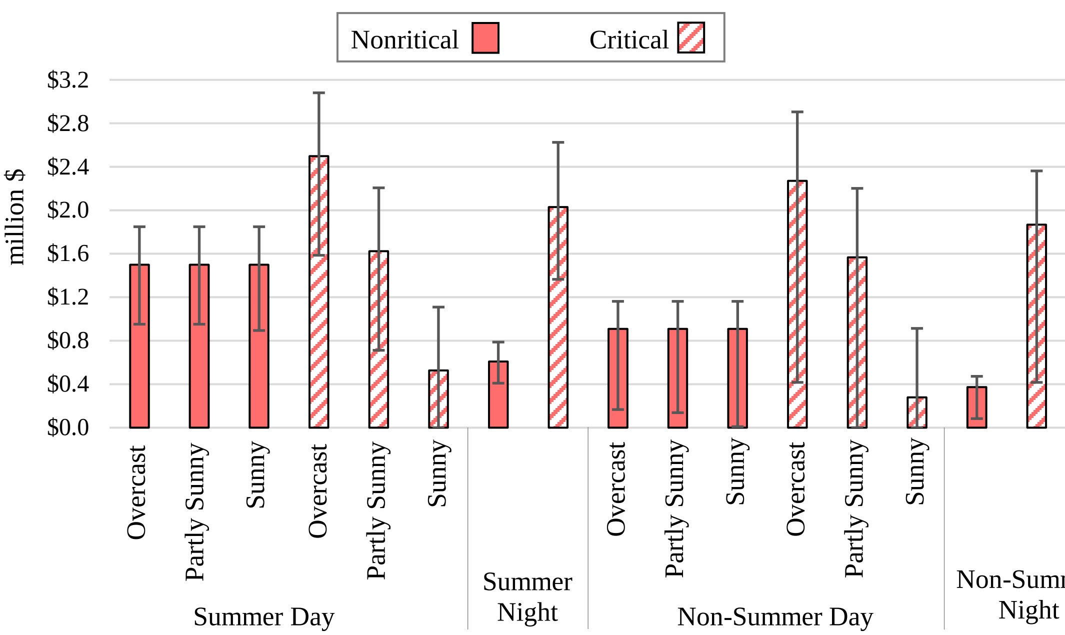

Figure 4-8- Scenario C (6.8MW Solar PV), imposed costs due to unmet critical and non-critical electrical loads during electric grid failure

Doubling the solar PV system capacity to 13.7 MW will improve the resilience performance of the energy system. This will enable the system to fully meet the critical loads and even partially cover the noncritical loads when it is sunny (see Figure 4-9).

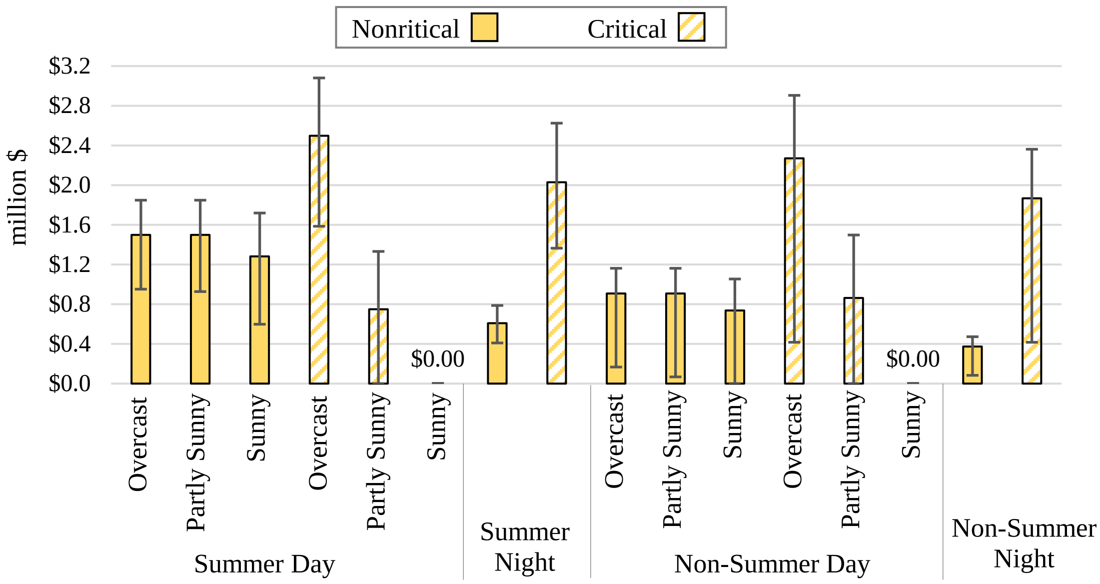

Figure 4-9- Scenario D (13.7MW PV), imposed costs due to unmet critical and non-critical electrical loads during electric grid failure

Comparing scenario D and scenario E results reveal that scenario E can provide better resilience compared to scenario D as all critical loads are met and some portion of the non-critical loads are covered as well. On the other hand, if the outage occurs during the night, the CHP system is able to cover the critical loads while in solar-only scenarios the energy system will not be resilient during nights.

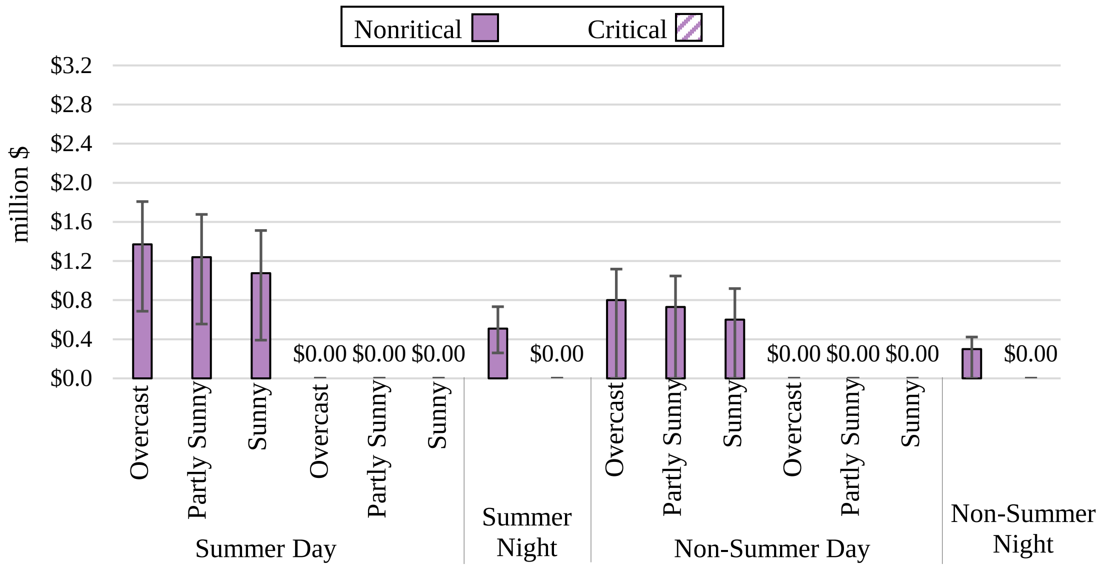

Figure 4-10- Scenario E (6.8MW PV + 9MW CHP), imposed costs due to unmet critical and non-critical electrical loads during electric grid failure

Figure 4-11 shows the energy system resilience in scenario F. It is evident that the diesel generators can cover all critical loads while also partially cover the non-critical electrical loads.

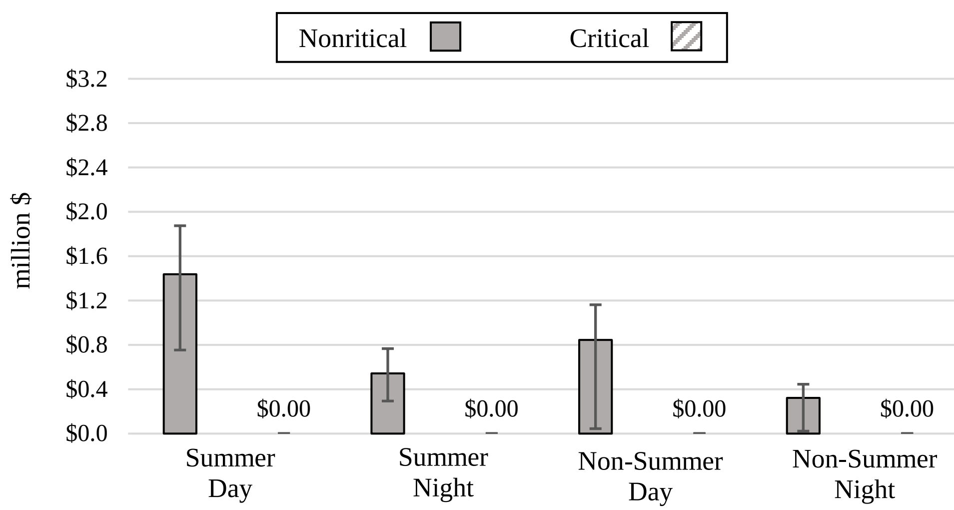

Figure 4-11- Scenario F (stand-by diesel generators), imposed costs due to unmet critical and non-critical electrical loads during electric grid failure

ReCI indices were calculated based on 95th percentile of loads during the selected operational temporal periods assuming that the system stakeholders would like to evaluate the system resilience when loads are quite high (Figure 4-12). It was found that utilization of the CHP system (with fast ramping rate) and emergency diesel generators can considerably improve resilience performance of the energy system. Regarding the scenarios with solar penetration (i.e. scenarios C, D, and E), average PV power output (partly sunny condition) was assumed for *ReCI* calculations. Implementation of solar PVs improves resilience performance of the system only during day time and is proportional to the solar penetration level. Comparing scenarios B and C, which have equal upfront cost, indicates that CHP systems, specifically with fast ramping characteristics, would improve energy systems resilience significantly.

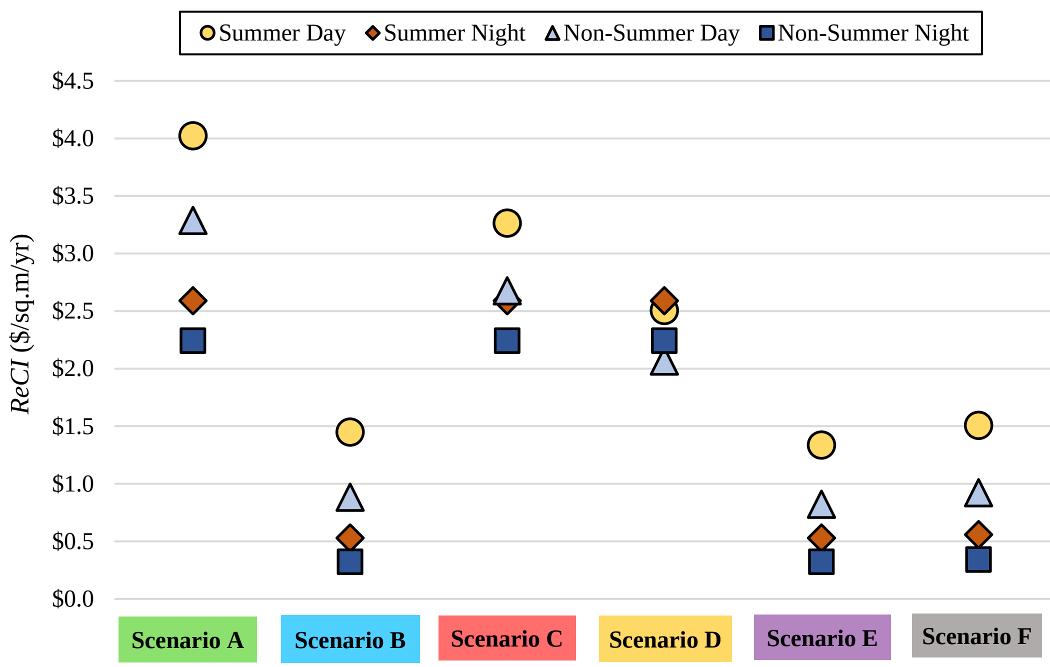

Figure 4-12- Resilience cost intensities (ReCI) for electric grid failure across all scenarios

4.3.3.4 Sustainability Compass and Decision Analysis

Results of the sustainability assessment of the energy system have been mapped on the Sustainability Compass (Figure 4-13). Sustainability status of all investigated scenarios are shown relative to the base case (scenario A) and to each other informing decision-maker how and to what extent each scenario affects the system performance in each sustainability criteria. Figure 4-13-a illustrates the IES performance in normal operation while Figure 4-13-b shows the system performance in confronting grid failure.

Comparing scenarios B and C, which have the same initial costs, reveals that scenario B has higher environmental impacts while it can improve resilience and economic performance of the system more significantly. If a stakeholder would like to double the investment, scenarios D and E would be the logical options. Results indicate that scenario E has much better economic and resilience performance while also reducing the overall environmental and health impacts compared to scenario A. Scenario F does not affect the *ExCI* index as the diesel generators will only run during outages. Also, the *EnCI* of the system will be higher in scenario F (compared to scenario A) as this option does not provide any savings during normal operation and the initial investments will result in a higher *EnCI* index. The *EnCI-ReCI* compass can be used to estimate how much to invest on resilience improvement measures as against potential imposed costs.

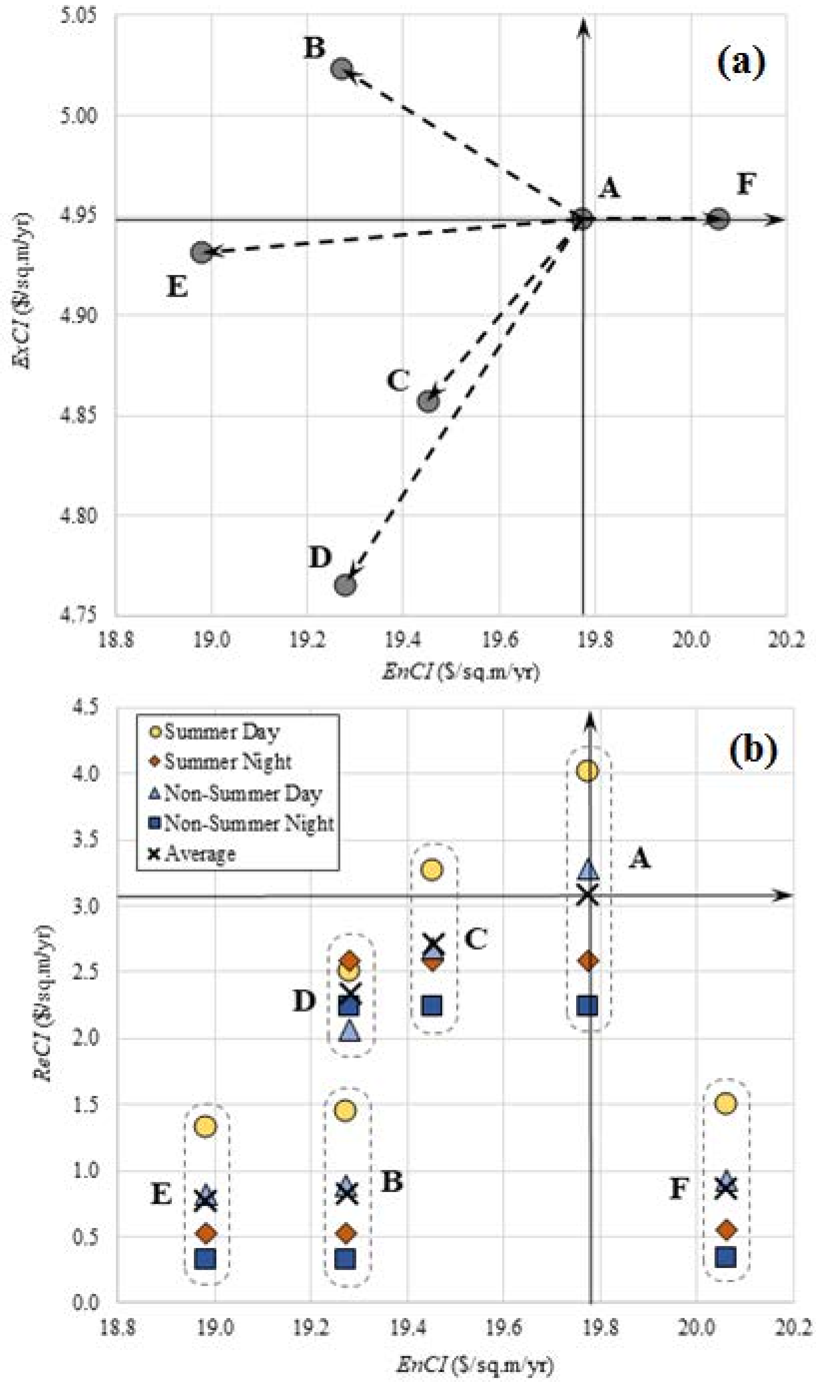

Figure 4-13-Sustainability Compass, EnCI versus ExCI changes

4.4. Summary and Future Works

Sustainable and resilient energy infrastructure are critical for sustainable development under normal conditions, and in confronting extreme conditions and disasters. Improving sustainability and resilience of energy systems have thus become a strategic goal both at national and local scales. This calls for a multi-criteria framework to assess sustainability of energy systems in different conditions enabling policy and decision makers to evaluate and track performance of such systems. This paper proposes a holistic assessment and quantification framework supporting sustainability-conscious design, operation, and development of energy systems at community scale.

As an extension to the EUI concept applied to individual buildings, we propose the use of three performance-based indices for sustainability benchmarking. The developed sustainability indices reflect normalized energy costs, environmental/health externalities and potential penalty costs associated with economic, environmental, and resilience dimensions respectively. A new way of communicating the analysis results via the "Sustainability Compass" diagram is proposed which would allow better decision-making since the direction and magnitude of changes in the sustainability indices under different scenarios is better revealed.

The proposed methodology has been illustrated using end-use monitored data for whole year operation of a university campus energy system; four energy development scenarios, with implementation of CHP system and various solar PV penetration levels, were identified and their sustainability performance were compared with the baseline case. Results of this analysis suggested that, with equal initial investments, CHP systems can provide 1.5 times more savings in *EnCI* (energy cost intensity) and 5 times more savings in *ReCI* (resilience cost intensity) indices compared to PV systems while causing more environmental/health impacts (higher *ExCI*, i.e. external cost intensity) relative to the base case. Given the uncertainties associated with *ReCI* index, it was found that only scenario E (both CHP and PV systems are implemented) can improve the energy system performance in all three sustainability criteria.

We anticipate three categories of extensions of the suggested sustainability assessment framework and of the Sustainability Compass representation. One category would be inclusion of other infrastructure systems, such as water system/infrastructure and transportation integrated with the community energy system. Second category would consider building construction and materials which may have both direct and indirect impacts on sustainability performance of the community. The third category is the extension of these concepts to optimally control and operate the energy systems based upon all sustainability criteria rather than solely based on economic variables.

Chapter 5 – Summary and Future Work

5.1 Summary

This study proposes a framework to assess, characterize and quantify key attributes of sustainability of integrated energy systems, which is one of the key elements of any community or facility, Sustainability of such systems, comprised of utility power plants, distributed generation technologies, and building heating and cooling systems, would essentially include two dimensions:

(a) system performance under normal conditions. A sustainable system has to be designed, operated, and supported such that its environmental impacts and costs are minimal; this is the concept of functional efficiency;

(b) system performance when stressed by internal or external disruptions posed by natural, manmade, or random events. In this circumstance, the system ought to be designed and managed such that losses of lives, assets, and functionalities are minimal. This can be achieved through various capacities, depending on type of the disruption and the system functions, such as robustness, adaptivity, and fast recovery, to name a few; these capabilities are generally referred to as resilience.

In this thesis, a new life-cycle and performance-based quantitative sustainability assessment framework have been developed which is focused on community scale energy systems. A more practical and specific definition of sustainable energy systems has been proposed and new quantitative sustainability indices and metrics have been suggested whereby sustainability concepts can be integrated more effectively into engineering design and planning practices. In addition, comprehensive methodologies have been developed for identifying and quantifying location and circumstance-specific environmental impacts under normal condition, and resilience of energy systems when disruptions occur. Specific features and key findings of each of the developed methodologies are summarized below:

(a) Functional efficiency under normal operation analysis enhanced by LCA (Chapter 2)

A pragmatic LCA methodology to quantitatively evaluate monetary costs of human health and environmental impacts of a specific community scale Integrated Energy Systems (IES) has been developed which capture the effect of real-time emissions from various energy systems including, utility power plants, distributed generation facilities, and building heating and cooling systems. The uncertainties associated with the results were analyzed using the Monte Carlo techniques. The developed approach described in this thesis can be integrated into design, operation, and development planning practices toward more sustainable engineered systems and infrastructure. Some of the capabilities of the proposed methodology were illustrated through a case study on a large university campus with more than 280 buildings. The external costs of electricity generation using on-site CHP system were found to be about 4.4 ¢/kWh (neglecting the recovered heat) which is considerably higher than both on-site solar systems (0.5 ¢/kWh) and utility-generated electricity (2 ¢/kWh). It was found that the amount of recovered heat plays a crucial role in external costs of a CHP system. In other words, the waste heat from the exhaust flue gas and from the motor jacket can be used to offset boilers fuel consumption by reducing their loading. The campus CHP system has overall efficiency of 71% which results in the external costs to be 1.86 ¢/kWh. Therefore, we can conclude that expanding the size of the CHP plant along with thermal heat recovery to offset the use of boilers would be a sustainable option.

(b) Performance based resiliency analysis (Chapter 3)

Through modeling of system response to potential internal and external failures (called failure modes) during different operational temporal periods (such as different diurnal and seasonal periods of the year), the proposed methodology quantifies resilience of the system based upon loss in the services which the system is designed to deliver. A three-dimensional matrix, called Loss Matrix, is introduced whose elements represent the undelivered system services under different scenarios, i.e. combinations of failure modes and different operational temporal periods. Assigning monetary penalty costs to such losses and including them in the objective function of an optimization model of the entire system allows the three-dimension loss matrix to be reframed into a two-dimensional Consequence Matrix where individual elements represent the imposed penalty costs to the system stakeholders due to undelivered services and/or non-optimal system performance. Normalizing the individual elements results in the Resilience Matrix of the system for different scenarios.

The performance-based resilience assessment framework developed in this study offers several advantages compared to the existing ones: (i) through a constraint optimization model of the system, the system performance during disruption can be realistically modeled accounting for physical, economic, and operational limitations; such models are usually available for operational control and optimization and can be modified to include penalty costs and possible failure scenarios to be used for resilience assessment purposes; (ii) the developed framework can be implemented for different types of engineered systems and is able, and meant to, handle multi-functional systems; (iii) quantification of resilience performance in monetary terms facilitates resilience considerations to be incorporated in cost-effectiveness analyses; (iv) it directly targets system performance when confronted a disruption, rather than focusing on system characteristics, e.g. faster recovery, which may or may not improve the system respond to the disruption.

(c) <u>Combining normal operation and resilience and introduction of the sustainability compass</u> (Chapter 4)

New sustainability indices were proposed for energy systems which capture the impacts on environment and people heath, economic performance of the system, and resilience performance, identified by normalized environmental/health externalities, energy costs, and penalty costs respectively. A new way of presentation of results, called "Sustainability Compass" diagram is proposed which facilitates communication of the assessment results and would allow sounder decision-analysis since different system attributes are captured and trade-offs between different scenarios are better identified and revealed.

The proposed methodology has been illustrated using end-use monitored data for a whole year of operation of a university campus energy system; four energy development scenarios, with implementation of CHP system and various solar PV penetration levels, were identified and their sustainability performance were compared with the baseline case. Results of this analysis suggested that, with equal initial investments, CHP systems can provide 1.5 times more savings in *EnCI* (energy cost intensity) and 5 times more savings in *ReCI* (resilience cost intensity) indices compared to PV systems while causing more environmental/health impacts (higher *ExCI*, i.e. external cost intensity) relative to the base case. Given the uncertainties associated with *ReCI* index, it was found that only scenario E (both CHP and PV systems are implemented) can improve the energy system performance in all three sustainability criteria.

5.2 Future Work

This research opens up a number of avenues worth exploring. These have been divided into immediate (or lower-level) issues, and broader extensions, the latter requiring a higher level of conceptual formulation and development effort.

<u>5.2.1 Immediate Extensions</u>

(a) Integration of the developed concepts to optimally control and operate energy systems based upon a larger set of sustainability criteria, which may not be translated into economic variables.

(b) More subtle consideration of the criticality of loads (rather than simply considering them to be *critical* and *non-critical* and expressing associated service loss penalties as a non-linear function with relevant uncertainties stated as, say fuzzy numbers.

(c) Including frequency of occurrences of different failure modes and their duration which is important for investments relate to enhancing resiliency.

(d) Aggregation of various scenario results of system resilience analysis into one composite resilience index.

(e) Apply the developed methodology to a real-world case using data collected for multiple years in which weather and building load variabilities, both seasonally and across years, are represented in a probabilistic manner.

(f) Emphasizing the social elements in the analysis through fuzzy weights applied during the decision analysis process.

5.2.2 Broader Extensions

(a) Inclusion of building construction and materials into the LCA analysis which may have both direct and indirect impacts on sustainability performance of the community; direct effects are those economic, environmental, and resilience impacts associated with the materials and construction techniques, while indirect effects could be, for instance, effects of the selected material on energy performance of buildings.

(b) Extending the developed framework to the energy infrastructure at aggregated levels (such as electric grid) which would include a whole new set of sustainability metrics.

(c) Defining the concept of “absolute sustainable system/community” as a reference point, akin to the exergy efficiency concept. The best sustainable building would be defined depending upon type of the building, geographical location, and climatic conditions since availability of renewable energies, as a key element, and power generation resources varies greatly from place to place.

(d) Inclusion of water, sewage, communication, and transportation system/infrastructure coupled with the community energy system. Analyzing the interconnection among these infrastructures, their reliance on each other, and service losses due to various failure modes will provide insight towards resilience of complex systems.

(e) Extending the current resilience assessment methodology which is limited to events that cause little or no physical damage, to more extreme events including disasters.

REFERENCES

[1] United Nations. Our Common Future (the Brundtland Report). Oxford, Oxford University Press: 1987.

[2] U.S. Energy Information Administration (EIA). Today in Energy 2017. http://www.eia.gov/todayinenergy/.

[3] Doukas H, Papadopoulou A, Savvakis N, Tsoutsos T, Psarras J. Assessing energy sustainability of rural communities using Principal Component Analysis. Renew Sustain Energy Rev 2012;16:1949–57. doi:10.1016/j.rser.2012.01.018.

[4] U.S. Energy Information Administration (EIA). Consumption and Efficiency 2017. https://www.eia.gov/consumption/.

[5] Wald ML. Fossil Fuels' Hidden Cost Is in Billions, Study Says. New York Times 2009.

[6] Hohmeyer O. Social Costs of Energy Consumption: External Effects of Electricity Generation in the Federal Republic of Germany. New York: Springer; 1988.

[7] Wicke L. Die ökologischen Milliarden: das kostet die zerstörte Umwelt - so können wir sie retten. Goldmann; 1988.

[8] Rabl A, Rabl VA. External Costs of Nuclear: Greater or Less Than the Alternatives? Energy Policy 2013;57:575–84.

[9] Rabl A, Spadaro J V. External Costs of Energy: How Much Is Clean Energy Worth? Sol Energy Eng 2016;138:1–8.

[10] Cohon J, Cropper M, Greenbaum D, Wassel R. Hidden Costs of Energy-Unpriced Concequences of Energy Production and Use. Washington, D.C.: National Academies Press; 2010.

[11] Corona B, Cerrajero E, Lopez D, San Miguel G. Full Environmental Life Cycle Cost Analysis of Concentrating Solar Power Technology: Contribution of Externalities to Overall Energy Costs. Sol Energy 2016;135:758–68.

[12] Mattmann M, Logar I, Brouwer R. Hydropower Externalities: A Meta-analysis. Energy Econ 2016;57:66–77.

[13] Zhang J, Xu L, Li X. Review on the Externalities of Hydropower: A Comparison Between Large and Small Hydropower Projects in Tibet Based on the CO2 Equivalent. Renew Sustain Energy Rev 2015;50:176–85.

[14] Hacatoglu K, Dincer I, Rosen MA. A new model to assess the environmental impact and sustainability of energy systems. J Clean Prod 2015;103:211–8. doi:10.1016/j.jclepro.2014.06.050.

[15] Krewitt W. External Costs of Energy - Do the Answers Match the Questions? Looking Back at 10 Years of ExternE. Energy Policy 2002;30:839–48.

[16] Georgakellos DA. Impact of a Possible Environmental Externalities Internalisation on Energy Prices: The Case of the Greenhouse Gases from the Greek Electricity Sector. Energy Econ 2010;32:202–9.

[17] Kosugi T, Tokimatsu K, Kurosawa A, Itsubo N, Yagita H, Sakagami M. Internalization of the External Costs of Global Environmental Damage in an Integrated Assessment Model. Energy Policy 2009;37:2664–78.

[18] Owen AD. Renewable Energy: Externality Costs As Market Barriers. Energy Policy 2006;34:632–42.

[19] Moslehi S, Arababadi R. Sustainability Assessment of Complex Energy Systems Using Life Cycle Approach-Case Study: Arizona State University Tempe Campus. Procedia Eng., vol. 145, Elsevier Ltd; 2016, p. 1096–103.

[20] Afgan NH, Carvalho MG, Hovanov N V. Energy system assessment with sustainability indicators. Energy Policy 2000;28:603–12.

[21] Evans A, Strezov V, Evans TJ. Assessment of Sustainability indicators for Renewable Energy Technologies. Renew Sustain Energy Rev 2009;13:1082–8.

[22] Diakoulaki D, Mirasgedis S, Tourkolias C. Assessment and Exploitation of Energy-related Externalities in the Industrial Sector. Energy Policy 2007;35:2925–38.

[23] Goncalves J, Martins A, Neves L. Methodology for real impact assessment of the best location of distributed electric energy storage. Sustain Cities Soc 2016;26:531–42. doi:10.1016/j.scs.2016.05.010.

[24] Gaterell MR, McEvoy ME. The Impact of Energy Externalities on the Cost Effectiveness of Energy Efficiency Measures Applied to Dwellings. Energy Build 2005;37:1017–27.

[25] Arababadi R, Moslehi S, El M, Haavaldsen T, Parrish K. Energy policy assessment at strategic , tactical , and operational levels : Case studies of EU 20-20-20 and U . S . Executive Order 13514. Energy Policy 2017;109:530–8.

[26] Sovacool BK, Perea MAM, Matamoros AV, Enevoldsen P. Valuing the manufacturing externalities of wind energy: assessing the environmental profit and loss

of wind turbines in Northern Europe. Wind Energy 2016;19:1623–47. doi:10.1002/we.

[27] Garcia R, Marques P, Freire F. Life-cycle assessment of electricity in Portugal. Appl Energy 2014;134:563–72. doi:10.1016/j.apenergy.2014.08.067.

[28] Messagie M, Mertens J, Oliveira L, Rangaraju S, Sanfelix J, Coosemans T, et al. The hourly life cycle carbon footprint of electricity generation in Belgium, bringing a temporal resolution in life cycle assessment. Appl Energy 2014;134:469–76. doi:10.1016/j.apenergy.2014.08.071.

[29] Varun, Sharma A, Shree V, Nautiyal H. Life cycle environmental assessment of an educational building in Northern India : A case study. Sustain Cities Soc 2012;4:22–8. doi:10.1016/j.scs.2012.03.002.

[30] Sim J, Sim J. The atmospheric environmental impact of a Korean traditional building ’ s life cycle , along with carbon footprint analysis. Sustain Cities Soc 2017;28:172–86. doi:10.1016/j.scs.2016.09.008.

[31] International Organization for Standardization. ISO 14040-Environmental management - Life Cycle Assessment - Principles and Framework. vol. 3. 2006.

[32] Šulga M. Life Cycle Assesment (LCA) Based Environmental Impact Minimization of Solid Fuel Boilers in Lithuanian Industry. Environ Res Eng Manag 2011;4:74–84.

[33] Longo S, Cellura M, Guarino F, Rocca V La, Maniscalco G. Embodied energy and environmental impacts of a biomass boiler : a life cycle approach. AIMS Energy 2015;3:214–26.

[34] Gazis E, Harrison GP. Life Cycle Energy and Carbon Analysis of Domestic Combined Heat and Power Generators. IEEE Trondheim PowerTech 2011:19–23.

[35] Vignali G. Environmental assessment of domestic boilers : A comparison of condensing and traditional technology using life cycle assessment methodology. J Clean Prod 2017;142:2493–508. doi:10.1016/j.jclepro.2016.11.025.

[36] Beccali M, Cellura M, Longo S. Report on Life cycle analysis. 2014.

[37] Dones R, Heck T, Bauer C, Hirschberg S, Bickel P, Preiss P, et al. ExternE-Pol Externalities of Energy : Extension of Accounting Framework and Policy Applications New energy technologies. 2005.

[38] Machol B, Rizk S. Economic Value of U.S. Fossil Fuel Electricity Health Impacts. Environ Int 2013;52:75–80.

[39] Goodkind AL, Polasky S. Health & Environmental Costs of Electricity Generation in Minnesota. 2013.

[40] Mariel P, Meyerhoff J, Hess S. Heterogeneous preferences toward landscape externalities of wind turbines - Combining choices and attitudes in a hybrid model. Renew Sustain Energy Rev 2015;41:647–57.

[41] Board of Governors of the Federal Reserve System-The Discount Rate 2018. https://www.federalreserve.gov/monetarypolicy/discountrate.htm (accessed December 3, 2018).

[42] NREL. Hourly Energy Emission Factors for Electricity Generation in the United States - Data.gov 2016. https://catalog.data.gov/dataset/hourly-energy-emission-factors-for-electricity-generation-in-the-united-states-73720 (accessed June 5, 2017).

[43] U.S. Environmental Protection Agency (EPA). eGRID Subregion Representational Map n.d. https://www.epa.gov/energy/egrid-subregion-representational-map (accessed July 6, 2017).

[44] U.S. Energy Information Administration (EIA). Arizona Net Electricity Generation by Source 2017. https://www.eia.gov/state/?sid=AZ (accessed July 9, 2017).

[45] U.S. Energy Information Administration (EIA). How much electricity is lost in transmission and distribution in the United States? 2017. https://www.eia.gov/tools/faqs/faq.php?id=105&t=3 (accessed September 3, 2017).

[46] U.S. Environmental Protection Agency (EPA). The Emissions and Generation Resource Integrated Database- eGRID2014. Washington, DC 20460: 2017.

[47] U.S. Energy Information Administration (EIA). Electricity Generation and Environmental Externalities: Case Studies. Washington, DC: 1995.

[48] U.S. Energy Information Administration (EIA). Heat Content of Natural Gas Consumed 2017. https://www.eia.gov/dnav/ng/ng_cons_heat_a_EPG0_VGTH_btucf_a.htm (accessed November 8, 2017).

[49] Deru M, Torcellini P. Source Energy and Emission Factors for Energy Use in Buildings. National Renewable Energy Laboratory. Golden, Colorado: 2007.

[50] Swiss Centre For Life Cycle Inventories. Ecoinvent Database 2.2 (2010). Ecoinvent Cent 2007;2.0.

[51] Halasah SA, Pearlmutter D, Feuermann D. Field Installation Versus Local Integration of Photovoltaic Systems and Their Effect On Energy Evaluation Metrics.

Energy Policy 2013;52:462–71.

[52] United States Census Bureau. Thematic Maps 2010. https://www.census.gov/geo/maps-data/maps/thematic.html (accessed May 12, 2017).

[53] Bozza A, Asprone D, Manfredi G. Developing an Integrated Framework to Quantify Resilience of Urban Systems Against Disasters. Nat Hazards 2015;78:1729–48. doi:10.1007/s11069-015-1798-3.

[54] Betty Biringer, Eric Vugrin DW. Critical Infrastructure System Security and Resiliency. 1st ed. CRC; 2013.

[55] Pimm SL. The Complexity and Stability of Ecosystems. Nature 1984;307:321–6. doi:10.1038/315635c0.

[56] Hatvani-Kovacs G, Belusko M, Skinner N, Pockett J, Boland J. Heat Stress Risk and Resilience in the Urban Environment. Sustain Cities Soc 2016;26:278–88. doi:10.1016/j.scs.2016.06.019.

[57] Zobel CW, Khansa L. Characterizing Multi-event Sisaster Resilience. Comput Oper Res 2014;42:83–94. doi:10.1016/j.cor.2011.09.024.

[58] Chang SE, Mcdaniels T, Fox J, Dhariwal R, Longstaff H. Toward Disaster-resilient Cities: Characterizing Resilience of Infrastructure Systems with Expert Judgments. Risk Anal 2014;34:416–34. doi:10.1111/risa.12133.

[59] Maliszewski PJ, Perrings C. Factors in the Resilience of Electrical Power Distribution Infrastructures. Appl Geogr 2012;32:668–79. doi:10.1016/j.apgeog.2011.08.001.

[60] Cimellaro GP, Reinhorn AM, Bruneau M. Framework for Analytical Quantification of Disaster Resilience. Eng Struct 2010;32:3639–49. doi:10.1016/j.engstruct.2010.08.008.

[61] Attoh-Okine NO, Cooper AT, Mensah SA. Formulation of Resilience Index of Urban Infrastructure Using Belief Functions. IEEE Syst J 2009;3:147–53. doi:10.1109/JSYST.2009.2019148.

[62] Cutter SL, Barnes L, Berry M, Burton C, Evans E, Tate E, et al. A Place-based Model for Understanding Community Resilience to Natural Disasters. Glob Environ Chang 2008;18:598–606. doi:10.1016/j.gloenvcha.2008.07.013.

[63] Ouyang M, Dueñas-osorio L, Min X. A three-stage resilience analysis framework for urban infrastructure systems. Struct Saf 2012;36–37:23–31. doi:10.1016/j.strusafe.2011.12.004.

[64] Ouyang M, Fang Y. A Mathematical Framework to Optimize Critical Infrastructure Resilience against Intentional Attacks. Comput Civ Infrastruct Eng 2017;00:1–21. doi:10.1111/mice.12252.

[65] Ouyang M. A mathematical framework to optimize resilience of interdependent critical infrastructure systems under spatially localized attacks. Eur J Oper Res 2017;262:1072–84. doi:10.1016/j.ejor.2017.04.022.

[66] Ouyang M, Dueñas-osorio L. Multi-dimensional hurricane resilience assessment of electric power systems. Struct Saf 2014;48:15–24. doi:10.1016/j.strusafe.2014.01.001.

[67] Ouyang M, Wang Z. Resilience assessment of interdependent infrastructure systems : With a focus on joint restoration modeling and analysis. Reliab Eng Syst Saf 2015;141:74–82. doi:10.1016/j.ress.2015.03.011.

[68] Lin Y, Bie Z. Tri-level optimal hardening plan for a resilient distribution system considering reconfiguration and DG islanding. Appl Energy 2018;210:1266–79. doi:10.1016/j.apenergy.2017.06.059.

[69] Alderson DL, Brown GG, Carlyle WM. Operational Models of Infrastructure Resilience. Risk Anal 2015;35:562–87. doi:10.1111/risa.12333.

[70] Matelli JA, Goebel K. Conceptual design of cogeneration plants under a resilient design perspective: Resilience metrics and case study. Appl Energy 2018;215:736–50. doi:10.1016/j.apenergy.2018.02.081.

[71] Vugrin ED, Turnquist MA, Brown NJK. Optimal recovery sequencing for enhanced resilience and service restoration in transportation networks. Int J Crit Infrastructures 2014;10:218–46.

[72] Turnquist M, Vugrin E. Design for resilience in infrastructure distribution networks. Environ Syst Decis 2013;33:104–20. doi:10.1007/s10669-012-9428-z.

[73] Biringer BE, Vugrin E, Warren D. Critical Infrastructure System Security and Resiliency. Boca Raron, FL: CRC Press; 2013.

[74] Mousavizadeh S, Haghifam MR, Shariatkhah MH. A linear two-stage method for resiliency analysis in distribution systems considering renewable energy and demand response resources. Appl Energy 2018;211:443–60. doi:10.1016/j.apenergy.2017.11.067.

[75] Lacommare KH, Eto JH. Cost of Power Interruptions to Electricity Consumers in the United States (U.S.). 2006.

[76] Centolella P., Farber-DeAnda M., Greening L. A. KT. Estimates of the Value of

Uninterrupted Service for The Mid-West Independent System Operator. 2010.

[77] Pipattanasomporn M, Feroze H, Rahman S. Securing critical loads in a PV-based microgrid with a multi-agent system. Renew Energy 2012;39:166–74. doi:10.1016/j.renene.2011.07.049.

[78] Sujil A, Agarwal SK, Kumar R. Centralized multi-agent implementation for securing critical loads in PV based microgrid. J Mod Power Syst Clean Energy 2014;2:77–86. doi:10.1007/s40565-014-0047-1.

[79] Maor I, Reddy TA. Cost penalties of near-optimal scheduling control of BCHP systems: Part I - Selection of case study scenarios and data generation. ASHRAE Trans 2009.

[80] Reddy TA, Maor I. Cost Penalties of Near-Optimal Scheduling Control of BCHP Systems : Part II — Modeling , Optimization , and Analysis Results. ASHRAE Trans 2009;115.

[81] Reddy TA, Moslehi S, Inanlouganji A. Predictive Scheduling and Control of IES: Mathematical Modeling and Results of Scenario Optimization. Technical Report, Submitted to Pacific Northwest National Laboratory. 2018.

[82] Strang G. Linear Algebra and Its Applications. 4th Editio. Delhi, India: Cengage Learning Intia Private Limited; 2011.

[83] Sullivan MJ, Mercurio M, Schellenberg J. Estimated Value of Service Reliability for Electric Utility Customers in the United States. Berkeley, CA: 2009.

[84] Natural Gas Pipeline Safety and Reliability : An Assessment of Progress, American Gas Foundation. 2015.

[85] System Advisor Model (SAM). National Renewable Energy Laboratory (NREL) 2010. https://sam.nrel.gov/.

[86] Fu R, Feldman D, Margolis R, Woodhouse M, Ardani K, Fu R. U.S. Solar Photovoltaic System Cost Benchmark : Q1 2017. 2017.

[87] Kintner-Meyer M, Subbarao K, Kumar NP, Bandyopadhyay G, Finley C, Koritarov VS, et al. The Role of Energy Storage in Commercial Building A Preliminary Report. 2010.

[88] Vazquez M, Rey-stolle I. Photovoltaic Module Reliability Model Based on Field Degradation Studies. Prog PHOTOVOLTAICS Res Appl 2008. doi:10.1002/pip.

[89] Liu M, Li W, Wang C, Polis MP, Wang LY, Li J. Reliability Evaluation of Large

Scale Battery Energy Storage Systems. IEEE Trans Smart Grid 2017;8:2733–43.

[90] Islam T, Hofmann A, Hyland M. Evaluation of Data Submitted in APPA's 2013 Distribution System Reliability & Operations Survey. Washington D.C.: 2014.

[91] Kowalski K, Stagl S, Madlener R, Omann I. Sustainable energy futures: Methodological challenges in combining scenarios and participatory multi-criteria analysis. Eur J Oper Res 2009;197:1063–74. doi:10.1016/j.ejor.2007.12.049.

[92] Atilgan B, Azapagic A. An integrated life cycle sustainability assessment of electricity generation in Turkey. Energy Policy 2016;93:168–86. doi:10.1016/j.enpol.2016.02.055.

[93] Santoyo-Castelazo E, Azapagic A. Sustainability assessment of energy systems: Integrating environmental, economic and social aspects. J Clean Prod 2014;80:119–38. doi:10.1016/j.jclepro.2014.05.061.

[94] Mainali B, Silveira S. Using a sustainability index to assess energy technologies for rural electrification. Renew Sustain Energy Rev 2015;41:1351–65. doi:10.1016/j.rser.2014.09.018.

[95] Diniz da Costa JC, Pagan RJ. Sustainability Metrics for Coal Power Generation in Australia. Process Saf Environ Prot 2006;84:143–9. doi:10.1205/psep.04126.

[96] Fthenakis V. Sustainability of photovoltaics: The case for thin-film solar cells. Renew Sustain Energy Rev 2009;13:2746–50. doi:10.1016/j.rser.2009.05.001.

[97] Frangopoulos CA, Keramioti DE. Multi-Criteria evaluation of energy systems with sustainability considerations. Entropy 2010;12:1006–20. doi:10.3390/e12051006.

[98] Dombi M, Kuti I, Balogh P. Sustainability assessment of renewable power and heat generation technologies. Energy Policy 2014;67:264–71. doi:10.1016/j.enpol.2013.12.032.

[99] Hadian S, Madani K. A system of systems approach to energy sustainability assessment: Are all renewables really green? Ecol Indic 2015;52:194–206. doi:10.1016/j.ecolind.2014.11.029.

[100] Iddrisu I, Bhattacharyya SC. Sustainable Energy Development Index: A multi-dimensional indicator for measuring sustainable energy development. Renew Sustain Energy Rev 2015;50:513–30. doi:10.1016/j.rser.2015.05.032.

[101] Sharma T, Balachandra P. Benchmarking sustainability of Indian electricity system: An indicator approach. Appl Energy 2015;142:206–20. doi:10.1016/j.apenergy.2014.12.037.

[102] Dincer I, Acar C. Smart energy systems for a sustainable future. Appl Energy 2017;194:225–35. doi:10.1016/j.apenergy.2016.12.058.

[103] Phillips J. Determining the sustainability of large-scale photovoltaic solar power plants. Renew Sustain Energy Rev 2013;27:435–44. doi:10.1016/j.rser.2013.07.003.

[104] Turney D, Fthenakis V. Environmental impacts from the installation and operation of large-scale solar power plants. Renew Sustain Energy Rev 2011;15:3261–70. doi:10.1016/j.rser.2011.04.023.

[105] Siew RYJ, Balatbat MCA, Carmichael DG. A review of building/ infrastructure sustainability reporting tools (SRTs). Smart Sustain Built Environ 2013;2:106–39. doi:10.1016/j.jenvman.2015.09.010.

[106] Roth S, Hirschberg S, Bauer C, Burgherr P, Dones R, Heck T, et al. Sustainability of electricity supply technology portfolio. Ann Nucl Energy 2009;36:409–16. doi:10.1016/j.anucene.2008.11.029.

[107] Begić F, Afgan NH. Sustainability assessment tool for the decision making in selection of energy system-Bosnian case. Energy 2007;32:1979–85. doi:10.1016/j.energy.2007.02.006.

[108] Karger CR, Hennings W. Sustainability evaluation of decentralized electricity generation. Renew Sustain Energy Rev 2009;13:583–93. doi:10.1016/j.rser.2007.11.003.

[109] Schlör H, Fischer W, Hake JF. Methods of measuring sustainable development of the German energy sector. Appl Energy 2013;101:172–81. doi:10.1016/j.apenergy.2012.05.010.

[110] Dapkus R, Streimikiene D. Sustainability of Electricity Generation Technologies in EU. Int J e-Education, e-Business, e-Management e-Learning 2013;3. doi:10.7763/IJEEEE.2013.V3.188.

[111] Lo Prete C, Hobbs BF, Norman CS, Cano-Andrade S, Fuentes A, von Spakovsky MR, et al. Sustainability and reliability assessment of microgrids in a regional electricity market. Energy 2012;41:192–202. doi:10.1016/j.energy.2011.08.028.

[112] Safaei A, Freire F, Henggeler Antunes C. A life cycle multi-objective economic and environmental assessment of distributed generation in buildings. Energy Convers Manag 2015;97:420–7. doi:10.1016/j.enconman.2015.03.048.

[113] Lako P. Combined Heat and Power- Technology Brief E04. 2010. doi:10.1533/9781845694548.154.

[114] Noreika M, Downes K, OLeary M, Stitzer J. CHP Implementation : Designing Combined Heat & Power Financial Incentives and Eligibility Requirements for Non-Residential Demand-Side Management Programs Combined Heat and Power as a Demand-Side Management Solution. ACEEE Summer Study Energy Effic. Ind., 2013, p. 1–11.

[115] Database of State Incentives for Renewables & Efficiency (DSIRE), Business Energy Investment Tax Credit (ITC) 2018. http://programs.dsireusa.org/system/program/detail/658 (accessed March 5, 2018).

[116] Database of State Incentives for Renewables & Efficiency (DSIRE), Non-Residential Solar & Wind Tax Credit (Corporate) 2016. http://programs.dsireusa.org/system/program/detail/1661 (accessed March 5, 2018).

[117] Kurtz J, Saur G, Sprik S, Ainscough C. Backup Power Cost of Ownership Analysis and Incumbent Technology Comparison. 2014.

[118] Matt CF, Vieira LSR, Soares GFW, Faria LPT De. Optimization of the Operation of Isolated Industrial Diesel Stations. 6th World Congr. Struct. andMultidisciplinary Optim., Rio de Janeiro: 2005.

[119] Sullivan MJ, Schellenberg J, Blundell M. Updated Value of Service Reliability Estimates for Electric Utility Customers in the United States. 2015. doi:LBNL-2132E.

APPENDIX A

OPTIMIZATION MODEL FOR SUPERVISORY CONTROL OF INTEGRATED ENERGY SYSTEMS

Abstract

Work undertaken towards modeling and optimization in support of optimal receding horizon scheduling and control of integrated energy systems (IES) composed of on-site power generation, electrical and thermal energy storage, heating and cooling equipment is described in this appendix. The objective function is defined as accumulative operational cost of the IES over the simulation period which has been selected as 24 hours. Various black-box models of equipment performance were integrated into the optimization framework to identify the optimal values for dispatch and loading of different system components which were selected as decision variables. These inherently non-linear performance models were then replaced by segmented linear models in order to simplify the optimization model to a MILP (Mixed Integer Linear Problem) problem to reduce the numerical and computational burden. Hourly values over a 24-hour period of electricity and fuel price structures and building electrical and thermal loads along with individual component capacities and performance constraints are the needed inputs to the model.

A case study IES systems was carefully selected and inputs properly defined so that different solution methodologies of optimization could be performed (different linearization schemes, different solution approaches, different solvers and programming languages). The IES modeled in this case study includes 2 prime movers, 2 boilers, 2 VC chillers and one absorption chiller as well as a battery storage; the optimization modeling was performed for 4 sample days, namely Summer day with high loads, Summer day with low loads, Winter day with high loads, and Winter day with low loads. The results

of our analysis were very consistent with those obtained by two other groups of researchers within the framework of a separate funded research study.

Nomenclature

$a1, a2, \ldots$	Model coefficients
C	Cost ($)
C_p	Specific heat (kJ/kg. ^{o}C)
CL	Charge level
DoD	Depth of Discharge of storage systems
E	Electrical energy (kWh)
EES	Electrical Energy Storage
F	Fuel consumption (kJ/h)
i	Component indicator
m	Mass flow rate (kg/s)
Q	Thermal energy (heating or cooling)
RD	Ramp Down rate of equipment
RU	Ramp Up rate of equipment
S	System/component availability indicator (binary values, 1: available, and 0: unavailable)
SOC	State of Charge (kWh or MMBtu)
t	Time step (h)
T	Temperature (˚C)
TES	Thermal Energy Storage

TL	Time Lock
X	Minimum allowable part-load-ratio

<u>Subscripts:</u>

a	Air
AC	Absorption chiller
$bldg$	Building
$boiler$	Boiler
buy	Buying electricity from utility
c	Cooling
CR	Capacity Ratio
CT	Cooling Tower
cdi	Condenser inlet
$chrg$	Charging
$cooling$	Cooling
db	Dry-bulb
$demand$	Demand
dis	Discharging
EES	Electrical Energy Storage
$elec$	Electricity
gas	Natural gas (or any other fuel)
$grid$	Electrical grid

h	Used for heating
$heating$	Heating
HRU	Heat recovery unit
HX	Heat Exchanger
in	Inlet
max	Maximum
min	Minimum
n	Number of components
on/off	Component on/off status
$onP/offP$	On-peak and off-peak hours
PLF	Part-Load Fraction
PLR	Part-Load Ratio
PM	Prime mover
PV	Photovoltaic
sat	Saturation
$sell$	Sellback electricity to utility
TES	Thermal Energy Storage
VC	Vapor compression chiller
w	Water
η	Efficiency
ε	Effectiveness

<u>Superscript</u>

* Rated condition/Capacity

A.1 Introduction

This appendix describes the scheduling and optimal dispatch of Integrated Energy Systems (IES) as well as results of the analyzed case study. Details of how the objective function, the underlying part-load models of the various systems along with the range bounds and constraints have been framed are provided. The part-load component performance models are non-linear, and combined with the equipment scheduling aspect which involve binary variables to identify on/off status of each component, the optimization problem falls in the mixed integer non-linear programming (MINLP) category. Lingo software package was used for the purpose of this optimization analysis. However, initial evaluations led us to conclude that the MINLP approach to IES optimizing problems are time consuming and do not seem to converge to proper global minimum. Hence, the part-load models have been reframed as segmented linear models, which was later independently verified to be a valid approach by two other research groups tasked to analyze the same scenario using optimization models and software developed independently.

A.2 IES Plant Subsystems and Components

Figure A-1 is a schematic of a generic IES depicting how some of the main subsystems and components, i.e. prime movers, boilers, vapor compression chillers, absorption chillers, wet cooling towers and heat recovery loop are often connected to serve the building/facility heating, cooling, and electrical loads. The sketch includes a solar PV system but thermal and battery storage sub-systems have not been included. An IES can contain additional (or fewer) individual equipment than that shown here.

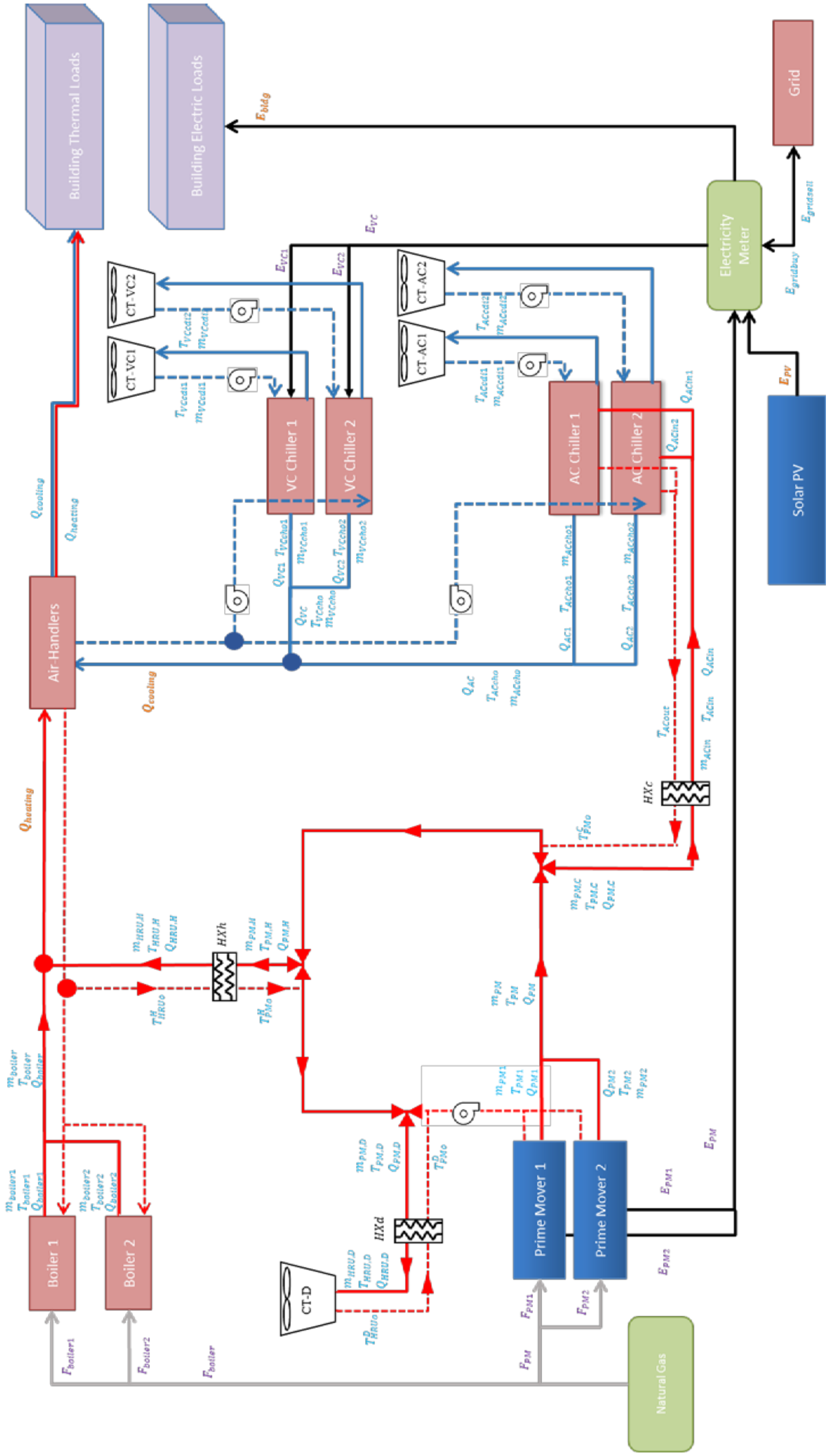

Figure A-1- Generic Schematic of an IES system without storage

A.3 Description of Mathematical Optimization Model

A.3.1 Model Scenarios

The test simulation scenario described in this section is meant to minimize operational costs of a grid-connected IES system which includes CHP systems, vapor compression chillers, absorption chillers, boilers, and PV system. The optimization includes costs of purchased electricity and fuel (natural gas) over a time period, usually 24-hour time horizon, with the understanding that scheduling and continuous control of individual equipment can be done in hourly time steps only. Note that demand charges were not considered in the model. The model can handle variable price rate structures and multiple components of each type. Solar photovoltaics are also included and sellback to grid can be an option. The optimization allows for energy dumping, both cooling and heating thermal energy if needed (even though this is usually not implemented practically by most IES system operators). Finally, the relevant models for electrical and thermal storage systems are also described.

A.3.2 Objective Function

Simulation time step is chosen as one hour. Operating cost is to be minimized over a 24-hour time horizon:

$$min\left\{\sum_{\mathrm{t}=1}^{24}\left[C_{gas}(t)\left(F_{boiler}(\mathrm{t})+F_{PM}(\mathrm{t})\right)+C_{elec,buy}(t).E_{grid,buy}(\mathrm{t})-C_{elec,sell}(t).E_{grid,sell}(\mathrm{t})\right]\right\} \tag{A-1}$$

where the individual terms are defined in the nomenclature. Note that the above objective function only includes operational costs and demand charges and maintenance costs are not included.

A.3.3 Model Constraints

The constraints are essentially mass and energy balances which are applied at both system level and at individual component level. Other practical constraints such as ramping rates, start-up costs, and time locks are also considered in this analysis, and discussed in the following sections.

A.3.3.1 Energy Balance Constraints at System Level

System level energy balance equations include electrical energy balance equation, heating energy balance equation, and cooling energy balance equation, as detailed below.

a) Electrical Energy:

Electrical energy balance equation includes distributed on-site electrical energy generation by the prime movers and solar PVs, purchased electricity from and sell-back to the utility grid, non-cooling electrical loads of the building, and electricity consumed by the electrical vapor compression chillers. Energy consumption of cooling towers fans should also be included if cooling towers performance is considered in the optimization model.

$$E_{PM}(t) + E_{PV}(t) + E_{grid,buy}(t) - E_{grid,sell}(t) = E_{bldg}(t) + E_{VC}(t) \qquad \text{(A-2)}$$

b) Heating Energy:

The total heating energy generated by boilers and recovered through the heat recovery units should be equal to, or larger than, the facility heating loads (Equation A-3). The excess amount can be **dumped** through a cooling tower. Equations (A-4.1) and (A-4.2) bound the amount of heat which can be recovered from the prime mover through the heat recovery unit and used for either heating or/and absorption cooling.

$$Q_{boiler}(t) + Q_{HRU}(t) = Q_{heating}(t) + Q_{h,dumped}(t) \qquad \text{(A-3)}$$

$$Q_{PM}(t) = Q_{PM,h}(t) + Q_{AC,in}(t) \tag{A-4.1}$$

$$Q_{PM,h}(t) * \varepsilon_{HX} \geq Q_{HRU}(t) \tag{A-4.2}$$

c) Cooling Energy:

The cooling energy balance constraint includes cooling energy provided by the absorption and vapor compression chillers (or any other cooling equipment that might be used) at each time step which ought to be equal to the total cooling demands with the excess amount to be dumped (or be stored if chilled water storage system is available).

$$Q_{AC}(t) + Q_{VC}(t) = Q_{cooling}(t) + Q_{c,dumped}(t) \tag{A-5}$$

A.3.3.2 Component Models and Practical Constraints

a) Prime Movers

At each time step, the total electrical power, fuel consumption, and heat generated by the combined heat and power (CHP) plant are summations of these variables across individual prime movers:

$$E_{PM}(t) = \sum_{i=1}^{nPM} E_{PM}(i,t) \tag{A-6}$$

$$F_{PM}(t) = \sum_{i=1}^{nPM} F_{PM}(i,t) \tag{A-7}$$

$$Q_{PM}(t) = \sum_{i=1}^{nPM} Q_{PM}(i,t) \tag{A-8}$$

Part-load performance of the prime movers are modeled using the regression model developed by Hudson [1]. This model can be applied to fuel cells, reciprocating engines, and microturbines. Generalized coefficients proposed by Hudson can be implemented for each type of the prime mover; alternatively, model coefficients specific to a particular system can be identified through regression analysis if monitored historical data is available.

$$F_{PM}(i,t) = \frac{E_{PM}(i,t)\times F^*_{PM}(i)}{E^*_{PM}(i)\times PLF} \quad \text{(A-9)}$$

Where:

$$PLF = \left[a0_{PM}(i) + a1_{PM}(i)\frac{E_{PM}(i,t)}{E^*_{PM}(i)} + a2_{PM}(i)\left(\frac{E_{PM}(i,t)}{E^*_{PM}(i)}\right)^2 + a3_{PM}(i)\left(\frac{E_{PM}(i,t)}{E^*_{PM}(i)}\right)^3\right]$$

The capacity of the prime mover needs to be bounded between the minimum allowable part-load-ratio (X_{PM}) and its rated capacity (E^*_{PM}). Also, a binary integer variable $S_{PM}(i,t)$ needs to be included which specifies whether the *i*th prime mover is available at time step t or not. Time-lock constraints (discussed later) are also introduced to identify the proper value for this variable. The following equation applies to each prime mover and similar equation is required for each component:

$$S_{PM}(i,t).X_{PM}(i).E^*_{PM}(i) \le E_{PM}(i,t) \le S_{PM}(i,t).E^*_{PM}(i) \quad \text{(A-10)}$$

The amount of heat generated by the prime mover can be determined as:

$$Q_{PM}(i,t) = F_{PM}(i,t) - 3600 \times E_{PM}(i,t) \quad \text{(A-11)}$$

where the term 3600 is introduced to convert kW to kJ/h.

Model coefficients for two types of prime movers, namely reciprocating engines and gas turbines, are listed in Table A-1 along with model coefficients for boilers, VC chillers, and absorption chillers.

Table A-1- Numerical values of the part-load model coefficients of various equipment ([1]*)*

	Reciprocating gas engine (Eq. A-9)	Gas turbine (Eq. A-9)	Vapor compression chiller (Eq. A-18)	Absorption chiller (Eq. A-22)	Boiler (Eq. A-14)
a_0	0.4866	0.3279	0.640844	-0.00383696	0.082597
a_1	1.0214	1.1542	-1.171278	-0.2129657	0.996764
a_2	-0.508	-0.4821	0.7008978	0.3856205	-0.079361
a_3	-	-	-0.3400201	0.4719114	-
a_4	-	-	0.1119608	0.3726551	-
a_5	-	-	1.046851	-0.0071625	-

Figure A-2 shows the variation of the part-load factors (PLF) curves for various generic types of prime movers (taken from [2]).

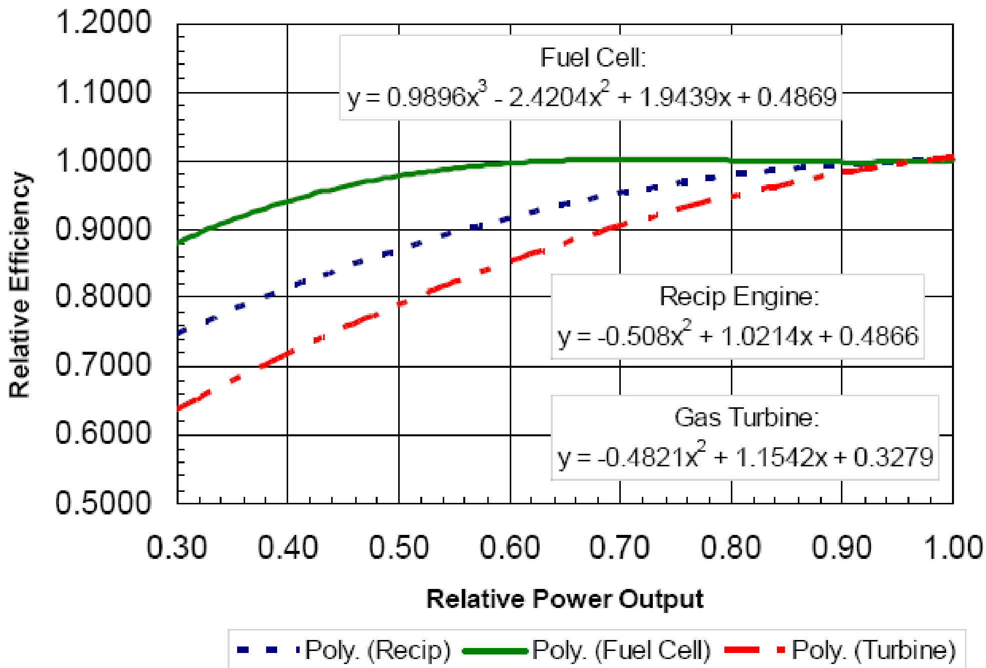

Figure A-2- Part-load electrical efficiency factors for different distributed generation equipment (PLF factors shown in Eq. A-9) (from [2])

b) Boilers

Equations (A-12) and (A-13) capture the fact that the total generated heating and fuel consumed by the boilers are the summation of these variables across individual boilers.

$$Q_{boiler}(t) = \sum_{i=1}^{nboiler} Q_{boiler}(i,t) \tag{A-12}$$

$$F_{boiler}(t) = \sum_{i=1}^{nboiler} F_{boiler}(i,t) \tag{A-13}$$

A second order part-load-performance model is adopted in this study:

$$F_{boiler}(i,t) = Q_{boiler}(i,t) \times \left(\frac{F^*_{boiler}(i)}{Q^*_{boiler}(i)}\right) / \, PLF \tag{A-14}$$

where PLF=$\left(a0_{boiler}(i) + a1_{boiler}(i)\left(\frac{Q_{boiler}(i,t)}{Q^*_{boiler}(i)}\right) + a2_{boiler}(i)\left(\frac{Q_{boiler}(i,t)}{Q^*_{boiler}(i)}\right)^2\right)$

and the limiting constraint on the capacity of the boilers reflects the condition that operating performance should be between its rated capacity and a pre-stipulated minimum:

$$S_{boiler}(i,t).\,X_{boiler}(i).\,Q^{*}_{boiler}(i) \leq Q_{boiler}(i,t) \leq S_{boiler}(i,t).\,Q^{*}_{boiler}(i) \qquad \text{(A-15)}$$

Boiler model coefficients are given in Table A-1, while the PLF factor is plotted in Figure A-3. Though this is non-linear, we note that the curve is fairly linear down to PLR = 0.5, and that 3 linear segments should capture the total variation quite well.

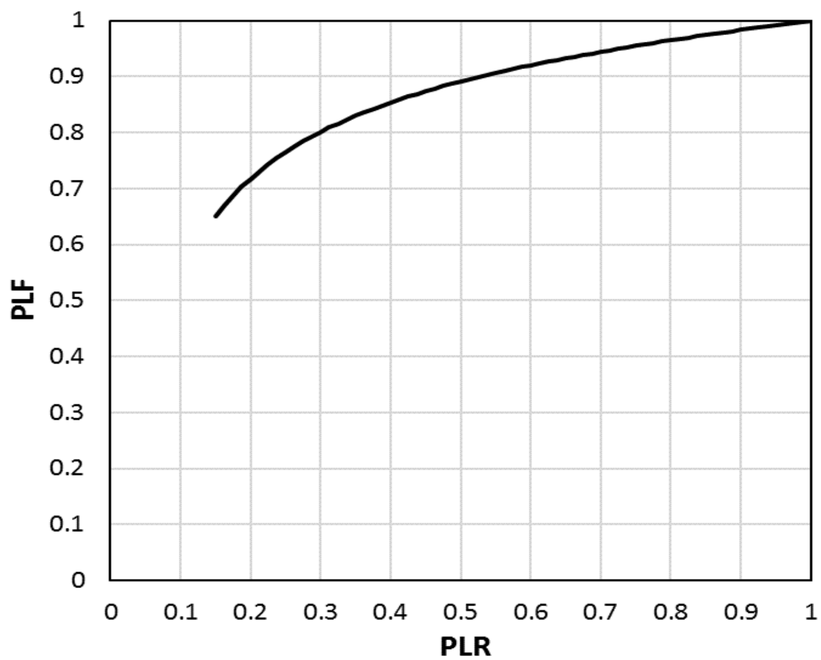

Figure A-3- Part-load performance of boilers- PLF factor from Eq. A-14 (adopted from [3]*)*

c) Vapor Compression Chillers (VC):

Total cooling energy generated and electricity consumed by the plant at each time step are simply the respective sums of the generation and consumption of individual vapor compression chillers.

$$Q_{VC}(t) = \sum_{i=1}^{nVC} Q_{VC}\,(i,t) \qquad \text{(A-16)}$$

$$E_{VC}(t) = \sum_{i=1}^{nVC} E_{VC}\,(i,t) \tag{A-17}$$

Although our previous analysis indicated that Gordon and Ng model [4] would outperform the black-box approach, we found that the models being non-linear in the basic variables, lead to numerical problems in that the optimization package has difficulty finding an optimum. However, no such difficulties were found with black-box model developed by [5]. Hence, in order to reduce the numerical complexity, we have adopted the later modeling approach.

$$E_{VC}(i,t) = E_{VC}^{*}(i) * PLF \tag{A-18}$$

where $PLF = \left[a0_{VC}(i) + a1_{VC}(i)\left(\frac{T_{VCcdi}(i,t)}{T_{VCcdi}^{*}(i)}\right) + a2_{AC}(i)\left(\frac{T_{VCcdi}(i,t)}{T_{VCcdi}^{*}(i)}\right)^{2} + \right.$

$\left. a3_{VC}(i)\left(\frac{Q_{VC}(i,t)}{Q_{VC}^{*}(i)}\right) + a4_{VC}(i)\left(\frac{Q_{VC}(i,t)}{Q_{VC}^{*}(i)}\right)^{2} + a5_{VC}(i)\left(\frac{T_{VCcdi}(i,t)}{T_{VCcdi}^{*}(i)}\right)\left(\frac{Q_{VC}(i,t)}{Q_{VC}^{*}(i)}\right)\right]$

The model coefficients are given in Table A-1 and plotted in Figure A-4. Notice that there are only two regressors in the model: the cooling load and the condenser water inlet temperature (which is equal to the cooling tower water leaving temperature). The chilled water set temperature is assumed to be fixed and so does not appear in the above equation. The capacity constraint for the vapor compression chillers is that operation should be between its rated capacity and a predefined minimum allowable part-load-ratio:

$$S_{VC}(i,t).\,X_{VC}(i).\,Q_{VC}^{*}(i) \le Q_{VC}(i,t) \le S_{VC}(i,t).\,Q_{VC}^{*}(i) \tag{A-19}$$

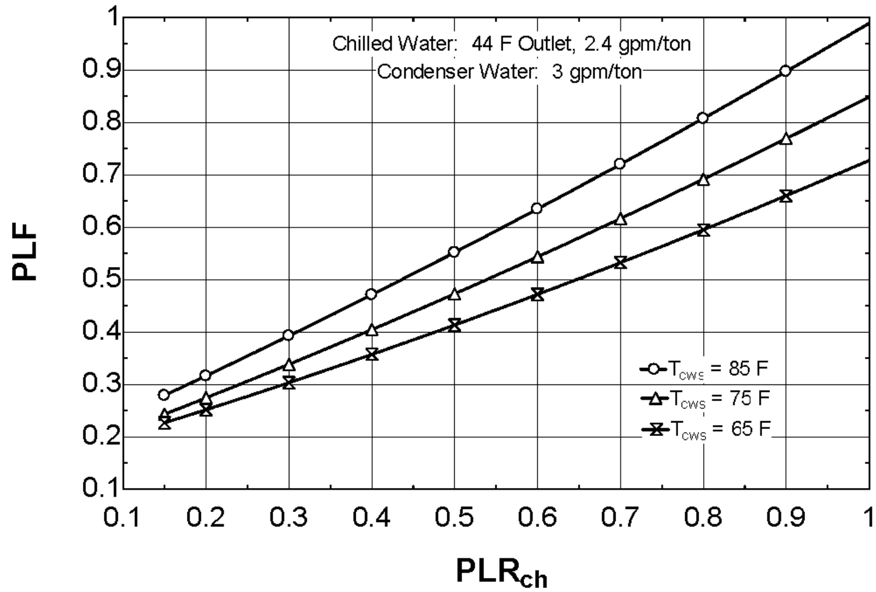

Figure A-4- Part-load performance of fixed-speed, electric-driven centrifugal chiller – PLF given by Eq. A-18 (from [5]*)*

d) Absorption Chillers (AC)

The total generated cooling thermal output and heat input to the AC units at each time step are given by:

$$Q_{AC}(t) = \sum_{i=1}^{nAC} Q_{AC}\,(i,t) \tag{A-20}$$

$$Q_{AC,in}(t) = \sum_{i=1}^{nAC} Q_{AC,in}\,(i,t) \tag{A-21}$$

The black-box approach is adopted in this analysis which relates the heat input to the generator of each absorption chiller based on the cooling output and the condenser water inlet temperature, at both part-load and rated conditions.

$$Q_{AC,in}(i,t) = Q^*_{AC,in}(i) \ * PLF \tag{A-22}$$

where $PLF = \left[a0_{AC}(i) + a1_{AC}(i)\left(\frac{T_{ACcdi}(i,t)}{T^*_{ACcdi}(i)}\right) + a2_{AC}(i)\left(\frac{T_{ACcdi}(i,t)}{T^*_{ACcdi}(i)}\right)^2 + \right.$

$\left. a3_{AC}(i)\left(\frac{Q_{AC}(i,t)}{Q^*_{AC}(i)}\right) + a4_{AC}(i)\left(\frac{Q_{AC}(i,t)}{Q^*_{AC}(i)}\right)^2 + a5_{AC}(i)\left(\frac{T_{ACcdi}(i,t)}{T^*_{ACcdi}(i)}\right)\left(\frac{Q_{AC}(i,t)}{Q^*_{AC}(i)}\right)\right]$

Model coefficients are given in Table A-1, and the part-load curves are plotted in Figure A-5. The chiller cooling output should be bounded between its rated capacity and a predefined minimum allowable part-load-ratio:

$$S_{AC}(i,t).X_{AC}(i).Q^*_{AC}(i) \le Q_{AC}(i,t) \le S_{AC}(i,t).Q^*_{AC}(i) \tag{A-23}$$

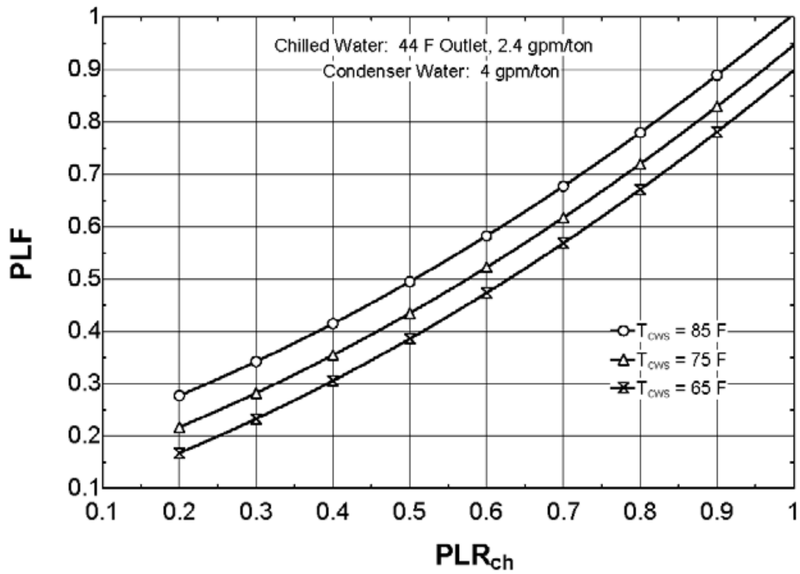

Figure A-5- Part-load performance of absorption chiller- PLF given by Eq. A-22 (from [5]*)*

Cooling tower models are required to predict the inlet water temperature to the chiller condenser which is assumed to be equal to the outlet water temperature from the cooling tower. However, the effect of the cooling tower has been neglected in this analysis by assuming that the outlet water temperature is equal to the rated value (an assumption made by the other two groups also).

e) Time-locks

Time locks are constraints which require that equipment must operate for a certain period of time after they are started. This is meant to prevent frequent start-stop operation. We have assumed a similar formulation to model turning off or turning on the various IES components. The following set of equations can be applied to any component.

$$\sum_{\tau=t-TL}^{t-1} s(i,\tau) \geq TL \times [s(i,t) - s(i,t-1)] \tag{A-24}$$

$$\sum_{\tau=t-TL}^{t-1} [1 - s(i,\tau)] \geq TL \times [s(i,t) - s(i,t-1)] \tag{A-25}$$

where *TL* represents time lock (hours) and τ is a dummy variable and s is the on/off binary variable for any component.

f) Battery Storage (Electrical Energy Storage- EES)

Energy balance equation should be framed to include battery charging and discharging:

$$E_{PM}(t) + E_{PV}(t) + E_{grid,buy}(t) - E_{grid,sell}(t) + \eta_{EES,dis} E_{dis}(t) - E_{chrg}(t) = E_{bldg}(t) + E_{VC}(t) \tag{A-26}$$

The battery model can be defined as:

$$SOC_{EES}(i,t) = \eta_{EES,storage}(i) \times SOC_{EES}(i,t-1) + \eta_{EES,chrg}(i) \times E_{chrg}(i,t) - E_{dis}(i,t) \tag{A-27}$$

where SOC is battery state of charge at each time step which should be bounded between some predefined charge level identified by depth of discharge (DoD) and the battery capacity as:

$$X_{EES}(i) \times E_{EES}^{*}(i) \leq SOC_{EES}(i,t) \leq E_{EES}^{*}(i) \tag{A-28}$$

where $X_{EES}(i) = 1 - DoD_{EES}(i)$, and charging and discharging rates (in Watts) are also limited depending on the state of charge at that time step:

$$0 \leq E_{chrg}(i,t) \leq E_{chrg,max}(t) \tag{A-29}$$

$$0 \leq E_{dis}(i,t) \leq E_{dis,max}(t) \tag{A-30}$$

It should be noted that **constant** charging and discharging rates were assumed for both battery and thermal storage system (next section) in this research project to simplify the problem.

g) Thermal Energy Storage (TES) System

Chilled water thermal storage system was also considered in one of the scenarios assumed. Cooling energy balance equation would include two extra terms associated with the thermal storage system as:

$$Q_{AC}(t) + Q_{VC}(t) + \eta_{TES,dis} Q_{dis}(t) = Q_{cooling}(t) + Q_{c,dumped}(t) + Q_{chrg}(t) \quad \text{(A-31)}$$

The TES model is defined as:

$$SOC_{TES}(i,t) = \eta_{TES,storage}(i) \times SOC_{TES}(i,t-1) + \eta_{TES,chrg}(i) \times Q_{chrg}(i,t) - Q_{dis}(i,t) \quad \text{(A-32)}$$

where SOC is storage system state of charge at each time step which should be bounded between some predefined charge level identified by depth of discharge (DoD) parameter and the storage capacity as:

$$X_{TES}(i) \times Q^*_{TES}(i) \leq SOC_{TES}(i,t) \leq Q^*_{TES}(i) \quad \text{(A-33)}$$

where $X_{TES}(i) = 1 - DoD_{TES}(i)$, and charging and discharging rates (in MMBtu) are also limited depending on the state of charge at that time step:

$$0 \leq Q_{chrg}(i,t) \leq Q_{chrg,max}(t) \quad \text{(A-34)}$$

$$0 \leq Q_{dis}(i,t) \leq Q_{dis,max}(t) \quad \text{(A-35)}$$

h) Ramping Constraints

Ramping constraints limit the rate at which power, heating, or cooling generation of a particular system component may increase or decrease between two successive time steps. In this study, ramping rates are considered for both ramping-up and ramping-down conditions, and expressed in the same unit as the output of the corresponding component. Ramping constraints for boilers (as an example) can be expressed as:

$$-RD_{boiler}(i) \leq Q_{boiler}(i,t) - Q_{boiler}(i,t-1) \leq RU_{boiler}(i) \tag{A-36}$$

where RU and RD are the ramp up and ramp down rates respectively.

A.4 Piecewise Linear Modeling of Nonlinear Models

This section provides some theoretical background of how to best approximate non-linear models using segmented linear models. Next, it applies the methodology to various equipment of the integrated energy system.

A.4.1 Piece-wise linear function using integer programming

Suppose that y = f(x) is a non-linear function. The aim is to approximate this non-linear function with a piecewise linear function for which the slope and intercept depend on x value. More specifically, there are n break points and the value of x could be in n-1 different closed intervals formed by these break points and the slope and intercept is different for each interval such that the function is still smooth.

The notation is as follows:

a_j: Slope at interval *j*

b_i: break point *i*

$f(b_i)$: Output value at break point *i*

$Z_i \in [0,1]$: The convex combination coefficient

$$y_j = \begin{cases} 1 & if\ x\ lies\ in\ the\ jth\ interval \\ & 0\ \ Otherwise \end{cases}$$

Note that when the value of independent variable lies in interval j, its value is in the range $[b_j, b_{j+1}]$. In this case we would have:

$$x = Z_j * b_j + Z_{j+1} * b_{j+1} \tag{A-37}$$

$$f(x) = \sum_{i=1}^{n} Z_i * f(b_i) \tag{A-38}$$

As the value of x should lie on only one of the intervals, we need to add the following constraint to the model:

$$y_1 + y_2 + \cdots + y_{n-1} = 1 \tag{A-39}$$

where all y_j are binary variables.

Also, as any interval is defined as points between two consecutive break points, the following constraint is also needed.

$$z_1 + z_2 + \cdots + z_n = 1 \tag{A-40}$$

as z_is are convex combination coefficients, they all should be positive.

Finally, as convex combination coefficient for a break point will be nonzero only if the point lies in one of the two intervals that formed by that point, we also added the following constraints to the model.

$$z_1 \leq y_1 \tag{A-41}$$

$$z_k \leq y_{k-1} + y_k \tag{A-42}$$

for *k = 2,3,…,n-1*:

$$z_n \leq y_{n-1}$$

Note that the first and last break points show up just in one interval and that is why we have different constraints for these points.

A.4.2 Model Intercept

While the above model is zero-intercept, the model developed by Group#2 does include different intercepts for different intervals. To be consistent and in order to take care of this issue, we changed the first slope, such that in the second break point, the value of the function defined above be equal to the first intercept of interest. For the subsequent intervals no change is needed and the model takes care of intercepts by calculating function value at break points and considering these border values in subsequent calculations. Table A-2 lists the values of the segmented linear model slopes used in our analysis.

Table A-2- Piecewise linear model parameters

Component	Interval	Lower Bound	Upper Bound	Slope
Prime mover	1	150	210	0.01397588
	2	210	370	0.00630502
	3	370	500	0.00657468
Boiler	1	1.2	2.1	5.340555788
	2	2.1	4	0.596682831
	3	4	8	0.265743355
Vapor compression chiller	1	0.3599795	1	72.9080578
	2	1	1.9	32.95726035
	3	1.9	2.399863	35.80207305
Absorption chiller	1	0.23746162	0.61	1.869511783
	2	0.61	1.05	1.189568592
	3	1.05	1.583077	1.507863263

A.5 Case Study

A.5.1 Description of Scenario

This section summarizes the analysis and validates the case study results for which specifications of the energy system components are listed in Table A-3.

Table A-3- Specifications of the BCHP system components

	Building Type	Large Office
Prime Mover	Quantity (Type)	1 (recip) + 1 (turbine)
	Rated electric output- kW	788+242
	Rated net gas- MMBtu/h	7.22+2.84
Electrical Energy Storage	Rated Capacity- MWh	2
Thermal Energy Storage	Rated Capacity- Cooling MMBtu	-
Boilers	Quantity	2
	Rated heat output- MMBtu/h	6.695
	Natural gas use- MMBtu/h	8.165
Vapor Compression Chiller	Quantity	2
	Cooling Capacity- MMBtu	7.2
	Electrical power input- kW	188.1
Absorption Chiller	Quantity	1
	Cooling capacity- MMBtu	1.86
	Heat Input- MMBtu	2.657

A.5.2 Linearization of Non-linear Component Models

Component models described earlier in this appendix are non-linear and further binary variables are required to identify which component is on/off at any time step. This makes the optimization problem a mixed integer non-linear problem. Due to large number of non-linear variables, global optimal solutions could not be found by the commercial software used, and therefore component models were re-expressed as linear or piecewise linear ones in order to overcome the convergence issue.

A.5.3 Results

In this case study, four sample days, i.e. a typical Summer day and a typical Winter day each with high taken to be 9 cents/kWh during on-peak hours (from 9AM to 7PM) and 3 cents/kWh during off-peak hours. The battery charging and discharging rates are limited to 500 kWh/h with the initial SOC of 50%. The battery SOC at the end of the 24 hours is forced to be equal to its initial SOC. During the summer days, when the heating loads are low, all heating loads are covered by the heat recovered from the prime movers and both boilers are off.

Results for the **Summer day with high loads** are depicted in Figure A-6; figure (a) illustrates electrical systems performance while figure (b) shows the battery SOC; heating and cooling loads and presented in figures (c) and (d) respectively. Following noteworthy points can be gleaned from the results of the optimization modeling for the Summer day with high loads:

- Battery gets fully charged before the on-peak hours and gets totally depleted till 12PM in order to minimize the amount of purchased electricity during the on-peak hours.

- Building electrical loads are entirely met by grid power before 6AM. From 6AM to 9AM the recip prime mover ramps up to feed the VC chillers, cover the rising heating loads, and charge the battery along with the grid power.
- The recip prime mover runs at its full capacity throughout the on-peak hours. The turbine also runs at full capacity from 9AM to 5PM after which the building electrical loads reduces.
- Building heating loads are entirely met by the recovered heat from the prime movers and both boilers are off over the 24-hour horizon.
- Cooling loads are mainly covered by the VC chillers while the absorption chiller is running only during on-peak hours when the prime movers generate enough heat.

Figure A-7 presents results of the optimization modeling for the **Summer day with low loads.** It is evident that the battery charging and discharging and other equipment loadings are almost similar to those of the Summer-high-load case. The only difference would be VC-Chiller 2 which is off throughout the day due to lower heating loads compared to the Summer-high-load case.

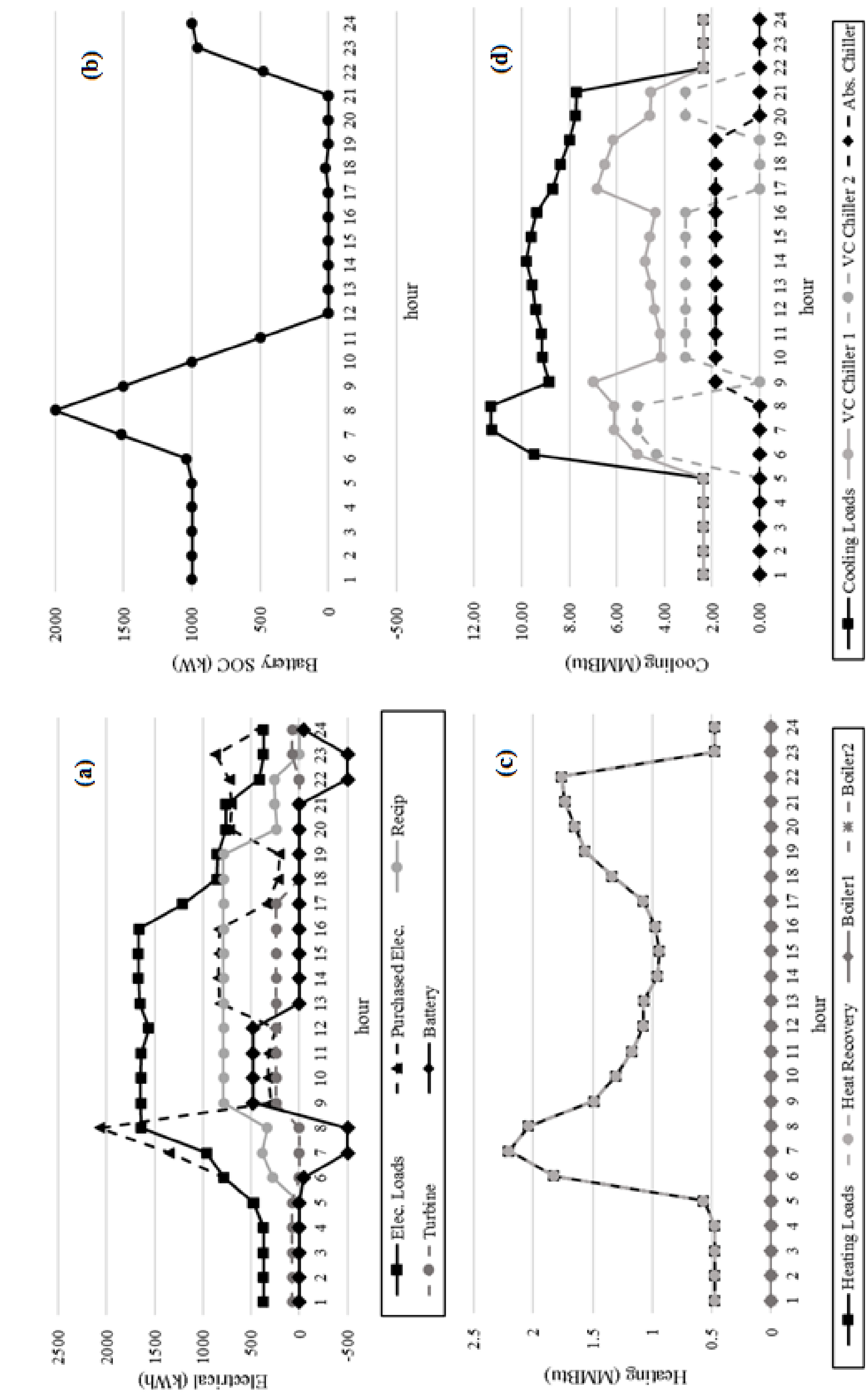

Figure A-6- Scheduling and dispatching results, Summer day with high loads

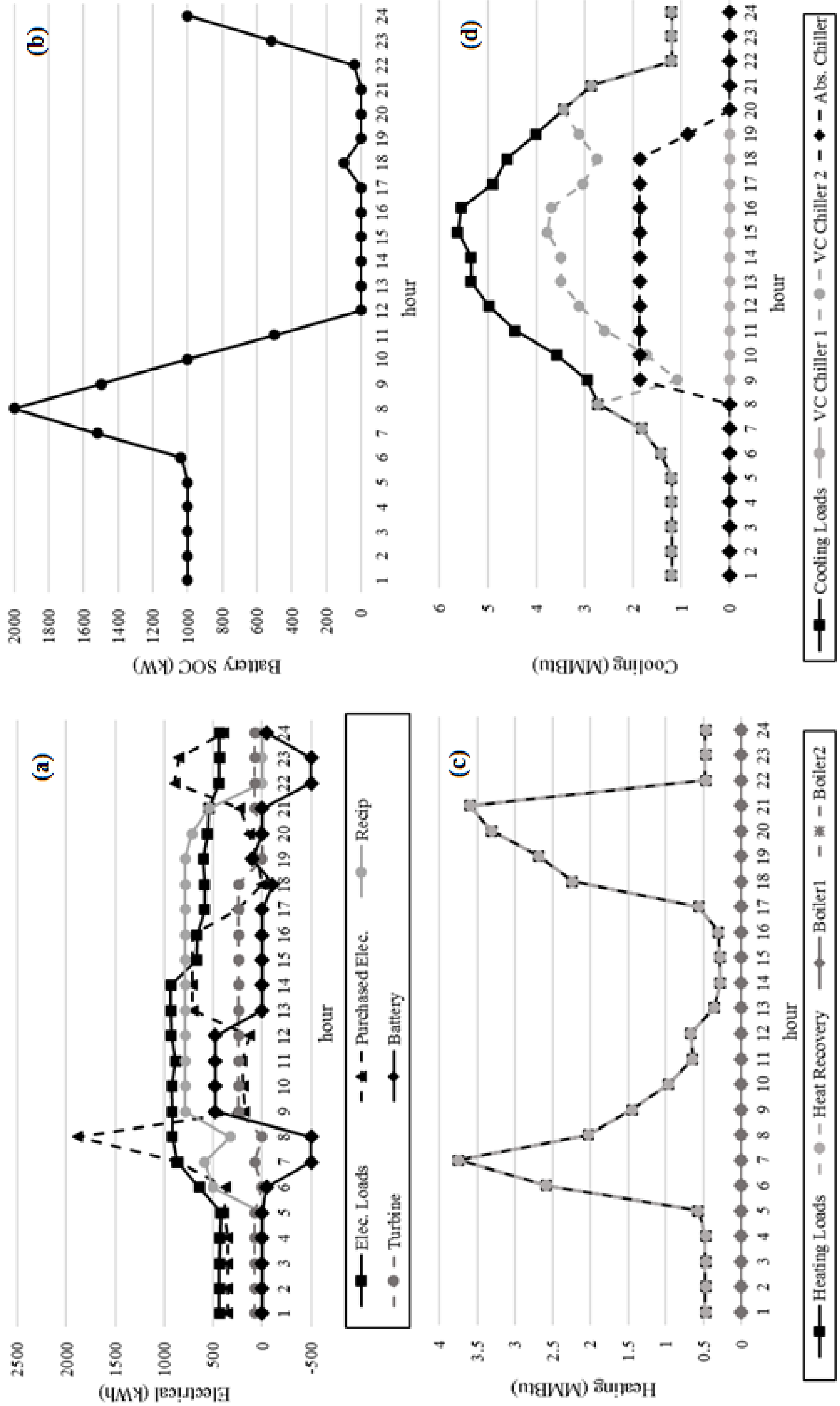

Figure A-7- Scheduling and dispatching results, Summer day with low loads

Figure A-8 and Figure A-9 show results of the analysis for the selected Winter days with high and low loads respectively. Battery charging and discharging trends are quite similar to those resulted for the Summer days. Note that differences in the battery recharging at the end of the day would not cause any difference in the operational costs as there might be multiple equally-optimal solution; in other words, there is no difference in charging the battery at 10PM or at 11PM. Salient points identified from the results for the selected Winter days are:

- Prime movers are running at maximum capacity during the on-peak hours in order to minimize the purchased electricity from the utility grid.
- Battery is fully charged before on-peak and depleted after four hours during the on-peak hours.
- Heating loads are covered by the recovered heat from the prime movers and also boiler1 while the second boiler remains off during the day.
- Cooling loads are very low before 5AM and after 11PM and the cooling generated by one VC chiller at 15% PLR is still larger than the cooling loads and therefore the excess amount should be dumped; note that we do not let the VC chillers to run below the 15% of their full capacity.
- VC chiller 2 is stand by throughout the day while the absorption chiller runs only five hours during the on-peak hours.

In Figure A-9 (c), loading is exchanges between boiler1 and boiler2 at 9AM. Note that the two boilers are identical and switching between them would not result in lower costs rather returns an equally optimal result. To prevent this issue, we could slightly alter the efficiency curve of one of the boilers so that the optimization model prefers one boiler over another; however, we decided not to do that as this might result in non-continuity in the segmented linear models.

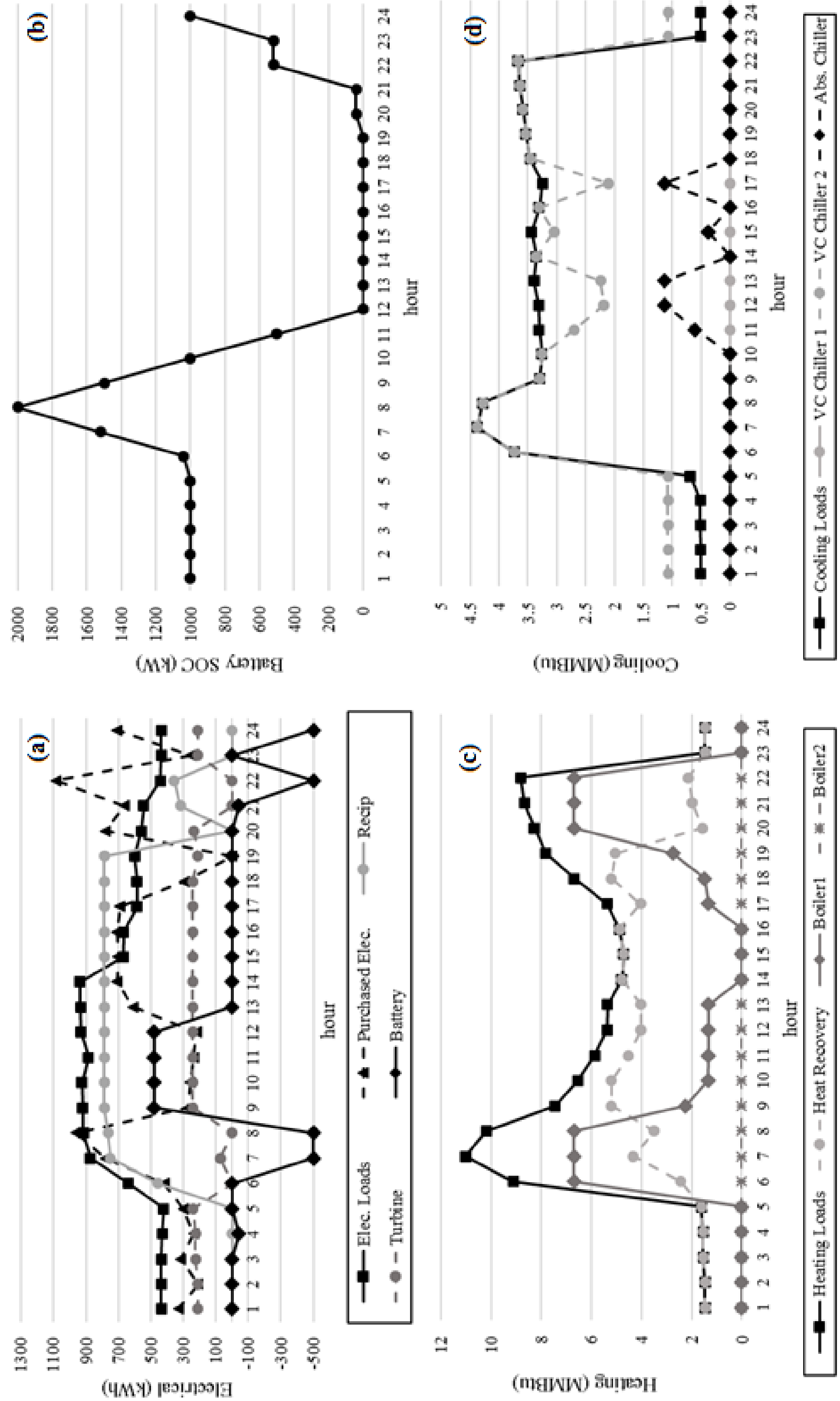

Figure A-8- Scheduling and dispatching results, Winter day with high loads

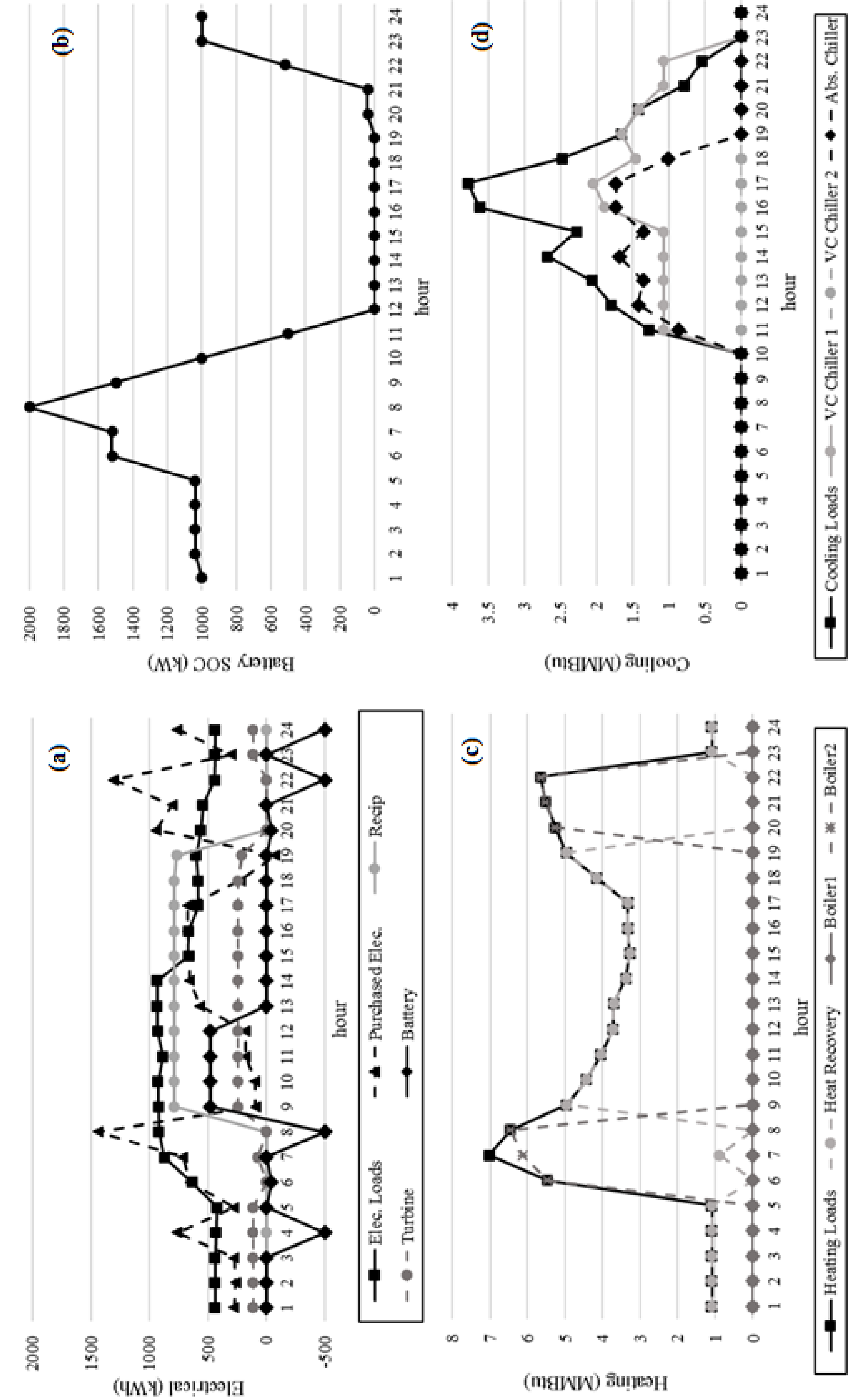

Figure A-9- Scheduling and dispatching results, Winter day with low loads

Table A-4 assembles results of the optimization analysis performed by different teams working on this project. We note that results obtained by ASU and Group#2 are close, thus confirming that the implemented optimization framework has been developed accurately.

Table A-4- Inter-comparison of operational costs results (penalty costs are included)

	Group#1	**ASU**	Group#2
Summer High	$1784	**$1787**	$1787
Summer low	$1688	**$1692**	$1689
Winter high	$2948	**$2591**	$2618
Winter low	$2086	**$1923**	$1936

Table A-5 shows the penalty costs in various investigated days associated with possible mismatches in energy balance equations due to errors in approximating nonlinear equipment output performance behavior by segmented linear models. Small penalty costs indicate that the segmented linear models are accurate and all the energy balance equations are satisfied.

Table A-5- Penalty costs due to linearized component models

	Group#1	**ASU**	Group#2
Summer High	$1.1	**$0.2**	$0.1
Summer low	$3.3	**$0.3**	$0.2
Winter high	$12.4	**$0.3**	$0.2
Winter low	$10.2	**$0.5**	$0.1

A.6 Conclusions

In this study, the accuracy of the developed optimization models was evaluated against those developed by Group#1 and Group#2 teams for several scenarios. The closeness of the results partially validates and confirm this objective. Mathematical formulation of the objective function, component part-load performance models, energy balance constraints, ramping and time-lock constraints have been described in this section. We have also developed a model to optimally identify the break-point of the segmented linear models used instead of regressive non-linear component models. Effect of linearization of the component models on total operational costs was found to be marginal confirming that the fitted segmented models can accurately approximate the actual performance of the equipment. Results of the case studies independently analyzed by different teams were very close although different solvers and software packages were used.

References

[1] Hudson, C.R., 2005. ORNL CHP Capacity Optimizer: User's Manual, Oak Ridge National Laboratory Report ORNL/TM-2005/267

[2] Maor, I. and T.A. Reddy, 2008. Near-Optimal Scheduling Control of Combined Heat and Power Systems for Buildings, Final Report for ASHRAE Research Project 1340-RP, submitted to ASHRAE, about 300 pages (single spaced), July.

[3] Birdsall, B., W. F. Buhl, K. L. Ellington, A. E. Erdem, and F. C. Winkelmann, 1990. "Overview of the DOE 2.1 Building Energy Analysis Program." Report LBL-19735, rev. 1. Lawrence Berkeley Laboratory, Berkeley, CA.

[4] Gordon, J.M. and NG, K.C., 2000. Cool Thermodynamics, Cambridge International Science Publishing, Cambridge, U.K.

[5] Braun, J.E., 2006. Optimized Operation of Chiller Equipment in Hybrid Machinery Rooms and Associated Operating and Control Strategies- 1200 RP, Final report of ASHRAE Research Project RP- 1200 RP, Braun Consulting, 87 pages, August.